EVALUATION OF PILLAR DESIGN SYSTEMS FOR LOW REEF PLATINUM MINING

Tawanda Zvarivadza

A research report submitted to the Faculty of Engineering and the Built Environment, University of the Witwatersrand, Johannesburg, in partial fulfilment of the requirements for the degree of Master of Science in Engineering.

Johannesburg, 2012

DECLARATION

I declare that this research report is my own, unaided work. It is being submitted for the Degree of Master of Science in the University of the Witwatersrand, Johannesburg. It has not been submitted before for any degree or examination in any other University.

.....

(Signature of candidate)

..... day of **.....** (year) **.....**

at **.....**

ABSTRACT

Platinum is amongst the extremely valuable resources so every effort has to be made to ensure its safe and economic extraction. The success of a bord and pillar mining method in the exploitation of platinum heavily depends on a comprehensive and competent pillar design method. Pillars need to be large enough to contain load and to be small enough to avoid loss of resource. An optimum pillar design method achieves such a scenario. Without this a mine is destined for disastrous consequences either ways. A mine stands to lose revenue and threatens sustainable development if it tries to be conservative and leave too large pillars. On the other hand, leaving too small pillars can lead to large scale pillar failure with damaging consequences such as entrapment of expensive mining machinery, loss of life by workers, loss of invaluable production sections and all the severe effects of ground subsidence due to underground failure of pillars. While a lot of research has been done on the pillar design for coal industry, very little advance has been achieved in terms of this sort of research on hard rock mining. Of the research which has been done there are still more gaps to be filled and considerations to be made to come up with reliable pillar design systems.

The main objective of this research was to make a critical evaluation of the current pillar design systems used in low reef platinum mining so that more benefit would be obtained in the performance improvement of these systems. An extensive literature survey was undertaken in order to determine the present status of the design systems. As part of the research a review of the work done by the author on one large scale platinum exploration project and several platinum mines in Zimbabwe was also done. Through this approach the inadequacies of the current pillar design systems were highlighted and a proposition of areas of further research to get more understanding on how some neglected factors influence pillar system stability were brought forward. The work on the exploration project presented an excellent opportunity to map out areas of much care and consideration when collecting the geotechnical parameters used in designing pillars. The exploration work also highlighted how rockmass classification methods can be utilised in determining the overall strength of pillars.

The evaluation concluded that the current pillar design systems for low reef platinum mining mainly consider w/h ratio and the strength of pillar material as important parameters in designing pillars. However there are many more important factors which are not considered which have a bearing on pillar system stability. Some of the unaccounted for factors which were discovered during the course of the research are; contact of the pillar with the roof and

floor, roof and floor conditions, effects of adversely oriented joints, spalling and side scaling effects, influence of pillar loading conditions, blasting damage effects, influence of weak layers and weathering, impact of k-ratio, time dependent effects, geology, fractured zones, effects of different types of discontinuities within the rock strata, the list goes on. The observed pillar failures in the studied platinum mines are a testimony that these parameters have to be considered in determining pillar strength lest an over estimation of strength is done. Furthermore, the empirical systems do not embrace the fact that pillar design is a system. As a system, considerations of the roof, the pillar and the floor is mandatory since neglecting one component of the system will affect all system components.

The current pillar design systems are empirically determined. To calibrate the pillar design curve in empirical designs, pillar failure has to occur. While this may work for the mines lying within the empirical limits of the data used to develop the formulae, it is prudent for engineers to utilise tools which do not rely on failures. For the new mines which are to be established a tool should be availed with the power and capacity to design the pillars without waiting for failure to take place. While research costs time and money its fruits are worth it. It is the recommendation of this research that more research has to be done to quantify the influence of the above mentioned parameters in a bid to come up with a system that accounts for all factors affecting pillar stability. At the current level of research different combinations of the pillar design systems can be utilised in order to reduce error levels in the designs.

ACKNOWLEDGEMENTS

Profound gratitude is expressed to my supervisor Professor J.N Van der Merwe for the untiring guidance and encouragement. I greatly appreciate his efforts and expertise which led to this project seeing day light.

Many thanks go to Badger Mining Consulting Company, in particular Mike Spengler, for availing and allowing me to use the project work at the Large Scale Platinum Exploration Project as part of this research. This work helped a lot in expressing some salient aspects of this project.

Todal Mining Company, in particular Ron Honey, is highly appreciated for engaging the author in the Large Scale Platinum Exploration Project to oversee the geotechnical work. The author learnt a lot of practical work relevant to this research during the course of the exploration project. His supervision and guidance services were readily available to the author even in the light of his busy schedule.

The author is greatly indebted to Professor T.R Stacey for the invaluable knowledge imparted by him through the Rock Engineering courses he delivers at the University of the Witwatersrand. These courses equipped the author with necessary knowledge to tackle the research. The University of the Witwatersrand together with its School of Mining Engineering is also thanked for affording the author an opportunity to embark on this research.

Pastor Gee and the Dominion Family Church were instrumental in giving the author a spiritual home and peace of mind. Their spiritual guidance is ever invaluable.

Special thanks go to my family and friends for being there for me in times of joy and need.

Above all, the author is thankful to the Almighty God for being a guiding figure in all aspects of his life. To God be the Glory.

In memory of my father Elias, mother Nicolet and aunt Susan.

TABLE OF CONTENTS

CONTENTS **PAGE**

LIST OF FIGURES

LIST OF TABLES

LIST OF ABBREVIATIONS

ATC	Automatic Temperature Control
BON	Base of Norite
CJ	Closed Cemented Joint
CR	Core Recovery
DRMS	Design Rock Mass Strength
FD	Fluoride
FLAC	Fast Lagrangian Analysis of Continua
GDP	Gross Domestic Product
IRS	Intact Rock Strength
ISRM	International Society for Rock Mechanics
LSZ	Lower Sulphide Zone
MH	Marker Horizon
MSZ	Main Sulphide Zone
MTPL	Multiple
OCJ	Open Cemented Joint
PGE	Platinum Group Elements
PGM	Platinum Group Metals
PSR	Possibly Structure Related
RIR	Rest Intact Rock
SF	Safety Factor
SP	Serpentine
SRK	Stephen, Robertson and Kirsten

UCS	Uniaxial Compressive Strength
UDEC	Universal Distinct Element Code
USA	United States of America
w/h	Width to Height Ratio
WIR	Wholly Intact Rock

LIST OF SYMBOLS

σ_c	Uniaxial Compressive Strength (MPa)
σ_{max}	Maximum Normal Stress (MPa)
ρ	Material Density (kg/m^3)
σ_1	Major Principal Stress (MPa)
σ_2	Intermediate Principal Stress (MPa)
σ_3	Minor Principal Stress (MPa)

CHAPTER 1: INTRODUCTION

1.0 Introduction.

This chapter gives brief background information necessary to comprehend the research project in question. As an introductory note the author discusses the Room and Pillar Mining method together with geology and geotechnical background of platinum mining on Zimbabwe's Great Dyke. The Zimbabwean Great Dyke is used for illustration purposes only since the discussion for this research may also hold for most low reef platinum mines with geotechnical and geological setting similar to the Great Dyke. Also addressed here are the definition of the research problem, justification of the research project and the objectives and aims of the research project. The author also gives an outline of the methodology adopted in finding a lasting solution to the research question. Content of research report is also presented in this chapter.

1.2 Background of Pillar design

As revealed by Ozbay et al (1995), pillars have been used as means of support since the early days of mining. Pillar supported mining methods such as the bord and pillar mining method requires a reliable design system for them to be successful. Several decades have passed now but not much has been attained in the field of pillar design research for hard rock mines. The theory on pillar design endeavours to bring up stable pillar designs however the deficiencies in them has resulted in several pillars designed this way collapsing as highlighted later on in this report. For low reef platinum mining, large tensile stresses accompanied by geological and geotechnical factors contribute to instability of pillar designs. Such experiences require a well formulated pillar design system which accounts for such factors so as to minimise pillar failure occurrences. Jager and Ryder (1999) mention that one of the fundamental tasks in the analysis and design of mine pillars is to determine an adequate pillar size for a given mining site where geological setting, ore materials and mining method have been explored. It is quite critical to have an optimum pillar size. Larger pillars mean that more ore has been left unmined signifying wastage and unsustainable exploitation of resources. On the other hand leaving smaller pillars is courting disaster since the pillars will be unable to offer the necessary support resulting in the collapse of the mine or sections thereof.

A pillar layout design system has to consider the hanging-wall, the pillar material and the floor as all these three work together for the success of the system. Ozbay et al (1995) describe the hangingwall in shallow hard-rock mining situations as a rockmass containing

well-defined discontinuities and subjected to deadweight tension. These factors have to be considered in this component of the system. They mention that when the hangingwall is unsupported, it becomes susceptible to backbreaks if critical spans are exceeded. Ozbay et al (1995) point out that at shallow depth the whole hanging wall overburden can be involved in a collapse extending to the surface so a support system which is robust, stiff and able to react quickly to any sign of convergence is required.

1.3 Geology and geotechnical background of the Great Dyke of Zimbabwe

This project covers low reef platinum mining pillar design practices on the Great dyke of Zimbabwe for both exploration and established mines. The student uses several literature and some practical encounters of platinum mining on the Great Dyke of Zimbabwe as bases of discussion. Below is a brief account of platinum mining geology and geotechnical background of the Great Dyke of Zimbabwe.

1.3.1 Geotechnical and geology aspects of the Great Dyke Ore Body

Great dyke is characterised with a dish shaped depression stratigraphically referred to as an open syncline. A type of rock known as gabbronorite makes an erosion resistant cap on the great dyke and constitutes the hills seen along the great dyke. Much knowledge about the great dyke is attributed to the work of Wilson and Prendergast (1987 – 2010). They studied the great dyke geology over several years and are considered to be the Great dyke geology Captains.

Wilson and Prendagast (2002) defines the Great Dyke as a narrow, elongate, mafic-ultramafic intrusion with rock-types and layered structure broadly similar to other major PGE-rich layered intrusions such as the Bushveld and Stillwater Complexes in South Africa and the USA respectively. The great dyke is generally known to be 550 km long and up to 11 km wide. Prendergast (2009) points out that the Great Dyke was emplaced into typical Archaean granite-greenstone terrain of the Zimbabwe Craton at around 2.58 Ga and now cuts across Zimbabwe from north to south. He mentions that the great dyke originally comprised a lower longitudinal series of partly separate, dyke-like bodies and an upper continuous and laterally-extensive lopolith which is now eroded away except above the lower dykes. Wilson and Prendergast (2002) bring to light that on a stratigraphical view, the Great Dyke is made up of a well-layered, lower Ultramafic Sequence of serpentinites, pyroxenites and minor chromitites, defining a series of macrocyclic units, and an upper Mafic Sequence of norite, gabbro and magnetite gabbro. This stratigraphical sequence is as shown in Figure 1.1.

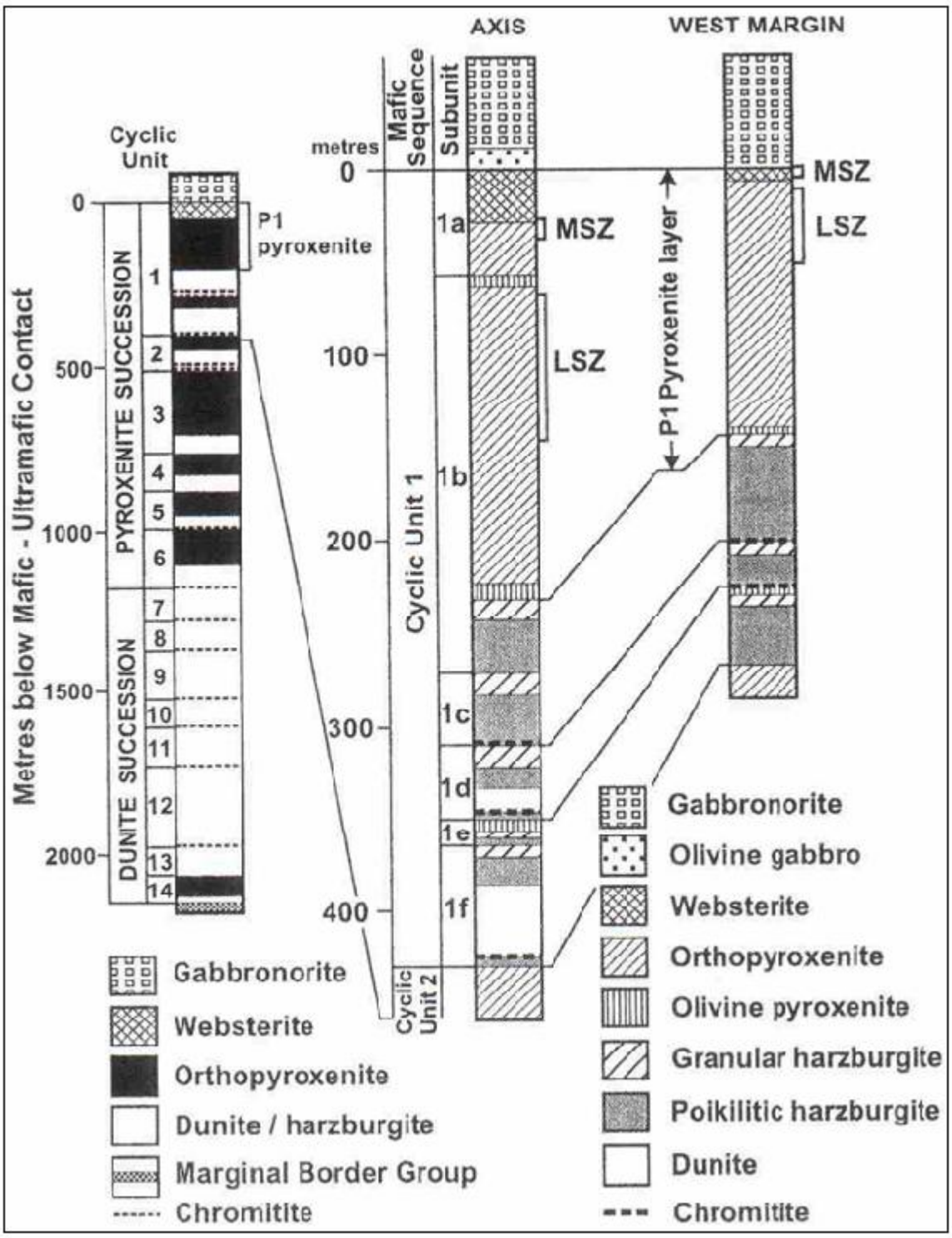

Figure 1.1: Stratigraphy of the Ultramafic Sequence in the Darwendale Subchamber, together with details of cyclic Unit 1 in the axial west marginal facies (Wilson and Prendergast, 2002)

Wilson and Prendergast (2002) point out that structurally, the various rock-types form parallel layers with an overall, doubly-synclinal, boat-like structure defined by both longitudinal and

transverse inward dips. They say that it is on this basis, and because of the style and continuity of ultramafic layering and the structural disposition of the upper mafic erosion remnants, the Great Dyke is subdivided into five principal subchambers, named from north to south the Musengezi, Darwendale, Sebakwe, Selukwe and Wedza Subchambers. Figure 1.2 presents a detailed layout of these five principal subchambers on the Great Dyke.

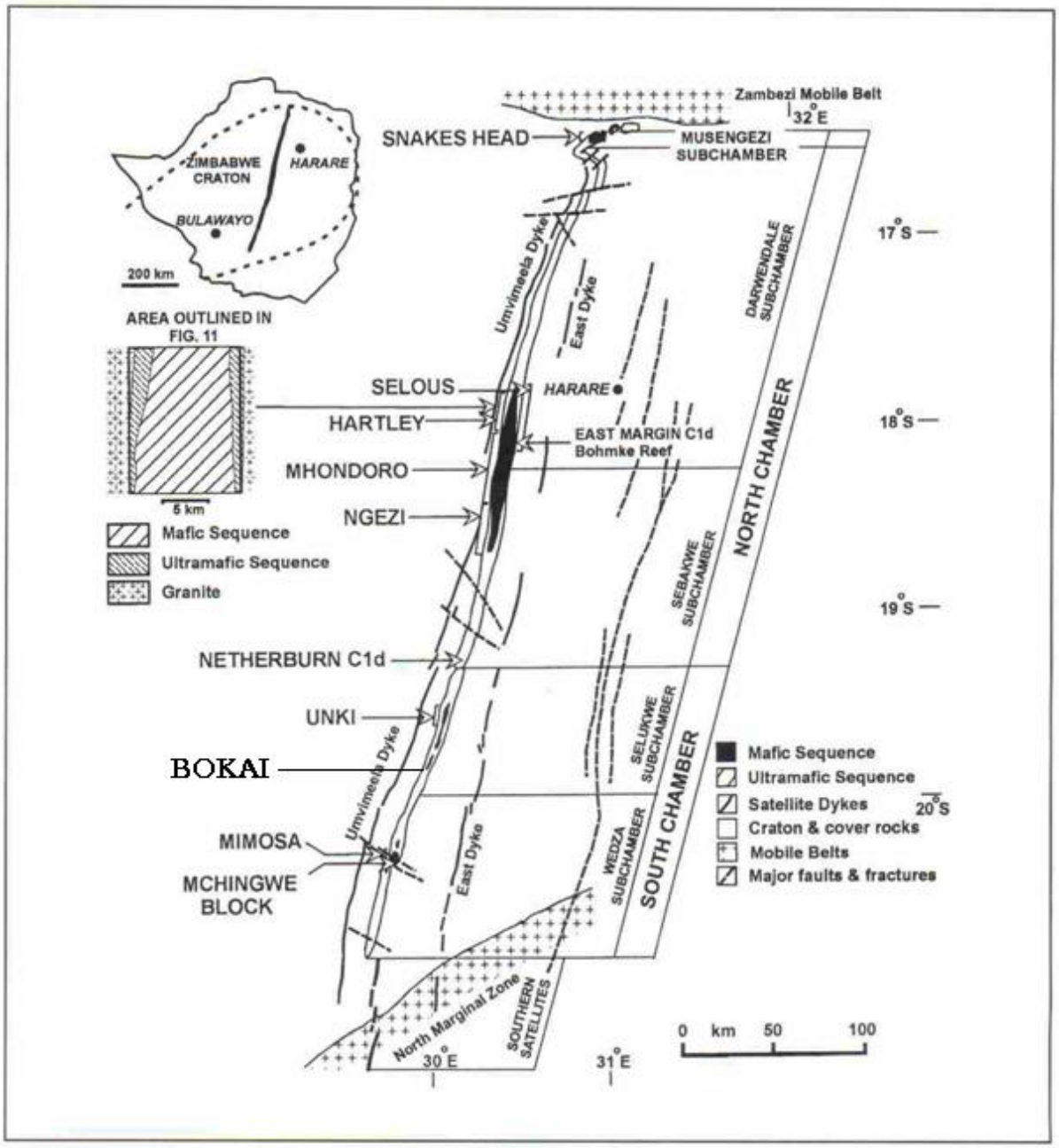

Figure 1.2: Location of the Great Dyke in the Zimbabwe Craton showing chambers and subchambers (Wilson and Prendergast, 2002)

The pointed platinum deposits make part of this research. A quick look at Figure 1.2 shows that the subchambers Wedza, Selukwe, and Sebakwe in the southern chamber are narrower than the subchambers Darwendale and Musengezi in the northern chamber. This shows that more platinum resources are hosted in the Northern Chamber compared to the Southern Chamber. Figure 1.3 gives a simplified version of the layout showing the complexes of economic importance within each chamber. The complexes named from north to south are: Musengezi, Hartley, Selukwe and Wedza Complexes. Platinum resources on the great dyke can last generations and generations hence the need to have a reliable pillar design system in the exploitation of these resources.

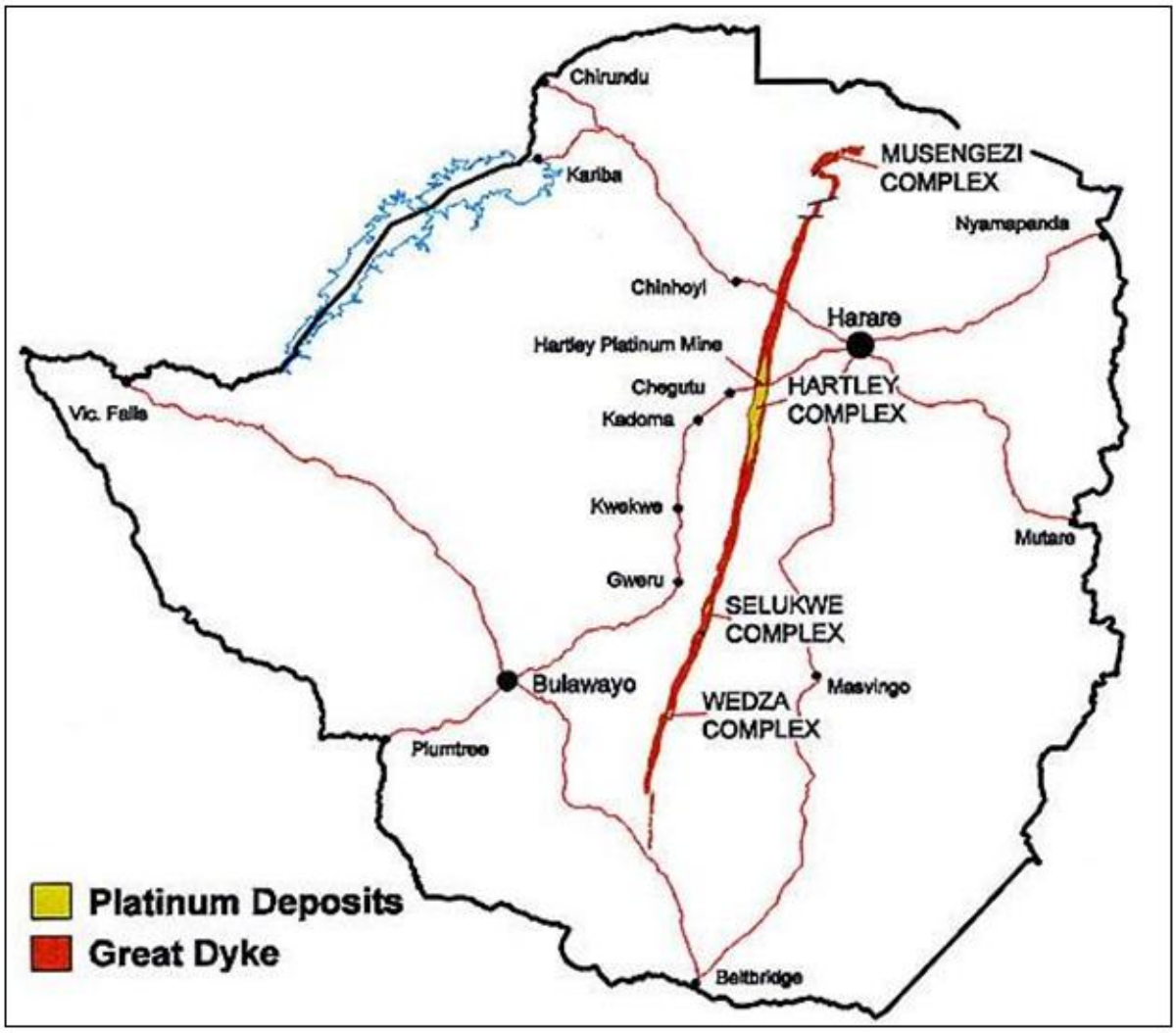

Figure 1.3: Great Dyke Platinum Complexes (Google Maps, 2010)

The distribution of platinum resources in million tonnes along the great dyke is as shown in Figure 1.4 while Figure 1.5 gives the photographic views of the great dyke.

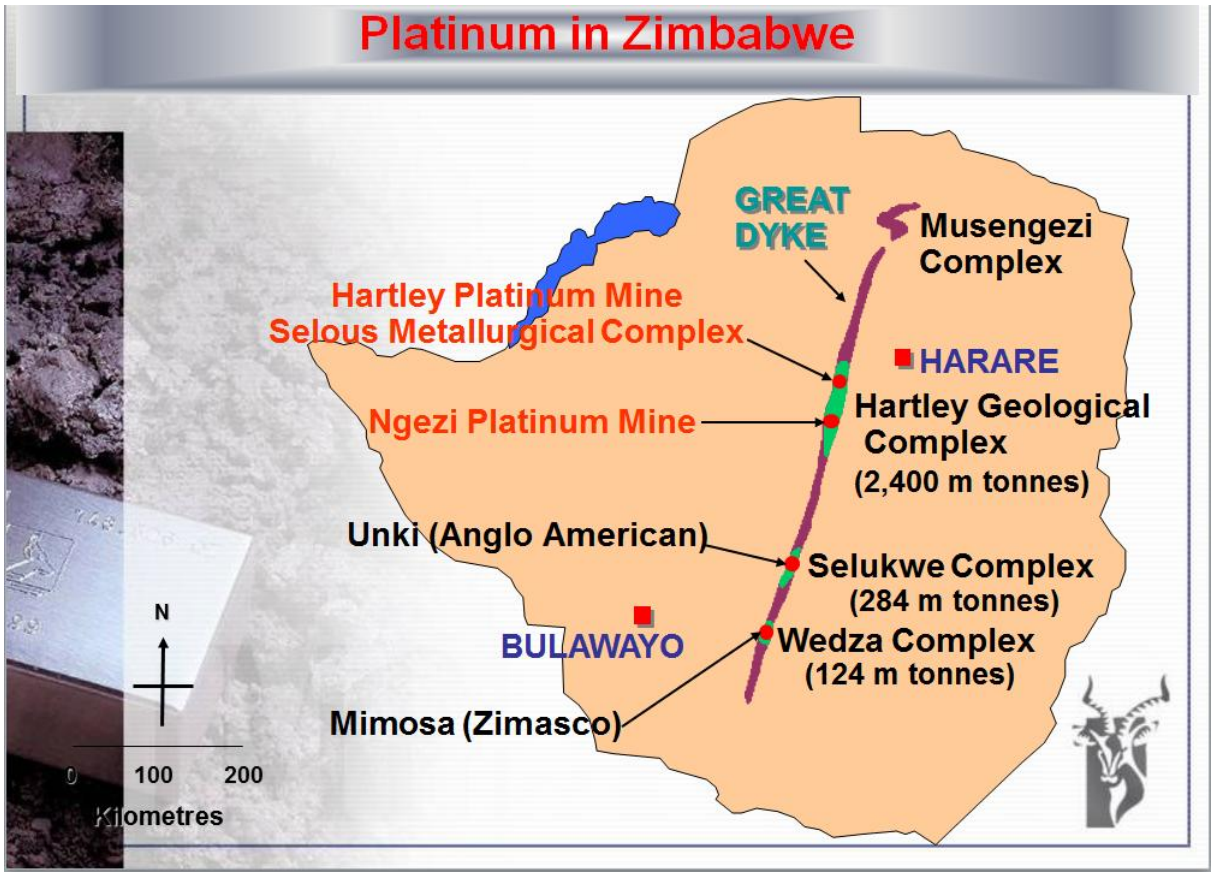

Figure 1.4: The distribution of platinum resources along the Great Dyke (Holding, 2008)

Figure 1.5: Photographic views of the great dyke: (a) aerial, (b) from the ground and (c) sectional view (Holding, 2008)

A high concentration of PGE and sulphide is found in the MSZ distributed vertically. It is this zone which is mined so more information of its structural and geotechnical stability is necessary in the preparation of pillar design systems. Wilson and Prendergast (2002) define the MSZ as a stratabound zone of disseminated sulphide mineralisation located at or just beneath the contact between the thin upper websterite and the thick lower bronzitite which make up the Pyroxenite No 1 Layer. They reveal that geotechnically the MSZ is kept in the same stratigraphic position beneath the upper mafic remnant in each of the five subchambers and it is essentially continuous within each remnant.

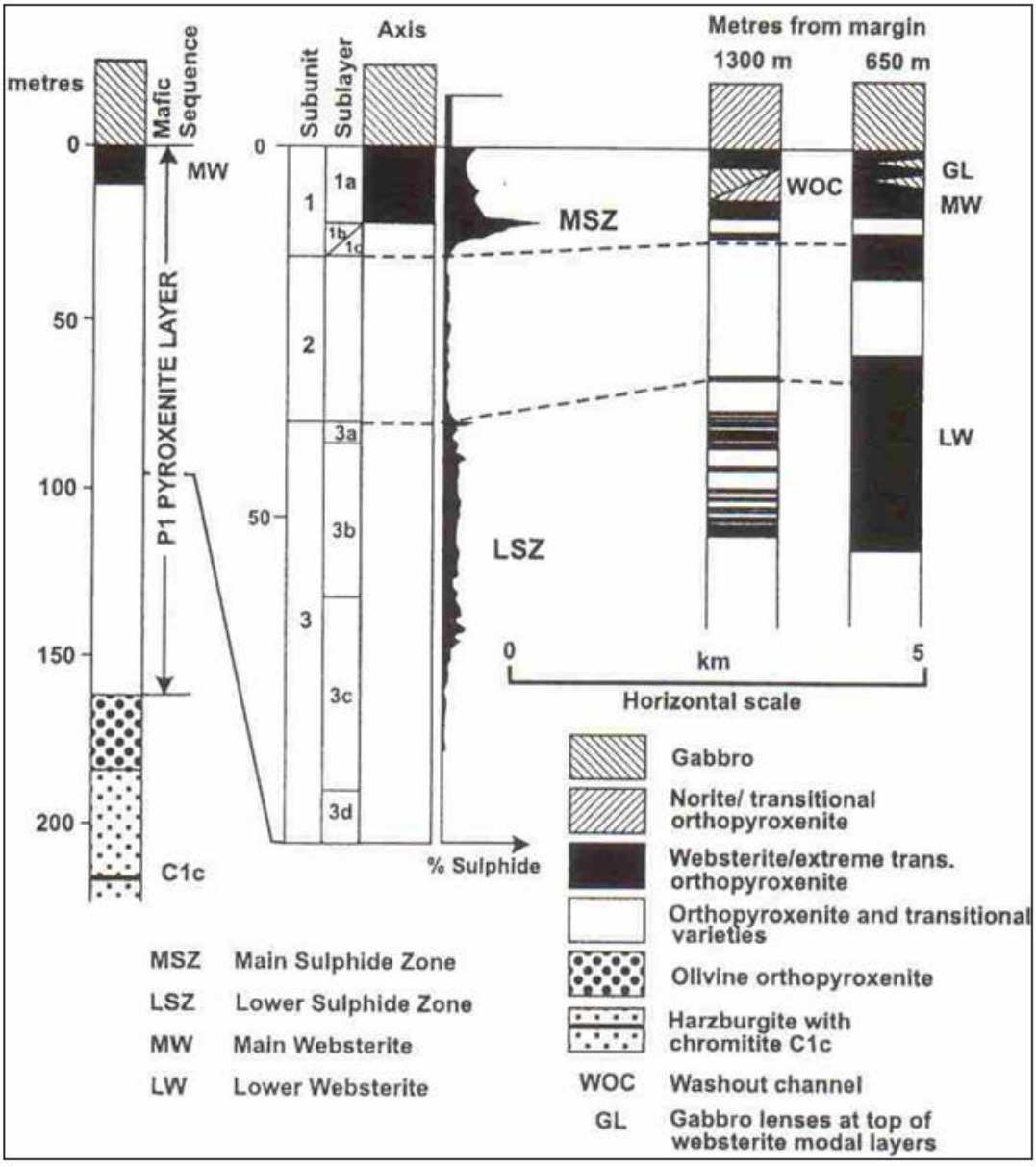

Figure 1.6: Stratigraphy of the P1 Pyroxenite in the Wedza Subchamber showing the transverse variations between the axis and the east margin the locations and general form of the MSZ and LSZ (Wilson and Prendagast, 2002)

The stratigraphy of the Pyroxenite No 1 layer is as given in Figure 1.6. Wilson and Prendergast (2002) indicate that in the narrow subchambers and towards the margins of the wider subchambers the MSZ is 2-3 m thick (and high grade) but up to 20 m thick (and low grade) in the axis of the wider subchambers. The other PGE-bearing zone which is of less economic interest is the LSZ. From their study, Wilson and Prendagast discovered that the LSZ occurs up to 10-60 m beneath the MSZ in all the five subchambers. They say that the LSZ is generally much thicker than the MSZ but contains significantly less sulphide and PGE per vertical metre.

1.3.2 Local geology and geotechnical aspects of platinum mines in Zimbabwe

The depth of great dyke orebody is relatively shallow and does not go beyond 500 m. This gives the platinum mines located on it a geotechnical challenge of large tensile zones extending to the surface. The tensile zones weaken the hangingwall such that the whole column of rock above the hanging wall is subject to collapse so pillar support has to be competent enough to handle this. On a geological note, Prendagast (2009) mentions that the relatively narrow Selukwe and Wedza subchambers are geologically more similar to each other and likewise the subchambers in the Northen chamber share a similar geological setting. He points out that the Selukwe Subchamber, which hosts the Bokai-Kironde Platinum Project as well as Unki mine, is 96 km long and up to 7 km wide and merges southwards with the Wedza Subchamber which hosts the Mimosa mine. A section through the great dyke at the Chironde claims for Bokai Platinum Project is shown in Figure 1.7 while a simplified geological map for Mimosa mine is presented in Figure 1.8.

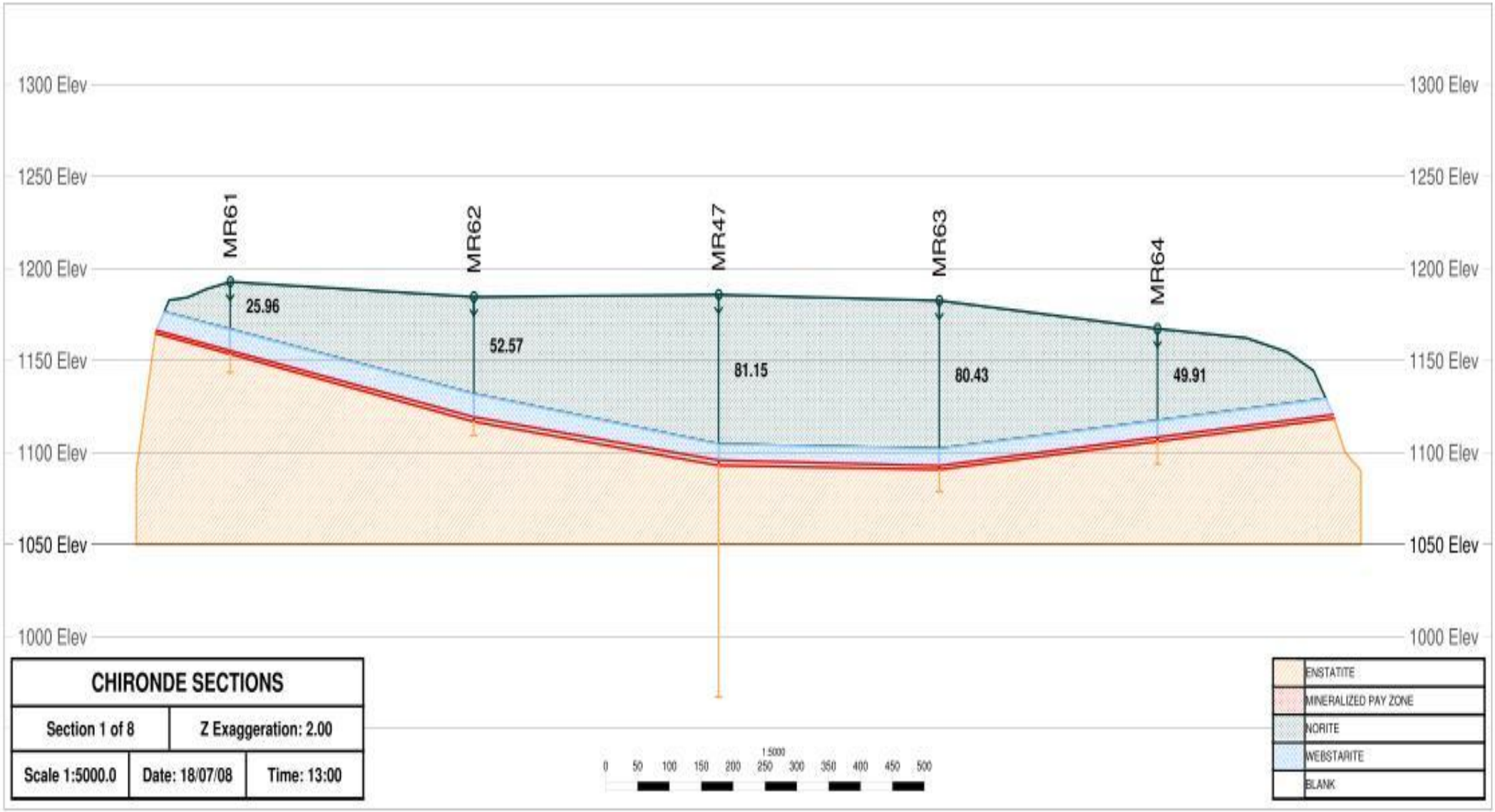

Figure 1.7: Section through the Great Dyke (Chironde Section), looking North: Norite, Websterite, Pay Zone, and barren Enstatite are shown (Todal Mining Geology Data Base, 2008)

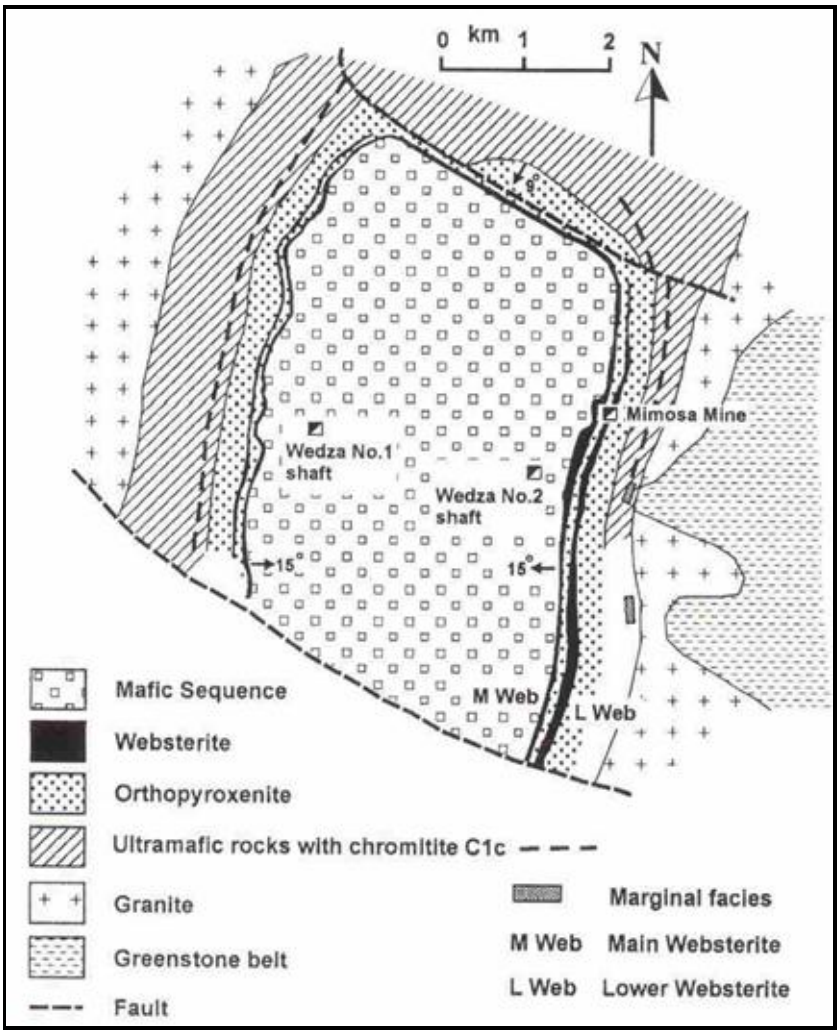

Figure 1.8: Simplified geological map of the Mimosa deposit in the Wedza Subchamber (Prendergast, 1991)

1.4 Bord and Pillar Mining Method in platinum mining

Bord and pillar mining involves the exploitation of mineral resources by making excavations in the ground separated by insitu rock. Except where geotechnical discontinuities like faults do not permit, bord and pillar mines are normally developed on a regular grid base. The existence of geotechnical and geological challenges calls for the modification of the mine layout to avoid pillar failure due to these obvious circumstances. The online Free Encyclopedia (2010) defines the bord and pillar mining method (also called room and pillar mining method) as a mining system in which the mined material is extracted across a horizontal plane while leaving "pillars" of untouched material to support the overburden leaving open areas or "rooms" underground. This encyclopaedia mentions that this method is usually used for relatively flat-lying, horizontal or flat dip deposits (where the country rock and ore are both competent) with inclination not exceeding 15º such as those that follow a

particular stratum. Young (1915) says that room and pillar mining is one of the oldest mining methods. He reveals that no orderly pillar design systems were available in the early days so early room and pillar mines were developed more or less at random, with pillar sizes determined empirically and headings driven in whatever direction was convenient. This approach results in pillar failures as others will be definitely under sized while others are oversized. There is normally a tendency of domino collapse of pillars where the failure of one pillar cascades into a chain reaction failure of pillars. In the present day bord and pillar mining the mine is divided into panels and these panel sections are separated by large pillars called barrier pillars which prevent the collapse in one section to spread to other sections. This way the mine is saved from progressive pillar collapse. However if these same barrier pillars are badly designed then they fail to arrest the chain reaction of pillar failure leaving the whole mine or greater part of it to collapse.

Hustrulid and Bullock (2001) also mention the fact that the selection of optimum pillar size is the road to successful bord and pillar mining. They also realise that if pillars are too large a significant quantity of valuable mineral resource is left behind reducing the profitability of the mine and on the other hand too small pillars are the architects of disaster in terms of pillar failure. To achieve a truly optimum pillar size there is need to have an accurate account of the pillar load and pillar strength. Several factors as discussed in this report have to be considered in determining accurate values of these parameters. Hustrulid and Bullock (2001) put forward that the load bearing capacity of the material above and below the material being mined and the capacity of the mined material itself determine the pillar size. An illustration of bord and pillar mining method is presented in Figure 1.9. In Figure 1.9, C is the pillar centre distance, w is the pillar width and B is bord (room) width.

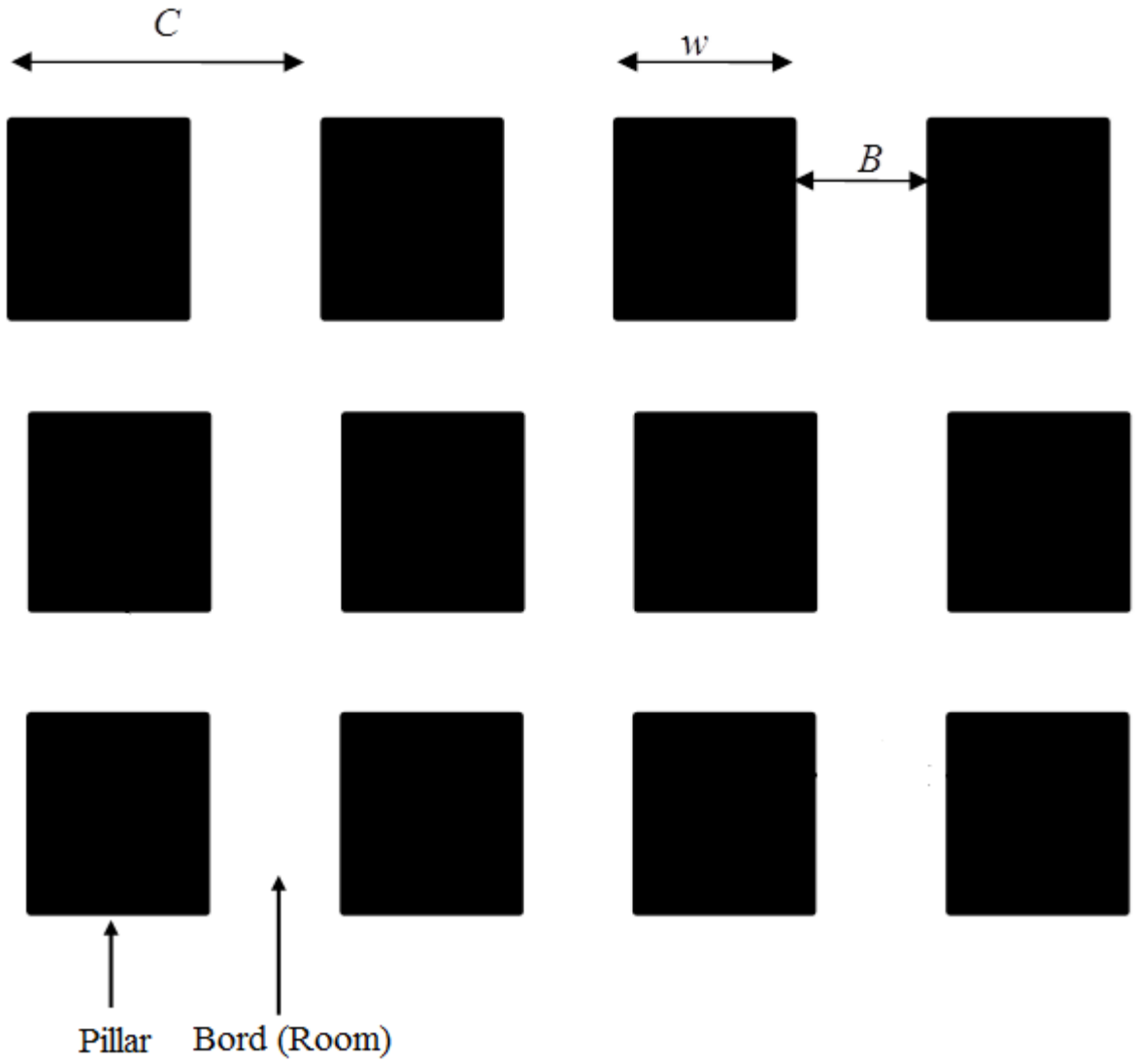

Figure 1.9: Illustration of Bord and Pillar Mining Method (Van der Merwe, 2011 - As modified by student)

1.5 Problem Definition

Evaluation of pillar design systems for low reef platinum mining is crucial if we are to know the inadequacies of the current practice. The determination of the knowledge gap in these systems helps in deciding further work to be done to enhance pillar design accuracy. While it is appreciated that not much empirical research on pillar design for hard rock tabular mine has been done because of rare occurrence of pillar failures, it must be realised that once such failure happens it has far reaching consequences. As such it is imperative to reflect on the work done to date with a view to suggest on further work to be done to improve pillar design accuracy in platinum mines. Successful pillar design revolves around high degree of

accuracy in the determination of pillar load and pillar strength, hence the main focus is on these in this research report.

1.6 Justification of the Research Project

The project had to be done because of the following:

- The need to identify challenges of the current pillar design systems for platinum mining and make necessary improvements thereof.
- To reduce rock support challenges such as heaving and side scaling due to unsound pillar design.
- When pillars collapse, expensive mining machinery and precious human life may be lost in mining sections resulting in gross loss. Coupled to this are the disastrous consequences of subsidence due to underground failure of pillars. Furthermore there are several economic challenges (direct or indirect) which emerge from non-performance of pillars.
- Premature failure of pillars leads to loss of mining sections which may contain high grade ores, hence the need of a competent support system which gives enough time for ore extraction.

1.7 Aims of the Project

The Research Project aims at achieving the following:

- To put forward all possible parameters to be considered in the development of a sound pillar design system so as to reduce uncertainty in the determination of pillar load and pillar strength.
- To increase safety margins in platinum mining so as to prevent equipment and human entrapment and also avoid the serious effects of subsidence.
- To enable the generation of more returns from platinum mining through exploitation of platinum from those sections that contain high grade platinum but experience pillar failure due to uncertainty in pillar design.

1.8 Objectives of the Project

The following are the objectives set to achieve the project aims.

- Utilisation of the student's current knowledge and practical exposure in platinum exploration and platinum mining as an aid to increased accuracy in pillar design.
- To integrate the current pillar design systems to come up with the most appropriate and reliable way of developing pillar design systems.

- Utilisation of Rock Mechanics theory to estimate the optimum excavation dimensions and get the optimum pillar design.
- To classify the relevant rock mass quality of the different stress zones in a project area
- To use rock mass rating to estimate the appropriate pillar design.

1.9 Methodology.

In a bid to come up with an effective and dependable pillar design system methodology for low reef platinum mining to address the aforementioned problems and attain the objectives and aims of the research project the author undertook the following:

- Utilised his current knowledge and practical exposure from a platinum exploration company and established platinum mines to formulate the appropriate pillar design system methodology.
- Carried out extensive literature survey on pillar design systems currently being used for low reef platinum mining and fish out their drawbacks and weak points and then suggested workable refinements which can bring a high degree of certainty.
- Analysed pillar failure patterns against pillar design system used to design them for an established mine so as to identify weak points.
- A geotechnical survey on pillar support layout standards of platinum mine was done to find out if pillar failure is attributable to failure to follow standards or other factors.
- Made use of rock strength tests results on drill core from a large scale platinum exploration project to design bord and pillar layout options using different methods used in practice and assessed them. Rock strength data from a developed platinum mine was also used for illustrative purpose.
- Established the scope of work to be undertaken during the exploration stage of platinum mine so as to give dependable bases for accurate pillar design.

1.10 Content of the Research Report

A review of the literature relevant to this research is presented in the next chapter. The review gives an insight into pillar load and pillar strength determination which are the inputs in determining safety factor. Pillar design theory, pillar types and their current design practises are some of the issues discussed by the author in Chapter 2. Covered also are pillar load, pillar strength and pillar foundation strength determination methods. Chapter 3 evaluates the pillar design systems presented in Chapter 2 and suggest further areas of improvement. The areas of special attention encompass pillar load and pillar strength determination methods,

which are important in safety factor determination. Geotechnical work undertaken by the author at a large scale platinum exploration project is discussed in Chapter 4. The work gives an insight into areas of particular attention in site geotechnical investigation if we are to come up with reasonably reliable pillar design parameters. Amongst the Geotechnical work discussed in Chapter 4 are oriented coal drilling, logging practice, core sampling procedure, laboratory tests and rock mass classifications. Pillar design results for the large scale platinum exploration project using different pillar design formulae presented in Chapter 2 are also discussed in Chapter 4. Pillar design systems as practiced at Platinum Mines Group X as well as a highlight of the inadequacy of these design systems, as currently practiced, are provided in Chapter 5. Conclusions and recommendations of this research are given in chapter 6. Bieniawski (1989) Rock Mass Rating System Table is shown in appendix 1. Appendix 2 gives core photographs of geotechnical boreholes BO53A, BO54A and BO55A selected for presentation in this research report. Geotechnical logs and downhole survey results for boreholes BO54A and BO55A are as given in appendices 3 and 4 respectively.

CHAPTER 2: LITERATURE REVIEW

2.0 Introduction

Since the research endeavours to enhance safety factor accuracy in pillar design through the evaluation of pillar design systems the author saw it critical to look into the following literature. This gives an insight into pillar load and pillar strength determination which are the inputs in determining safety factor. Pillar design theory, pillar types and their current design practises are some of the issues discussed by the author in this chapter. Covered also are pillar load, pillar strength and pillar foundation strength determination methods.

2.1 Pillar Design Theory

While much research has been done on pillar designs for the coal industry following the South African CoalBrook disaster of 1960, little has been done on pillar design for hard brittle rock which includes low reef platinum mining. Up to now no comprehensive pillar design layout for the bord and pillar mining method used in platinum mining has been developed. While pillars seem to be competent at current depth pillar failures with disastrous consequences can be witnessed as depth increases. Martin and Maybee (2000) reveal that mining operations start to encounter rock pillar failure problems as the mining depth increases. However, before a detailed evaluation of the present practice can be given, the current level of literature is presented in this chapter.

Different pillars are used in low reef platinum mining depending on the function the pillar is to serve. In hard rock tabular mining in general a great combination of pillar types is utilised. Spencer (2010) gives these types as Shaft Pillars, Bracket Pillars, Boundary Pillars, Water Barrier Pillars, Barrier Pillars, Crown Pillars, Sill Pillars, and Sequential Grid Mining - Scattered Mining with Dip Pillars, Non Yield Pillars**,** Yield Pillars and Crush Pillars. Salamon (1983) classified these pillars into three main classes which are: support pillars, protective pillars and control pillars. He explains that support pillars are a system of pillars usually laid out systematically to offer support to the undermined hangingwall. According to this classification protective pillars protect surface structures, underground mining excavations or separate one mine from its neighbour while control pillars are those laid out systematically and cut in deep level mines to curb rock bursts by reducing energy release rates.

Of all the mentioned pillars the ones normally used in low reef platinum mining are non-yield pillars, yield pillars, barrier pillars and crush pillars. As such this literature concentrated on these four.

The insitu rock supporting the roof, which is left between openings during mining is referred to as the pillar. Coates (1981) simply defines a pillar as insitu rock between two or more underground openings. Sjoberg (1992a) mentions that it is more practical in mining to define a pillar as portion of rock left only to carry load or reduce deformations in order to maintain stability in the mine. While all efforts are undertaken to cut pillars in less ore bearing zones there is always a need to strike a balance between ore left behind and mining operation stability.

The current pillar design systems are based on empirical determinations of pillar design parameters. This approach relies entirely on the failure of pillars for an empirical pillar design curve to be calibrated. The approach cannot be used for mines outside the empirical range the pillar design is meant for. More of the evaluations are as presented in chapter 3. Several formulas are currently in use to determine pillar strength. For the calculation of load the Tributary Area Theory (TAT) which applies to regular mining layouts is used. Coates (1981)'s method is also used to determine pillar load for large rectangular pillars like regional pillars. Parameters currently accounted for in the design of low reef platinum mining pillars are strength, load, w/h ratio and pillar foundation bearing capacity. Normally w/h ratio is generally used as a first indication of pillar strength. Martin and Maybee (2000) compared extensive data collected from back analysis and concluded that most pillars fail at a w/h ratio of less than 1.5 while there is substantial increase in pillar strength at a w/h ratio of more than 2. Stacey and Page (1986) mention that foundation failure rather than pillar failure can be expected at a w/h ratio of more than 7 provided pillar and foundation material are the same. At width to height ratio of more than 10, pillars are generally considered to be indestructible. Numerical modelling tools are also being utilised to aid pillar design.

2.2 Theory on Pillar Load Determination

2.2.1Tributary Area Theory Method

Pillar stresses are normally calculated using the Tributary Area Theory (TAT), which accounts for the full cover load (Ozbay et al, 1995). Ozbay et al (1995) explain that the theory is used in regular mining layouts of large lateral extents, several times greater than the mining depth and assumes that each pillar in the layout supports an equal amount of load to the surface. This allocates full cover load to each pillar in the layout. Also note that same size pillars must be used in the regular mining layout for the TAT to be applicable. The TAT is commended by Ozbay et al (1995) as it appears to be operationally convenient, leading to

fixed pillar-design dimensions for any given seam material and depth. Roberts et al (2002) consider the TAT to imply the assumption that a pillar carries the full load of the overburden above the pillar itself and half of the surrounding roadway.

The Average pillar Strength can be expressed as a function of extraction ratio as follows:

$$\mathrm{APS} = \frac{\sigma_V}{1 - e} \quad \text{----------1}$$

$\sigma_v = \rho g h$

Where:

APS is the Average Pillar Stress

σ_v is the vertical component of the virgin stress, MPa

e is the areal extraction ratio

ρ is rock density, kg/m^3

g is gravitational acceleration, m/s^2

h is depth below ground surface, m

Brady and Brown (1992) give a simple diagram to explain the calculation of *e* (a = b for square pillars and a ≠ b for rectangular pillars) as shown in Figure 2.1.

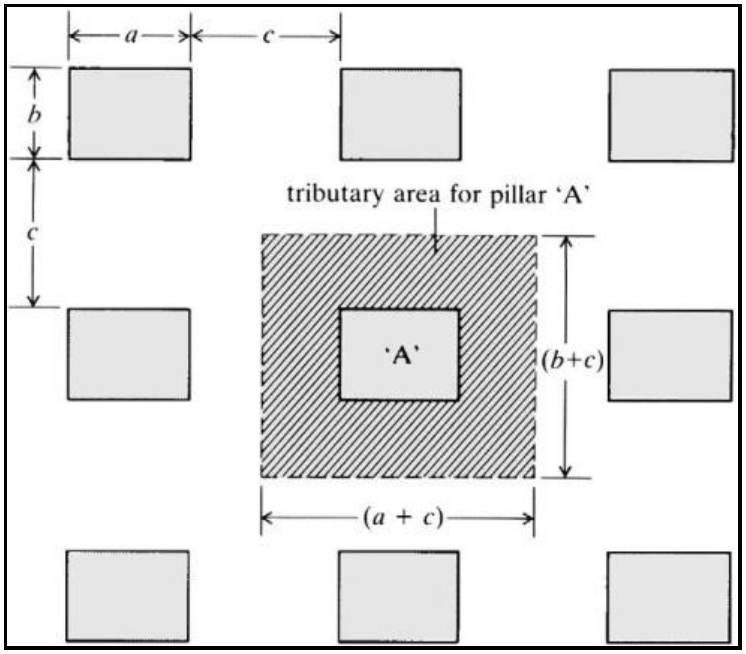

Figure 2.1: Plan showing the geometry for tributary area analysis of pillars in uniaxial loading (Brady and Brown, 1992)

Brady and Brown (1992) gave a formula for calculating extraction ratio using the shown dimensions as follows:

$$e = \frac{(a + c)(b + c) - ab}{(a + c)(b + c)} \quad \text{----------2}$$

Looking at the diagram it can be noticed that the formula can then be stated as

e = [Pillar base area / (Pillar base area + Pillar tributary area)]

Ryder and Jager (2002) also suggested the cross sectional view given in Figure 2.2 for the calculation of extraction ratio.

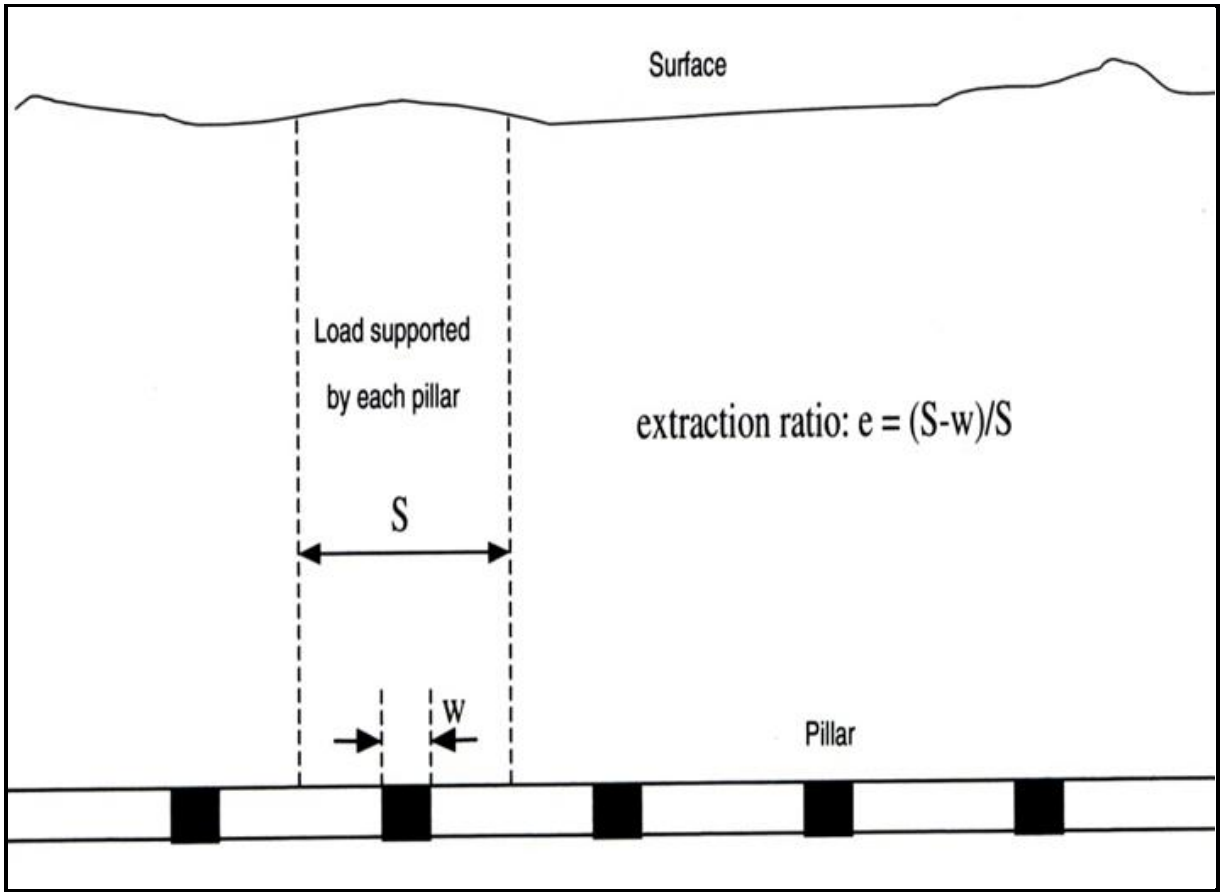

Figure 2.2: Vertical Section for the calculation of extraction ratio (Ryder and Jager, 2002)

Hoek and Brown (1980) came out with the tributary area theory for calculating stress for square pillars. The formula was driven using the diagram in Figure 2.3.

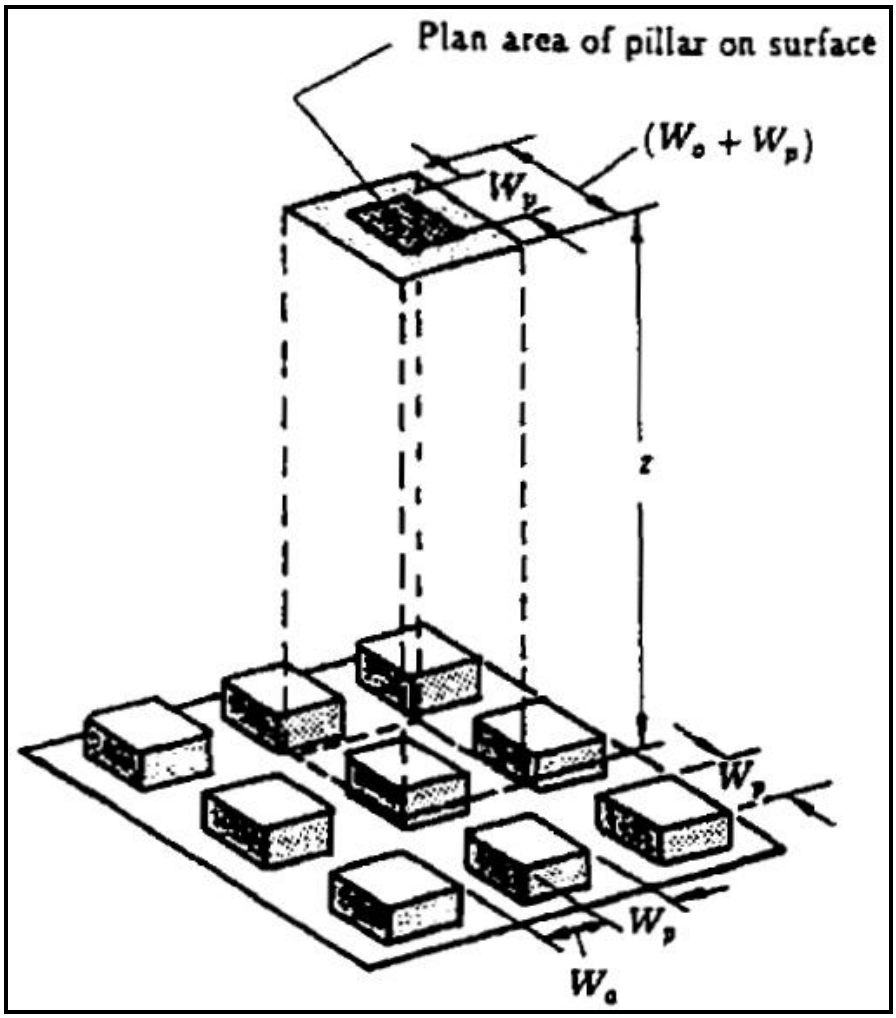

Figure 2.3: Tributary area theory for square pillars (Hoek and Brown, 1980)

From this layout they deduced the formula for calculating average pillar stress as:

$$APS = \sigma_v \left(1 + \frac{W_0}{W_p}\right)^2 \quad \text{----------3}$$

Where:

APS is the Average Pillar Stress,

σ_v is the vertical component of the virgin stress, MPa

W_0 is the excavation width

W_p is the pillar width

2.2.2 Coates Method

Coates (1981) brought up his formula for load calculation after realising that while the Tributary Area Theory can be utilised, it is insufficient since it does not consider geometrical and rock properties in its formulation. He went on to consider these parameters in the

formulation of his formula. Coates (1981) admitted that his formula is only applicable in the centre of the mining area with undisturbed long rib pillar and in situations where mine span does not exceed half of depth. The formula built up by Coates (1981) which is applicable for calculating pillar load in deep and long mining zones is as detailed below:

$$APS = \sigma_v \, x \quad 1 + \frac{2e \;\; 1 + h_s \;\; - kh_s(1 - w + w_p n)}{h_s n + 2 \;\; 1 - e \;\;\; 1 + h_s \;\; + \frac{2eb(1-w)}{\pi}} \quad ----------4$$

$$e = \frac{B_o}{B_{o+B_P}}, \quad k = \frac{\sigma_h}{\sigma_v}, \quad w = \frac{\nu}{1-\nu}, \quad w_p = \frac{\nu_p}{1-\nu_p}, \quad n = \frac{E(1-\nu_p^2)}{E_p \;\; 1-\nu^2}, \quad b = \frac{B_P}{L}, \quad h_s = \frac{H}{L}$$

Where:

APS is Average Pillar Stress

σ_v is vertical component of the virgin stress, MPa

e is the areal extraction ratio

H is height of stope, m

σ_h is the horizontal component of the virgin stress, MPa

k is the general expression for k-ratio

w k-ratio for abutments

w_p k-ratio for pillars

n is a simplifying expression relating Poisson ratio and Young Modulus

b is pillar width to extraction span width ratio

h_s is height of stope to extraction span width ratio

υ is Poisson's ratio for abutments

υ_p is Poisson's ratio for pillars

E is Young's Modulus for abutments

E_p is Young's Modulus for pillars

B_o is room width, m

B_p is pillar width, m

L is width of extraction span, m

It is evident from the formulation of both TAT and Coates Methods that they do not consider both overburden stiffness and seam stiffness. These play a pivotal role in determining pillar load as discussed in section 3.1.2 of this research report.

Note: Coates' method reduces to the usual TAT when L → infinity as shown in the calculation below:

When L → infinity, b = 0 and $h_s = 0$ such that

$$APS = \sigma_v \, x \quad 1 + \frac{2e \;\; 1 + h_s \;\; - kh_s \;\; 1 - w + w_p n}{h_s n + 2 \;\; 1 - e \;\;\; 1 + h_s \;\; + \frac{2eb \;\; 1 - w}{\pi}} \quad ----------5$$

$$APS = \;\; \sigma_v \, x \quad 1 + \frac{2e \;\; 1 + 0 \;\; - 0}{0 + 2 \;\; 1 - e \;\;\; 1 + 0 \;\; + 0} \;\; = \sigma_v \times \;\; 1 + \frac{2e}{2 - 2e} \;\; = \sigma_v \;\; \frac{2 - 2e + 2e}{2 - 2e}$$

$$= \sigma_v \;\; \frac{2}{2(1 - e)} \;\; = \frac{\sigma_v}{1 - e} \quad \text{(Which is the same as equation 1)}$$

Coates (1981) mentions that his formula considers geometrical (layout) and rock characteristics given below:

- the span of the mining zone with respect to its depth (L),
- height of the pillars (H),
- pillar locations within the mining zone,
- horizontal stress (σ_v) and
- modulus of deformation of the pillar and wall rock materials (E_p and E respectively).

2.2.2.1 Comment on Coates Method

While the rock properties are expected to be the same for the pillar and the abutments since they are of the same material, Coates (1981) differentiated them in cognisance of practical conditions. Abutments have sharp edges on which there is stress concentration as compared to the pillars. This difference in stresses acting on pillars and abutments brings about the difference in the elastic modulus and Poisson ratio for the two.

2.2.3 Numerical Modelling

This is a modern tool which has been relied on for simulating rock behaviour of late. Different types of packages can be used to model pillar loading system environments to give a picture of the load on pillars. The modelling package to be used depends on the type of problem at hand. Some of the softwares available for numerical modelling are Examine2D, Lamodel, Phase2, FLAC, UDEC and MAP3D. Each package has its own limitations and assumptions which the user needs to be aware of. As an example, Hoek et al (1997) point out

that two dimensional models like Examine2D assume that pillars are actually rib and their out of plane length is significantly longer than their width. Each of the softwares either uses the Distinct Element, Finite Difference, or Boundary Element solutions or uses a combination. These solution codes enable 3D stress-strain analysis packages to compute stresses, strains and displacements around three dimensional excavations in tabular orebodies. As an example, Besol Manual (1997) informs that some boundary element based modelling packages use a special form of boundary element code called displacement discontinuity modelling to replace excavation geometry by thin slits of irregular shape modelling the rock mass as a homogeneous isotropic, linear elastic body. However the use of numerical modelling to simulate rock behaviour requires knowledge and expertise from the user. It is of vital importance to emphasise that the user needs to know the limitations and assumptions of each package if they are to get a meaningful interpretation of the model results.

2.3 Theory on Pillar Strength Determination

There are vast issues that the current formulae used to determine hard rock pillar strength do not address. Most of the strength formulae developed for hard rock pillars have an empirical base. They were proposed after studies from different mines using failed pillar information in the data base of those mines. The formulae take the power form or linear form but have a common aspect of considering the w/h ratio of the pillars under study. The forms of the pillar strength formulae are as given in equations 6 and 7.

Power $$\sigma_s = K\, w^{\alpha}/h^{\beta} \quad ----------6$$

Linear $$\sigma_s = K\ \ A + B\frac{w}{h} \quad ----------7$$

Where:

σ_s is the strength of a pillar with width w and height h.

K is the adjusted or non-adjusted strength of a unit cube of pillar rock determined statistically or through the use of laboratory test results.

α, β, A and B are constants.

There are several representative coal pillar strength formulae from which the currently used hard rock pillar strength formulae were inspired. These are:

Holland and Gaddy (1956) $\sigma_s = K \ \overline{w}/h \ ----------8$

Holland (1964) $\sigma_s = K \ \overline{w/h} ----------9$

Salamon and Munro (1967) $\sigma_s = K\, w^{0.46}/h^{0.66} ----------10$

*Bunschinger (1876) $\sigma_s = K \ 0.778 + 0.222\frac{w}{h} ----------11$

Bunting (1911) $\sigma_s = 1000 \ 0.70 + 0.30\frac{w}{h} ----------12$

Bieniawski (1968a) $\sigma_s = K \ 0.64 + 0.36\frac{w}{h} ----------13$

*Cited in Du et al (2008)

While there are a lot of factors to consider in calculating pillar strength, rock mass strength of pillar material, the shape and size of the pillar are the three factors which Stacey and Page (1986) put forward as the three factors on which pillar strength depend. They mention that width and height, and gross structural features such as clay bands, faults, and joints are the parameters that define pillar shape and size. These formulae at times overestimate pillar strength even when used to determine pillar strength in fields within their empirical limits, resulting in pillar failure. This is an indication of some inadequacies. However Martin and Maybee (2000) propose that these formulae developed empirically should not be used for w/h ratios of more than 2. What they basically mean is that the formulae should not be used for barrier pillars.

Barrier pillars are considered to be indestructible as their width to height ratio is normally above 10. Stacey and Page (1986) point out that pillar confinement increases with increasing w/h ratio such that at w/h ratios above 5 pillar strength increases rapidly as a result of the confinement in the core of the pillar.

2.3.1 Salamon and Munro (1967)

Some of the formulae used to calculate pillar strength are derived through the adjustment of Salamon and Munro (1967)'s formula. According to Salamon (1999), this formula was developed by Salamon and Munro (1967) after the collapse of the CoalBrook North Colliery in 1960. They studied 125 pillars in the South African coalfields and came up with the following formula for calculating coal pillar strength:

$$\sigma_s = K\, w^{\alpha}/h^{\beta} \quad \text{---------- 14}$$

Where:

σ_s = the strength of a coal pillar

K = statistically determined (through back analysis) strength of a unit cube of coal

w = the pillar width

α, β = empirical constants

h = the height of a pillar

Note: Equations 6-14 are only valid for square pillars. For rectangular pillars an effective width w_e, has to be used in place of w. W_e is calculated as suggested by Wagner (1980) as:

$$w_e = \frac{4A}{C} m \quad \text{---------- 15}$$

Where:

A = Pillar plan area

C = Pillar plan circumference

The data base they used gave them the values 0.46 and -0.66 for the empirical constants α and β respectively.

2.3.2 Hedley and Grant (1972)

The authors used the approach adopted by Salamon and Munro (1967) and the formula they came up with is the one widely used by hard rock mines to design pillars. Their data base consisted of pillar failure statistics for Eliot Lake Uranium Mines in Canada which are hard rock mines. Ozbay et al (1995) mention that the orebody is stratified conglomerates, and hanging and footwalls consist of layered quartzite, argillite, and limestone formations. In their data base, 28 pillars covering depth range from 150 to 1 040 meters were used. Of these pillars, three were considered to be crushed or totally failed while two were taken to have failed partially. The remaining 23 pillars were considered stable. This data base yielded the values 0.5 and 0.75 for the empirical constants α and β respectively. In deducing these exponents a narrow range of w/h ratio of 0.7 to 1.5 was considered. They statistically determined the strength of a unit cube of hard rock to be 133 MPa. Kersten (1984) mentioned that the work by Hedley and Grant (1972) gained much publicity after being popularized by Wagner and Salamon (1979). Hedley and Grant (1972)'s equation is as follows:

$$\sigma_s = 133\frac{w^{0.5}}{h^{0.75}} \quad \text{----------16}$$

Although their equation was initially meant for square pillars Hedley and Grant (1972) later felt that it could also be used for rectangular pillars in their field of study. The rectangular pillars in the Eliot Lake Uranium Mines field were regarded as rib pillars since their length were in the order of 10 times their width. Hedley and Grant (1972) mapped out the relationship between pillar safety factor and pillar performance in their field of study and came out with the graph shown in Figure 2.4.

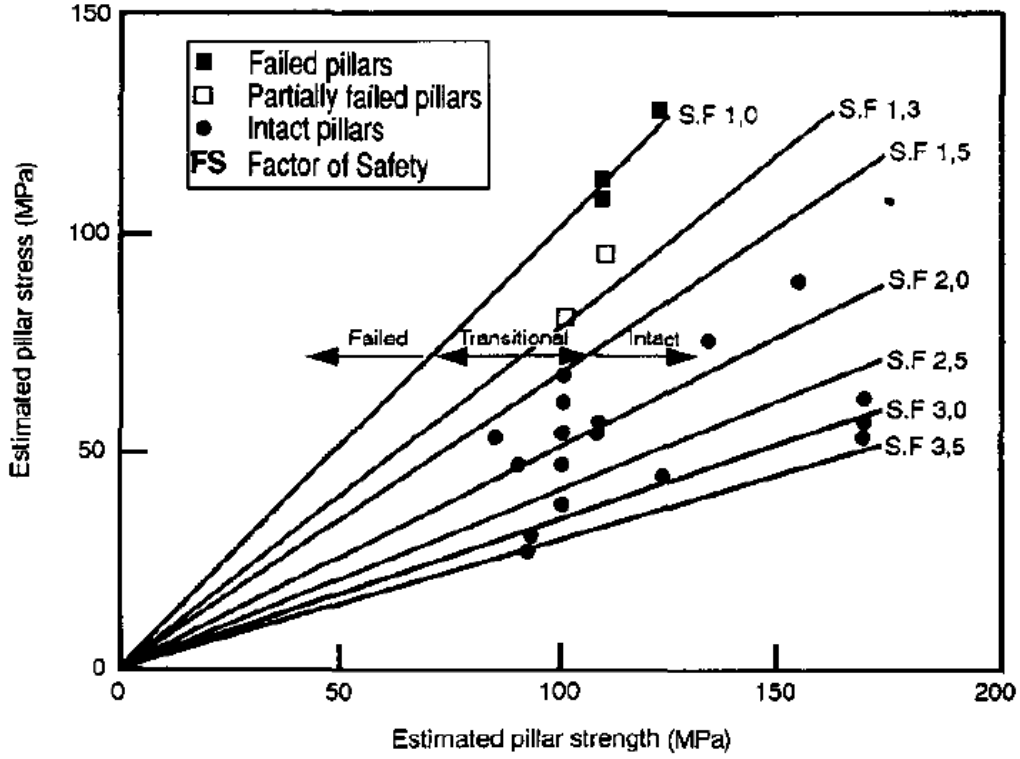

Figure 2.4: Relationship between pillar factor of safety and pillar performance as obtained from Elliot Lake Quirke Mines (Hadley and Grant, 1972)

2.3.2.1 Pillar Stability graphs

These are graphs used to represent pillar data and pillar strength. They are used to give a visualisation of the relationship between pillar stress and pillar width to height ratio. A description of pillar stability graphs is given by Potvin et al (1989) as follows:

"The y-axis of the graph has been chosen to represent a relative index of pillar loading. It is calculated as the ratio of average induced pillar load versus the compressive strength of the intact rock. The x-axis of the chart takes into account pillar shape by plotting the ratio of the pillar width to pillar height. This will account for the increased strength provided by the shape and confinement of the pillar."

Note: On the pillar stability graphs pillars are classified as stable, unstable or failed depending on the level of deterioration. Stable pillars are intact and can withstand the load for which they were developed, unstable pillars are those that have undergone deterioration to the extent that they can fail unpredictably although they can sustain load for some time and failed pillars are those that have completely lost their ability to withstand load.

The pillar stability graph as determined from Hedley and Grant (1972)' equation is as shown in Figure 2.5.

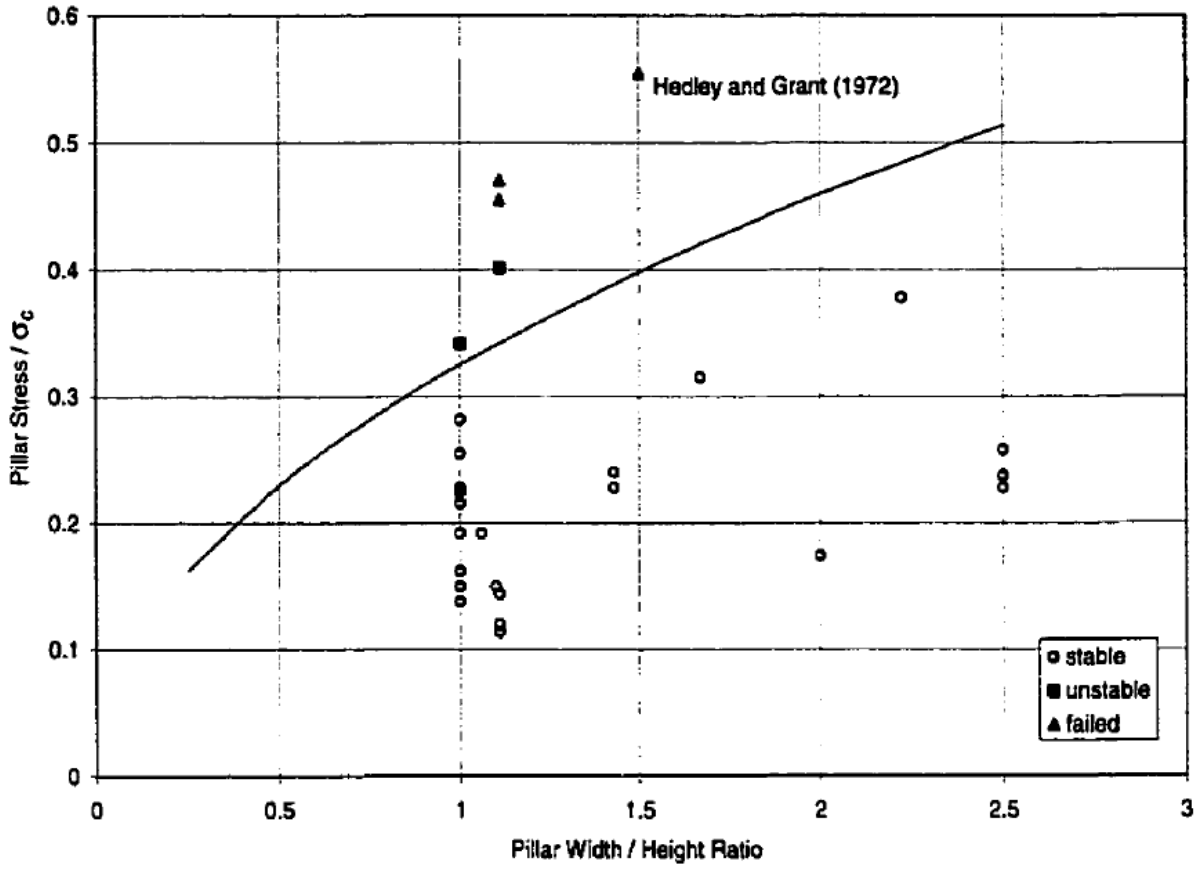

Figure 2.5: Pillar Stability graph for Hedley and Grant (1972)

2.3.3 Potvin et al (1989)

The authors came up with an empirical curve driven from a study of rib pillars in Canadian open stope mines. Since the Hedley and Grant (1972) curve was developed based on the response of smaller pillars, Potvin et al (1989) considers it to be conservative. They consider their pillar strength curve to be less conservative as the response of larger pillars was also incorporated in their data base. Potvin et al (1989) equation is as follows:

$$\frac{\sigma_s}{UCS} = 0.4162\frac{w}{h} \quad \text{----------17}$$

Where:

UCS is the Uniaxial Compressive Strength of the intact pillar rock.

The pillar stability graph for Potvin et al (1989) is as given in Figure 2.6.

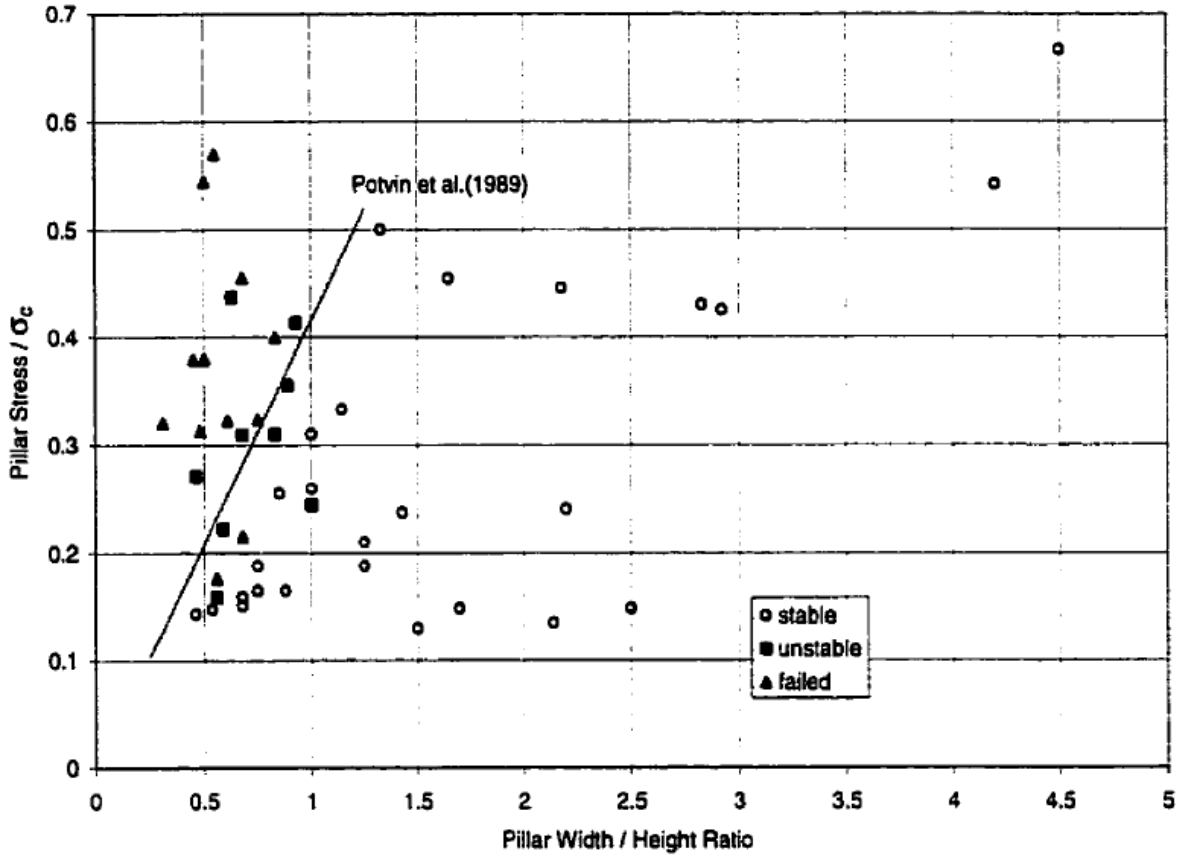

Figure 2.6: Pillar stability graph for Potvin et al (1989)

2.3.4 Von Kimmelmann et al (1984)

Von Kimmelmann et al (1984)'s empirical formula was determined after a study of Selebi Phikwe mines in Botswana. The data base used consisted of 57 massive sulphide pillars of which 47 were square pillars and 10 were long or rib pillars. This data base provided an outstanding opportunity for the three to determine an empirical stability graph as shown in Figure 2.7.

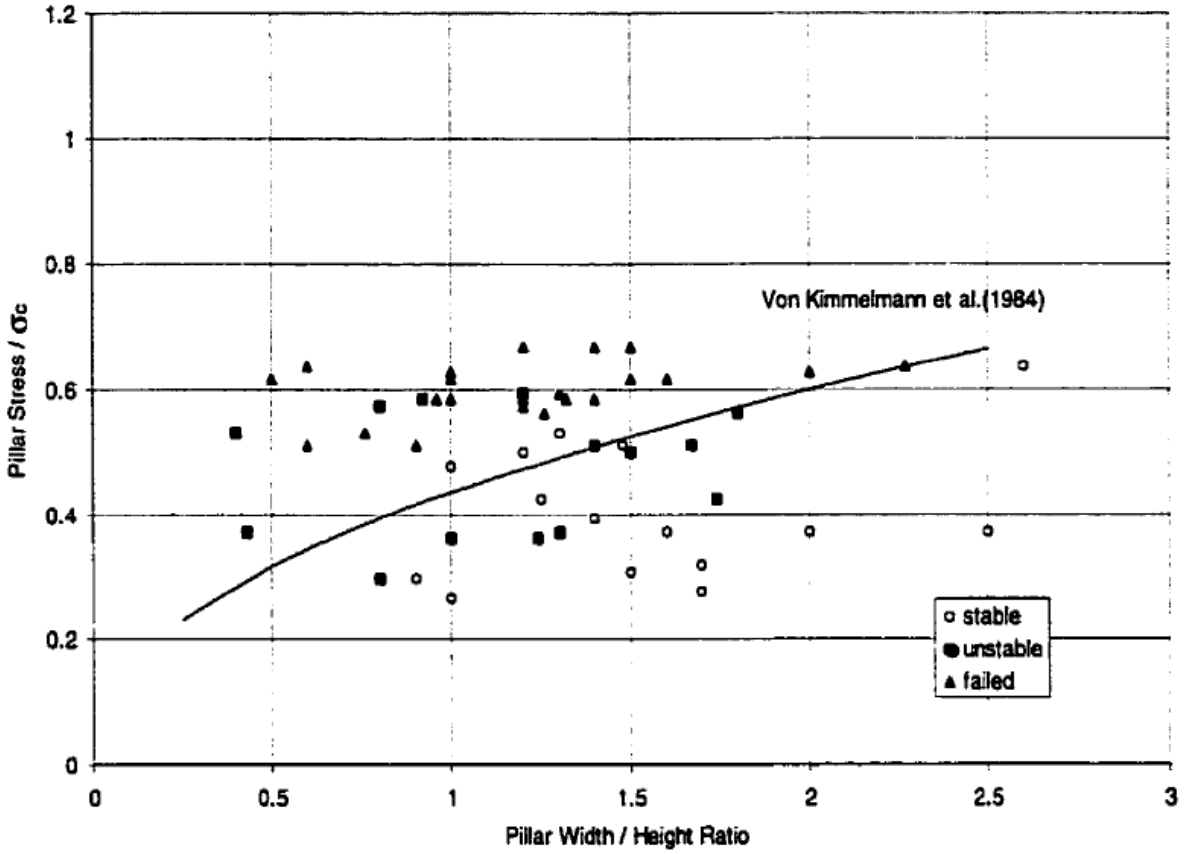

Figure 2.7: Pillar stability graph for Von Kimmelman et al (1984)

The empirical formula developed by them is almost identical to that of Salamon and Munro (1967) with the exception that they statistically determined the value of the strength of a unit cube of rock to be 65 MPa. This value gave them an empirical pillar design curve having a range of safety factor from 1.2 to 1.3. The formula developed by the three is as given below:

$$\sigma_s = 65\frac{w^{0.46}}{h^{0.66}} \quad \text{----------} \quad 18$$

2.3.5 Sjoberg (1992b)

The formula used by Sjoberg (1992b) in his study of pillars at Zinkgruvan Mine in Sweeden takes the form of that suggested by Obert and Duvall (1967) as follows:

$$\sigma_s = \sigma_{pl} \;\; 0.78 + 0.22\frac{w}{h} \quad \text{----------} \quad 19$$

Where:

σ_{pl} is the strength of a pillar with a *w/h* ratio of 1.

The UCS for the rockmass in which Sjoberg (1992b) did his studies was 240MPa. His database consisted of sill pillars. Plotting his results, Sjoberg (1992b) established that 74 MPa was a value for σ_{pl} which fitted his data very well. The pillar stability graph developed by Sjoberg (1992b) is as shown in Figure 2.8.

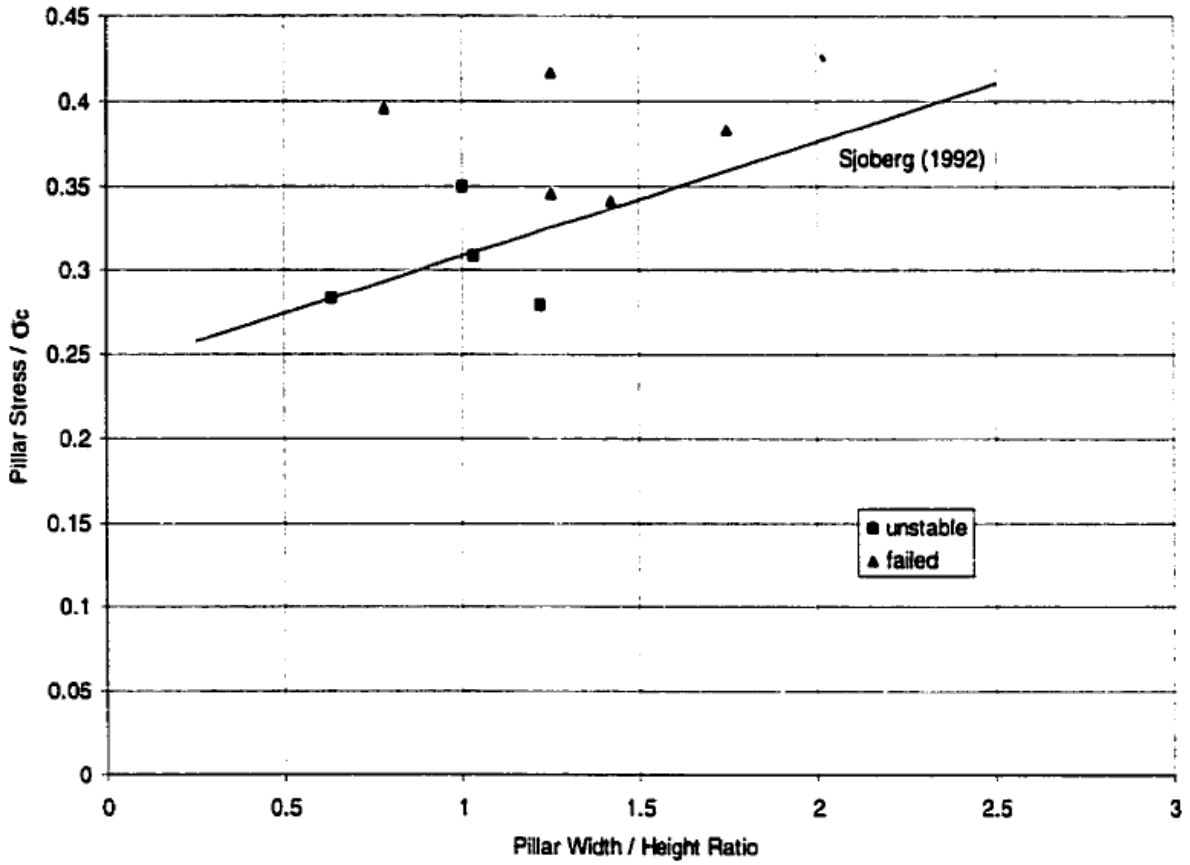

Figure 2.8: Pillar stability graph for Sjoberg (1992b)

2.3.6 Krauland and Soder (1987)

Krauland and Soder (1987) also used the formula suggested by Obert and Duvall (1967) as follows:

$$\sigma_s = \sigma_{pl} \quad 0.78 + 0.22\frac{w}{h} \quad ----------20$$

Equation 19 is differentiated from equation 20 by the difference in σ_{pl} values. Ploting their results, Krauland and Soder (1987) saw that a value of 35.4 MPa for σ_{pl} gave a curve of best fit for their data. The UCS for the rockmass in which they did their studies was 100 MPa. The pillar stability graph as determined by Krauland and Soder (1987) is as given in Figure 2.9.

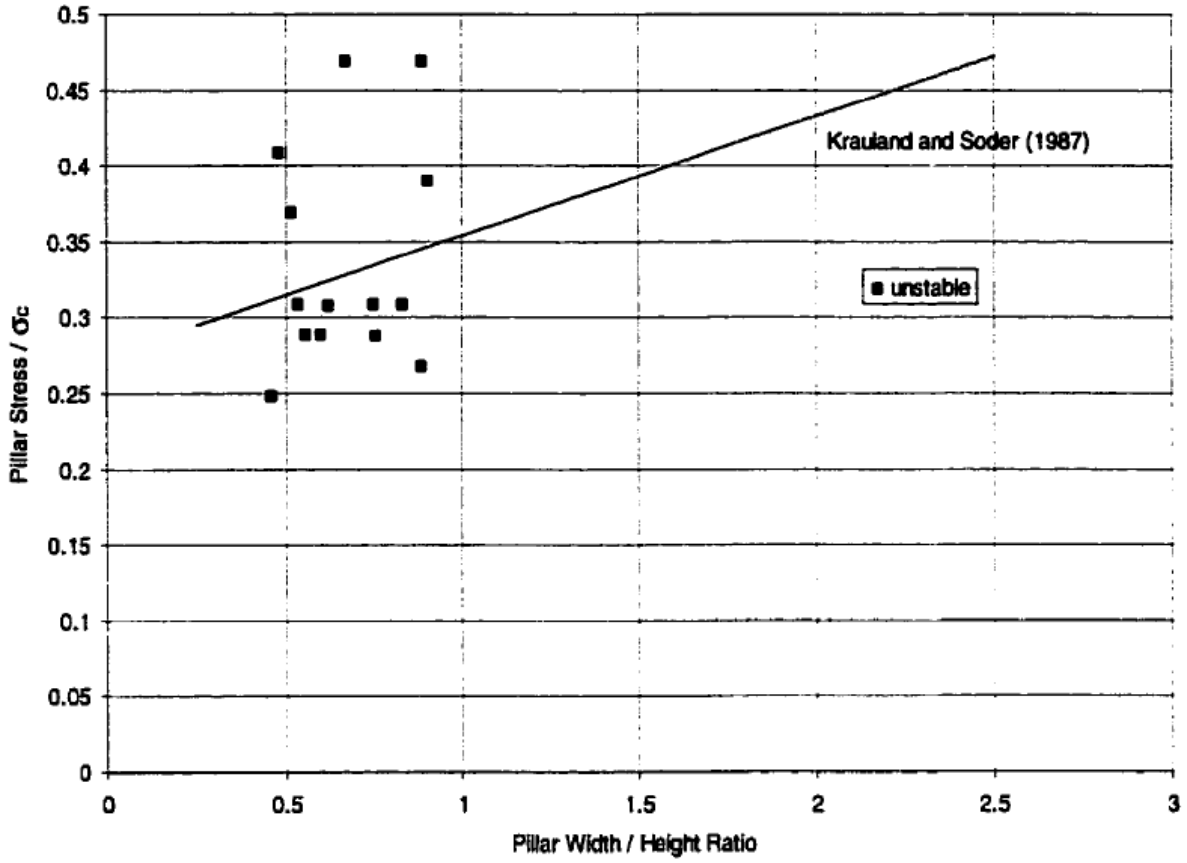

Figure 2.9: Pillar stability graph for Krauland and Soder (1987)

2.3.7 Lunder and Pakalnis (1997)

Lunder and Pakalnis (1997) used a combination of databases from other authors who came before them. The increased data in their data base brought a Greater Statistical Representation of field observations. Some of the databases used include those from Hedley and Grant (1972), Brady (1977), Von Kimmelman et al (1984), Krauland and Soder (1987), Hudyrna (1988), Sjoberg (1992b) and Lunder (1994). Lunder and Pakalnis (1997) came up with a formula to determine pillar strength which considers pillar confinement; as such they called it the Confinement Formula and is given as follows:

$$\sigma_s = \quad K * UCS \quad * \quad C1 + C2 * kappa \quad ---------- 21$$

Where:

K is rock mass strength size factor which Lunder and Pakalnis (1997) averaged at 44%

UCS is pillar material Unconfined Compressive Strength in MPa

Cl, C2 are empirical constants determined to be 0.68 and 0.52 respectively

Kappa is the mine pillar friction term

The formula for calculating kappa is given as:

$$\text{Kappa} = \tan\ \cos^{-1}\ \frac{1 - \text{Cpav}}{1 + \text{Cpav}} \quad \text{-----------------------} \quad 22$$

Where: C_{pav} is average pillar confinement defined as the ratio of average minor stress to average major principal stress at the mid height of the pillar. The formula for calculating Cpav is as given below:

$$C_{pav} = 0.46\ \log\ \frac{w}{h} + 0.75^{\ \frac{1.4}{w\ h}} \quad \text{-----------------------} \quad 23$$

Lunder and Pakalnis (1997) also developed pillar stability graphs for designing pillars using the average pillar stress divided by UCS as shown in Figure 2.10.

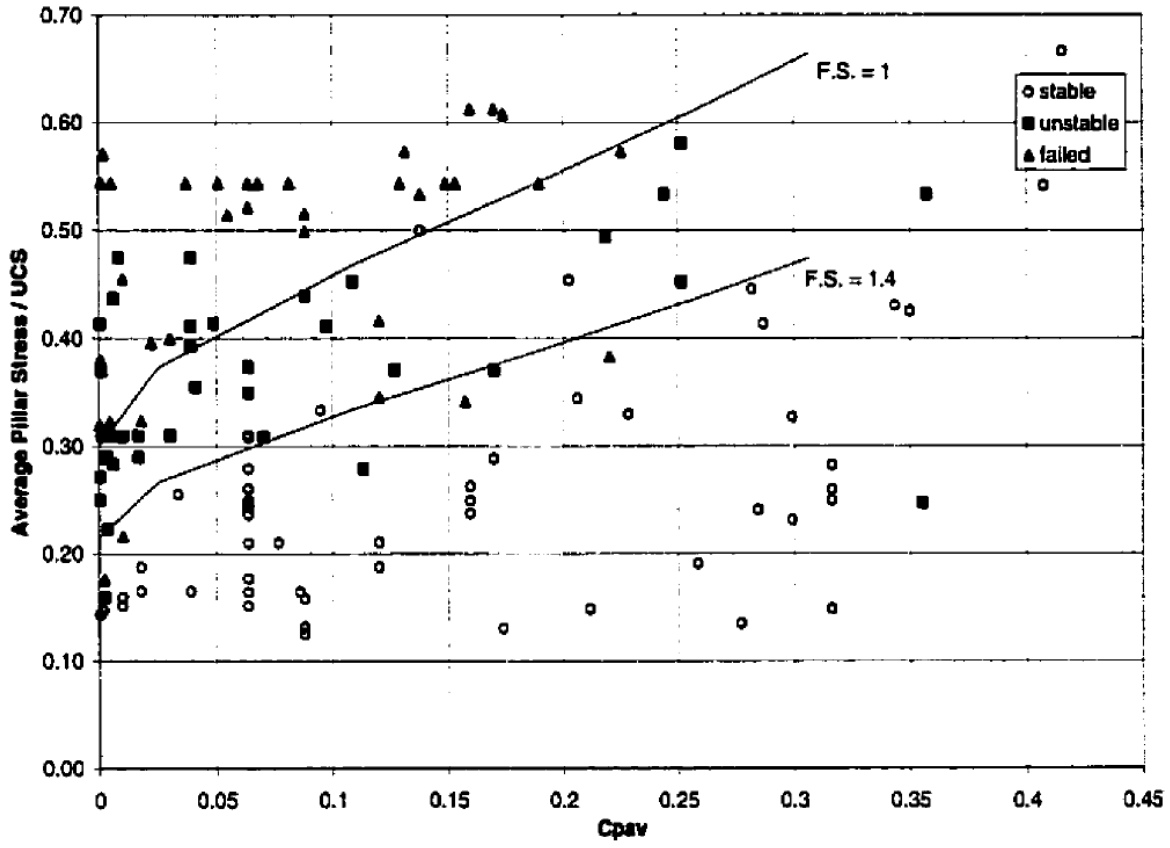

Figure 2.10: Pillar Stability Graph developed using average pillar confinement ((Lunder and Pakalnis, 1997)

They also developed pillar stability graphs using w/h ratios of pillars as shown in Figure 2.11.

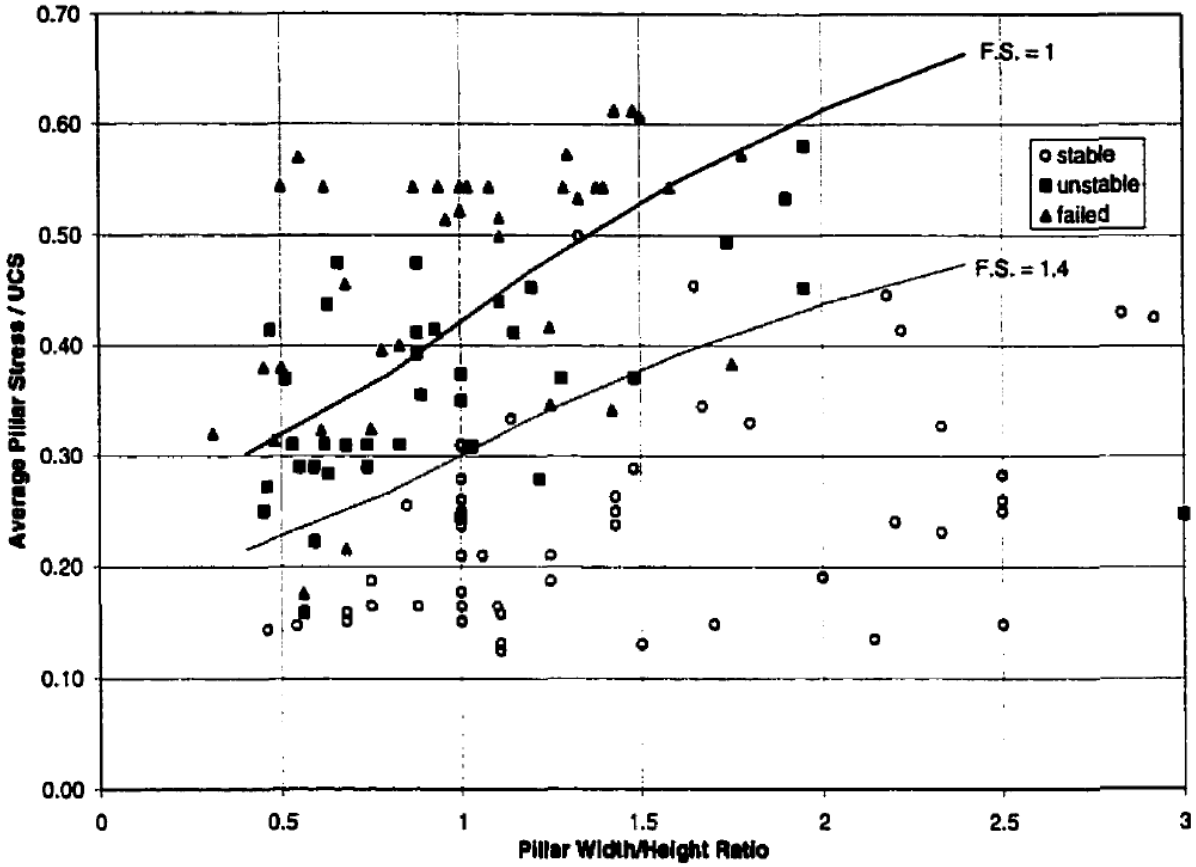

Figure 2.11: Pillar Stability Graph developed using pillar width-to-height ratio (Lunder and Pakalnis, 1997)

2.3.8 Salamon (1982)'s extended formula

In 1982 Salamon extended the formula they had developed for coal pillars with Munro in 1967. This followed after they realised the growing capacity of pillars to carry more load with increasing w/h ratio. The extended formula for calculating pillar strength is as given below:

$$\sigma_s = K\frac{R_0^b}{V^a} \text{ x } \frac{b}{\mathcal{E}} \text{ x } \left(\frac{R}{R_0}\right)^{\varepsilon - 1} + 1 \text{ MPa} \quad \text{---------- 24}$$

$V = W_{eff}^2$ x h,

$R = \frac{W_{eff}}{H}$

$W_{eff} = 4\frac{A}{C}$ (Defined according to Wagner (1980)'s definition of squat-pillar width)

$= 4\frac{\text{Pilar plan area}}{\text{Pillar plan circuference}}$

Where:

R_o is the critical width-to-height ratio ($R_o = 5$)

ε is the rate of strength increase (2.5)

a is 0,0667 (as determined by Madden, 1991)

b is 0,5933 (as determined by Madden, 1991)

V is pillar volume (w_1*w_2*h), m^3

R is pillar effective width to height ratio

σ_s is pillar strength, MPa

K is design rock mass strength, MPa

W_{eff} is the effective width, m

h is height of pillar, m

A is pillar area, m^2

C is pillar perimeter

This formula is known as the squat pillar formula. The validity of this formula was assessed by Wagner and Madden (1984) when they tested sandstone samples in the laboratory. They found that the squat pillar formula produced results in tandem with their laboratory results. Since no pillar with w/h ratio more than 3.75 was known to have collapsed at the time when this formula was established, the value of R was taken to be 5 by Salamon and Wagner (1985). Madden et al (1998) reveal that although ε could be taken as 2.5 a realistic estimate was difficult to determine for it. For hard rock mines the same formulae can be used in designing barrier pillars provided that the w/h > 5 since this is the criterion for using the squat pillar formula.

2.4 Determination of Foundation Strength

Too small pillars result in higher stresses while large pillars like barrier pillars impose much force on their foundations, hence the need to strike a balance to achieve optimality. For the latter case, if the foundation is weak then these pillars would punch into the foundations. It is therefore necessary to know the foundation strength when designing pillars especially the barrier pillars. Jager and Ryder (1999) refer to regional pillars as those pillars with a w/h ratio greater than 10 or more and fail by punching the foundation on which they stand rather than failing through crushing on their own right. They proposed a design criterion for barrier pillars as given below:

Design APS $\leq f_a$ x UCS of the weakest foundation strata

Either the UCS of the footwall or hanging wall material is used. It is the weakest value amongst these two which is used with the design criterion. It can easily be noticed that this

approach is meant to build some conservatism in the criterion there by not overestimating the design APS. The COMRO (1988) point out that f_a is an empirical factor which is typically taken as 2.5. As noticed by Jager and Ryder (1999), friction, dilation properties and presence of weak layers are not accounted for by this criterion.

Terzaghi (1943) and Hansen (1970) developed formulae for calculating foundation strength as outlined below.

2.4.1 Terzaghi (1943)'s Formula

Terzaghi (1943) developed his formula after observations on soil bearing capacity. Stacey and Page (1986) mention that Terzaghi's formula is the most widely used formula for determining the bearing capacity of foundations. They present the formula as outlined below:

$$q_u = cN_c + qN_q + \gamma B_p N_\gamma \quad ---------- 25$$

$$N_\gamma = 1.5\ (N_q - 1)\ \tan\phi \quad ---------- 26$$

$$N_c = (N_q - 1)\ \cot\phi \quad ---------- 27$$

$$N_q = e^{\pi \tan\phi} \tan^2\left(\frac{\pi}{4} + \frac{\phi}{2}\right) \quad ---------- 28$$

Where:

q_u is foundation strength, MPa

c is cohesion of foundation rock

B_p is foundation depth

ϕ is internal friction angle of foundation rock

Stacey and Page (1986) explain that q (MPa) is a parameter which is normally zero unless the failure is likely to take place in a weak bed some distance below or above the floor or roof contact while N_c, N_q and N_γ are bearing capacity factors which depend on the angle of friction of the foundation material.

2.4.2 Hansen (1970)'s Formulae

The work of Hansen (1970) considered different shapes of pillars since shape is a parameter that affects bearing capacity of foundations. The bearing capacity equations he proposed were an extension of the earlier work of Meyerhof between 1951 and 1963. In the formulation of his equations for determining pillar foundations bearing capacity Hansen (1970) considered Terzaghi'formula and made changes of his own. Bowles (2002) brings to light that Hansen (1970)'s equations allow any D/B (Depth of base/Width of base) so they can be used for both

shallow footings and deep bases. The equations developed by Hansen (1970) are as outlined below:

Rib Pillar $$q_u = cN_c + 0.5\gamma B_p N_\gamma \quad ---------- 29$$

Rectangular Pillar $$q_u = cN_q S_q \cot\phi + 0.5\gamma B_p N_\gamma S_\gamma - c\cot\phi \quad ---------- 30$$

Square Pillar $$q_u = cN_q(1+\sin\phi)\cot\phi + 0.3\gamma B_p N_\gamma S_\gamma - c\cot\phi \quad ----- 31$$

$$S_\gamma = 1 - 0.4\frac{B_p}{L_p} \quad ---------- 32$$

$$S_q = 1 + \sin\phi \text{ x } \frac{B_p}{L_p} \quad ---------- 33$$

Where:

B_p is pillar width

L_p is pillar length

γ is specific weight in MN/m^3 and is allocated a positive sign for floor rock and negative sign for roof rock

S_γ is a factor depending on the shape of the pillar

S_q is a factor depending on the shape of the pillar

2.4.3 Comment on Terzaghi (1943) and Hansen (1970)'s Formulae

Stacey and Page (1986) point out that Salamon (1982)'s effective width can be used for pillar width in Terzaghi's formula. Smith and Smith (1998) mention that the bearing capacity of a foundation is calculated by dividing the foundation strength attained using Terzaghi (1943) or Hansen (1970)'s formulae by a safety factor. They say that the value of SF is usually not less than 3 for relatively unimportant structures and for important structures it can go as high as 5. Hedley (1976) states that regional pillars are important structures in a mine and therefore their SF can be taken as 4.5.

2.5 Theory on different pillar types used in shallow platinum mining

The study done by Ozbay et al (1995) on pillar systems as practiced in shallow hard rock tabular mines in South Africa showed that there are basically four types of pillars in use for shallow mining practice. The types they identified are non-yield, crush, yield and barrier pillars. Ozbay et al (1995) summarised the operational characteristics of these pillars as given in Figure 2.12. The depths at which the different pillars can be used are as shown in Figure 2.13.

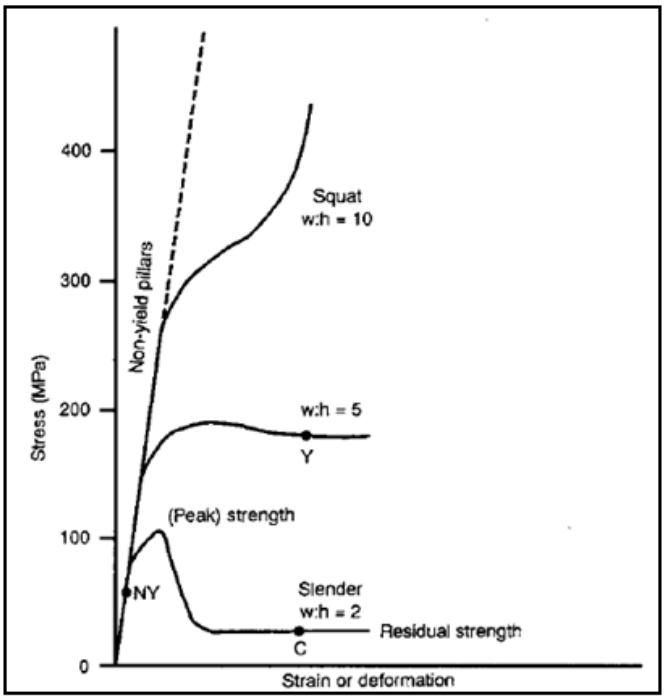

Figure 2.12: Typical stress-strain behaviour of hard rock pillars of different width-to-height ratios. Typical operating points are shown for NY (non-yield and barrier), C (crush), and Y (yield) pillars (Ozbay et al, 1995)

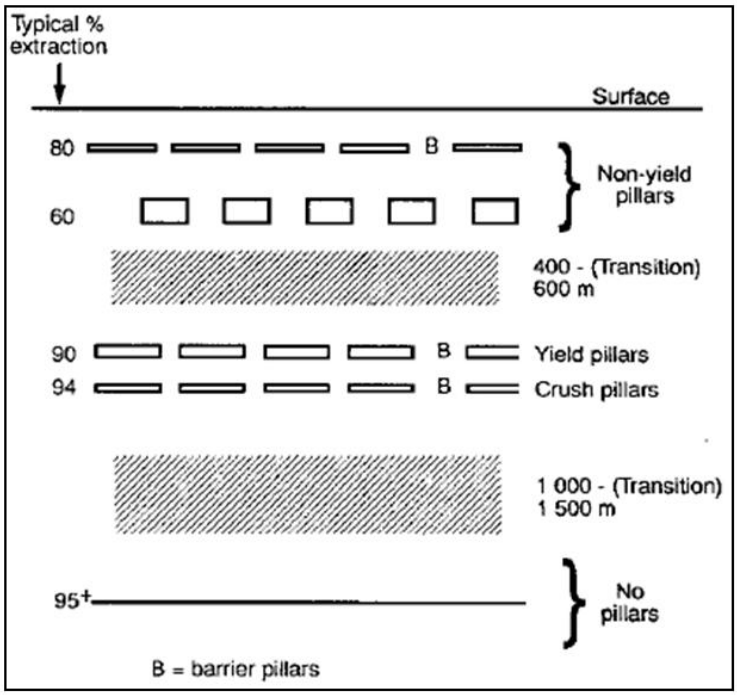

Figure 2.13: Typical pillar-mining systems at different depths, B = barrier pillar (Ozbay et al, 1995)

2.5.1 Non-yield pillars

Non-yield pillars can be defined as that system of rigid pillars that are designed in such a way that they do not fail. These pillars protect surface structures from disastrous consequences of mining subsidence due to underground mine workings. In the underground mining environment itself these pillars ensure mining excavations are safe and open such that neither equipment nor workers are entrapped. Ozbay et al (1995) define non-yield pillars as those pillars which are intended to remain essentially intact and elastic during the life of the mine and have stress/strain characteristics as indicated in Figure 2.12.

Ozbay et al (1995) pointed out that at very shallow depths, the tensile zone in the hangingwall can extend up to surface, and under these conditions the design of pillars is similar to the design of room and pillar systems in coal mining. They say the main consideration is to ensure that the strength of pillars at all times exceeds, by a suitable factor of safety, the maximum average pillar stress (APS) imposed by the coverload of superincumbent strata. The width-to-height (w/h) ratios of these pillars are on occasions as low as 0.7 at very shallow depths, but are usually in the range 2 to 5 and even higher (Ozbay et al, 1995).

2.5.1.1 Current design practice for non-yield pillars

Non-yield pillars are designed in such a way that they do not have to fail during the life of the mine. The strength of the pillar is such that it exceeds the load it carries by a certain percentage, usually at least 50% at the current practice. Most hard rock mines use a safety factor of 1.6 however Ryder and Ozbay (1990) suggest that the safety factor has to be individually selected, and safety factors below 1.3 are not advisable unless regional pillars are well established. Hedley and Grant (1972) formula which was developed after modifying Salamon and Munro (1967)'s formula is used to design non yield pillars. The general form of the Hedley and Grant (1972) formula with different values of K is used. It is represented as follows:

$$\sigma_s = K\frac{w^{0.5}}{h^{0.75}} \quad \text{----------34}$$

Where

σ_s is the pillar strength

K is the strength of a unit cube of rock

w is the pillar width

h is the height of a pillar

Ozbay et al (1995) reveals that there is inconsistence in the selection of a *K* value since in practice the following range is used for K:

$$\frac{\text{UCS}}{3} \leq \text{K} \leq \text{UCS} \quad ---------- 35$$

Where:

UCS is the Uniaxial Compressive Strength

Spencer (2010) makes known that the Hedley and Grant (1972) formula does not consider geological losses and the influence of any oversize pillars. Ozbay et al (1995) point out that the Hoek and Brown (1980) failure criterion is also used to the reef UCS in order to predict the unconfined rockmass strength for good quality rock comprising a pillar. The criterion is given as follows:

$$\sigma_1 = \sigma_3 + (\text{m}\sigma_c\sigma_3 + \sigma_c^2\text{s})^{0.5} \quad ----------36$$

Where:

σ_1 is the rockmass strength

σ_c is the laboratory UCS

σ_3 is the confining stress

m and s are the material constants as described by Hoek and Brown (1980)

When pillar w/h ratio rises beyond 5 there is a swift increase in strength so to this effect a formula developed by Salamon (1982) can be used to calculate pillar strength. This formula was earlier discussed in this research (equation 24) and is known as the squat pillar formula.

2.5.2 Crush pillars

As the mine deepens the tensile zone becomes smaller such that pillars are only needed to support the hanging wall up to the furthest active weak parting unlike near surface where pillars are expected to support the overburden to the surface. Ozbay et al (1995) mention that deeper levels permit the safe use of reduced levels of support resistance like small w/h ratio pillars (w/h < 3) which can provide reduced support resistance in their post-peak residual strength state. They define crush pillars as pillars intended to crush while they are still part of the face, but which have sufficient residual strength to provide the required support resistance to the immediate hangingwall, back at the face and in the back areas. Crush pillars normally

have a width to height ratio of 1.7 to 2.5. The deformation range in which crush pillars yield at their residual strength level was given by Ozbay et al (1995) as shown at point C in Figure 2.12. The residual strength of hard rock crush pillars can be determined using a method suggested by Roberts et al (2005).

2.5.2.1 Current design practice for crush pillars

Empirical studies are used in the design of crush pillars. Ozbay et al (1995) reveal that Cahnbley (1993) points out that the appropriate pillar size is determined by using a size which has proved to be successful in other similar geological situations. Ozbay et al (1995) mention that the initial pillar layout is then adjusted by decreasing the w/h ratio of pillars until sufficient support is provided by the crush pillars. They say that to achieve stable crushing of the crush pillars $2.5 \leq w/h \leq 1.5$. Ozbay et al (1995) indicates that w/h ratios can also be determined based on pillar failure mode while structural weaknesses in a pillar provide the crushing mechanism.

2.5.3 Yield pillars

Yield pillars are pillars which are intended to have a SF > 1 or even SF equal to 1 when first formed, but then yield in a stable manner at stress levels near to peak strength (point Y in Figure 2.12) (Ozbay et al, 1995). As mentioned by Ozbay and Roberts (1988), there exists a zone as we go down depth where the stresses are too high for non-yield pillars to be used and too low for immediate stable crushing of crush pillars. It is in this transition zone where yield pillars are utilised. In practice yield pillars are intact when formed and then are gradually weakened as the load on them increase beyond their load bearing capacity causing them to yield. For the pillars to yield in a stable manner, Ozbay et al (1995) point out that the condition of pillar post-peak stiffness being less than the stiffness of the loading strata has to be satisfied.

2.5.3.1 Current design practice for yield pillars

No much study has also been done for yield pillars since also empirical studies done in other places are the ones used to design yield pillars in areas of similar geological settings. As noted by Noble and Lougher (1993), there is discrepancy between theory and practice where by theoretical studies show that levels of regional or local stiffness render slender hard-rock pillars instable yet practical observations show that stable loading of such pillars can take place at w/h ratios of less than 2.51. To further highlight the inconsistence between theory and practice Ozbay et al (1995) argue that while Spencer and Kotze (1990) suggested that

pillars with w/h ratios ≥ 5 cannot fail in a stable manner, their practical observations witnessed 5x5 m pillars bursting.

2.5.4 Barrier pillars

Panel pillars are separated using regional pillars also known as barrier pillars since they bar the collapse in one panel to spread to other panels which can lead to a pillar run. Regional pillars provide regional stability to the whole mine. Like non yield pillars, barrier pillars are designed in such a way that they have to stand for the entire life of the mine. Given this requirement barrier pillars have to be strong enough to be indestructible in their duty to provide regional stability. Salamon (1974) suggests that a w/h ratio of more than 10 can be chosen to ensure indestructibility of the barrier pillars. However he warns that possibility of foundation failure should be assessed since punching or footwall heaving can occur in highly stressed situations where hanging walls or footwalls are relatively weak. Generally, like all other pillars, where barrier pillars intersect geological weaknesses they have to do so at 90° rather than running parallel to them to ensure minimum possible portion of the pillars are affected by these geological weaknesses. This way pillar instability is reduced. Ozbay et al (1995) mentioned the purpose of leaving barrier pillars as follows:

- to compartmentalize the mining into distinct regions, so that, if a collapse should occur in one region, it will be prevented from spreading into neighbouring stopes.
- to reduce excessive closures and surface subsidences which would otherwise occur in panels supported only by crush pillars.
- to assist in the control of the tensile zone and the prevention of surface subsidence.
- to increase effective strata stiffness substantially so as to reduce the possibility of large-scale instabilities (pillar runs) in stopes supported by non-yield pillars.
- to restrict volumetric stope closures and corresponding seismic energy release potentials.

2.5.4.1 Current design practice for barrier pillars

The squat pillar formula as discussed earlier on is currently utilised by the industry to determine strength of regional pillars. The load is calculated using the tributary area theory. An industrial survey done by Ryder et al (1995) found out that there are mixed opinions with regards to the design of pillars as evidenced by a wide range of barrier pillar designs, sizes and spacings used in the industry. They mention that a conservative rule of thumb, supported

by many theoretical results, used in determining barrier pillar spacing is to keep the span, L, less than about one-quarter of the depth, H, that is

$$\frac{H}{L} > 4$$

Based on this, Ryder and Ozbay (1990) proposed the criteria for selecting pillar barrier spacing as outlined below:

1. The height of the tensile zone is lower at H/L = 4 than it is at H/L = 2, thus reducing the load placed on the in-stope yield or crush pillars for tensile-zone control.
2. The hangingwall stiffness falls off fairly rapidly for H/L < approximately 2 and this could prejudice the stability of certain in-stope non-yield pillar layouts.
3. In-stope closures and surface subsidences in a yielding-pillar layout increase in direct proportion to span, L, but are often at acceptable levels if H/L is approximately 4.
4. In shallow non-yield pillar layouts, much lower H/L ratios may be acceptable since the in-stope pillars themselves provide substantial tensile zone control. However, for adequate compartmentalization L should rarely exceed 250 m.

Ryder and Ozbay (1990) suggest that numerical modelling can also be utilised in a bid to get an operational regional pillar span. They also reveal that adequate safety factors to arrest regional instability become more difficult or impossible to achieve at low H/L ratios.

2.6 Conclusions

A robust pillar design system thrives on accurate determination of Safety Factor. The inputs in the determination of Safety Factor, pillar strength and pillar load, need to be reliably determined for a dependable Safety Factor. Pillar load can be determined using TAT, Coates Method or Numerical Models. TAT is used in regular mining layouts of large lateral extents, several times greater than the mining depth and assumes that each pillar in the layout is of same size and supports an equal amount of load to the surface. Since TAT does not consider geometrical and rock properties in its formulation, Coates Method was developed to account for these but like TAT, it does not consider overburden stiffness and seam stiffness which play a pivotal role in determining pillar load as discussed later in this research report. Numerical models are used when depth/span becomes too great or when pillar sizes are different.

There are several formulae for determining pillar strength. They can be grouped into two main forms, the linear form and the power form. The main factors accounted for in these

formulae are the w/h ratio and the strength of pillar material as determined statistically or in the laboratory. This approach is inadequate as it leaves out a lot of factors influencing pillar strength as discussed later in this research report. The evaluation of the presented literature on pillar design systems is as given in Chapter 3.

CHAPTER 3: EVALUATION OF THE DISCUSSED PILLAR DESIGN SYSTEMS

3.0 Introduction

The previous chapter looked into the pillar design systems currently being used in platinum mining. This chapter seeks to evaluate them and suggest further areas of improvement. The areas of special attention encompass pillar load and pillar strength determination methods, which are important in safety factor determination.

3.1 Pillar Load determination methods

3.1.1 Tributary area Method

This theory applies to regular mining layouts with same size pillars. It assumes that in an underground excavation of large lateral extend greater than the mining depth each pillar supports an equal load to the surface. This way the theory simplifies pillar design as it conveniently offers fixed pillar-design dimensions for any given seam material and depth (Ozbay et al, 1995). However not all pillars in the mining layout will carry an equal load. Ozbay et al (1995) reveal that pillars near permanent abutments or lines of regional pillars carry lower stresses than the Tributary Area Theory method predicts, regardless of the extent of mining. They point out that while these deviations are small at shallow depths and low extraction ratios and in fact negligible in most aspects of coal design, they can be quite significant in hard rock mines which adopt much higher extraction ratios. It is crucial to note a revelation by Ozbay et al (1995) that in practical mining potholes or fault losses are often left as unintentional pillars resulting in lower extraction ratios which gives lower APS values than initially planned for. The Tributary Area Method is applicable to layouts that are wholly regular where the spans are large.

Van der Merwe (1998) argues that the conditions under which the Tributary area theory is applicable are when panel width is more than or equal to the depth provided that the pillar area is of the same size. As revealed by Roberts et al (2002), as w/h ratio goes below 1.25 and extraction ratio goes past 65% the tributary area theory becomes less accurate. Overburden stiffness and percentage extraction ratio also bound the performance of the tributary area theory as a tool for pillar design. On the other hand, Roberts et al (2002) indicate that as long as the designer accepts the constraints presented by the tributary area theory in calculating pillar stress levels, the theory can be utilised for practical design purpose.

3.1.2 Use of Numerical Modelling to assess the influence of mining parameters on pillar loads

Numerical modelling work carried out by Roberts et al (2002) using lamodel show that pillar loading is not only influenced by panel width to depth ratio. Their numerical analysis found out that overburden stiffness and seam stiffness also play a pivotal role in determining pillar load. Roberts et al (2002) varied overburden stiffness and seam stiffness using the lamodel boundary element code and came up with the following findings:

- Pillar loads decreased with increasing overburden stiffness. They observed that abutment loads increase as pillar loads decrease.
- Greatest deviations from TAT were observed at large depths, high extraction and low overburden stiffness. However they noted that the deviation from TAT was less than one per cent for typical mining parameters.
- The results for seam stiffness were similar to those obtained while varying overburden stiffness, though the relative magnitudes indicate that the results are less sensitive to seam stiffness than overburden stiffness.

3.1.3 Areas of further work to be done

Since the Tributary Area Theory is the widely used method for determining pillar load in the mining industry, adjustments to the theory with a view to enhance accuracy are critical. It is imperative to formulate the theory in such a way that it accounts for all variables affecting the pillar loading system within the tributary area. The loading conditions are affected by encounters of such factors as adversely oriented joins, pillar material properties themselves and overburden stiffness among others.

It is vital to note that TAT remains the simplest method for determining pillar load, but when depth/span becomes too great or when pillar sizes are different, the commonly used method is numerical modelling.

3.2 Pillar Strength Determination Methods

It can be seen from the presentation in chapter 2 that the current formulas for determining pillar strength borrow from the pioneering work by Bunschinger (1876) (linear formulas) and Holland and Gaddy (1956) (power formulas). The main factors accounted for are the w/h ratio and the strength of pillar material as determined statistically or in the laboratory. This

approach tends to be inadequate as factors such as discontinuities, characteristics of the surrounding strata and the effects of deterioration and time impact on the strength of a pillar. Joint properties like frequency, orientation and condition also have a significant influence on the strength of pillars. Scaling, Creep and other forms of time dependent factors affecting pillar strength have to be considered if a stable pillar system has to be established. That is to say all factors influencing pillar strength instability must be accounted for in the pillar design systems. It is crucial to note that the presented formulae do not embrace the systematic concept of the bord and pillar layout as they only consider the pillar itself without considering the roof strata and the floor strata which make contact with the pillar and are part of the bord and pillar layout. Failure propagation occurs if one or more components of a system is in fault hence all the elements of the system must be adequately accounted for in the design. While the consideration of the ore seam by the formulae may yield reliable results for this system component, other components have to be addressed likewise.

Several factors like specimen preparation, transportation, moisture content, testing laboratory temperature and storage condition of specimens have a significant influence on the strength of the rock specimen determined in the laboratory. It is therefore advised that the tests be done under scientifically recognised specifications.

One of the greatest drawbacks of the current formulae is that they are empirically based. The reason why this is a drawback is that failure has to occur to develop an empirical curve of pillar stability. Engineers need a tool which predicts failure in order to make reliable designs. A theoretical framework for pillar design can be established through numerical modelling to prevent dependence on collapse as called for by the empirical designs. The empirical designs for pillars designed elsewhere in areas lying out of these empirical ranges have to be done based on observation of pillar failures. This is costly and unsafe so a method should be always be available which does not depend on collapse.

3.2.1 Explanation of factors affecting pillar strength

3.2.1.1 Insitu Rock Strength

Pillar strength is a function of the insitu rock material strength comprising it. The stronger the pillar material the stronger the pillar will be when other factors are considered to be constant. However the influences of several factors if present have to be factored in determining a true value of the pillar strength. For example, it is possible to have a pillar with significantly high

material strength but the influence of discontinuities greatly reduces the overall strength of the pillar.

3.2.1.2 Pillar size and shape

The diagram in Figure 3.1 presents pillar types currently being used in mining of which the cylindrical and the cubical pillars are frequently used. Experiments in the laboratory show that the cylindrical pillar tends to be the stronger because it has no corners where stress concentrations can be experienced leading to pillar abutment failures. The load is uniformly distributed across the area of application.

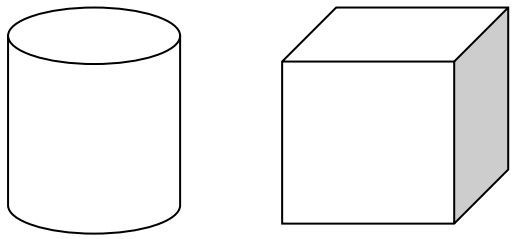

Figure 3.1: Pillar shapes used in mining

Experiments done by several authors show that specimen strength decreases with increasing size, however the strength decreases to a particular residual strength and not zero. The decrease in strength due to an increase in size can be explained by factors such as increase in discontinuities and grain boundaries within the specimen. Some of the results obtained by authors showing the relationship between pillar strength and pillar size are as shown in Figures 3.2 to 3.4.

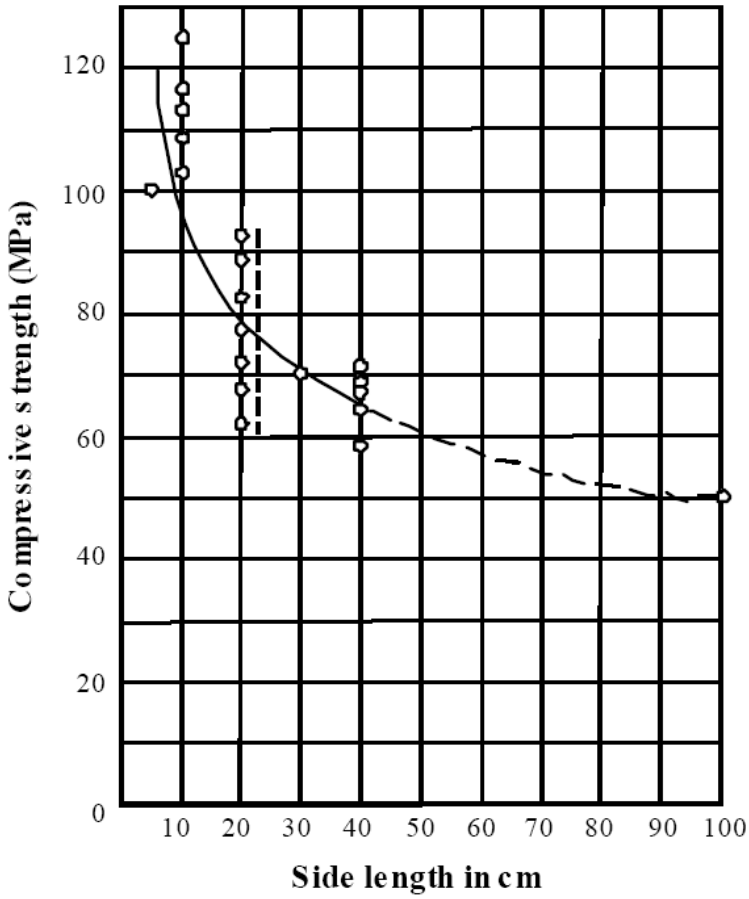

Figure 3.2: Relationship between pillar strength and pillar size for iron ore rock (Jahns, 1966)

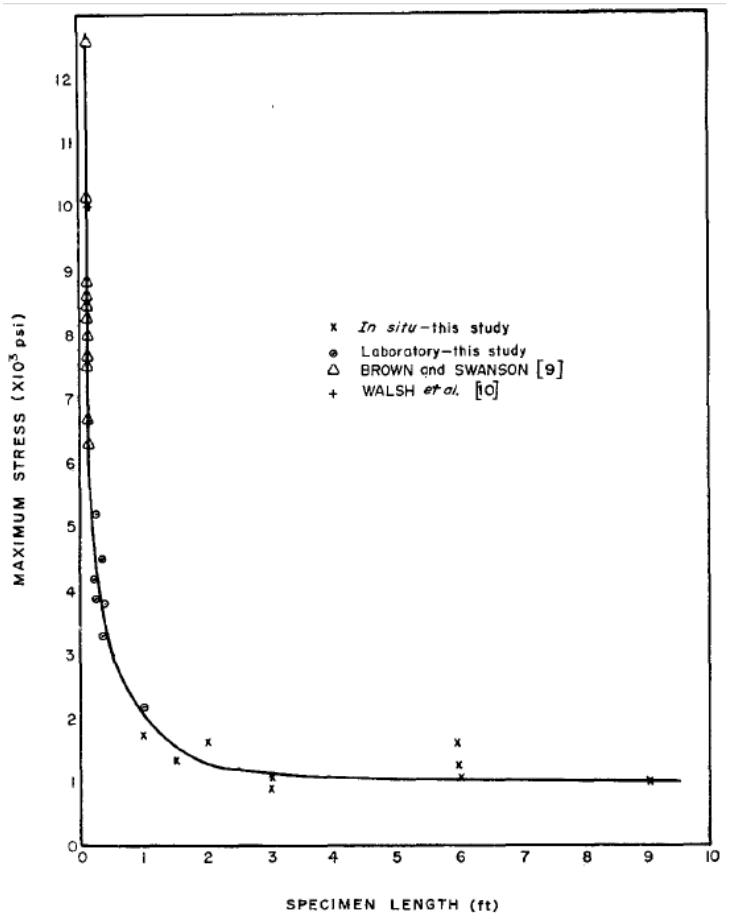

Figure 3.3: Maximum stress versus specimen length-Cedar City quartz diorite (Pratt et al, 1972)

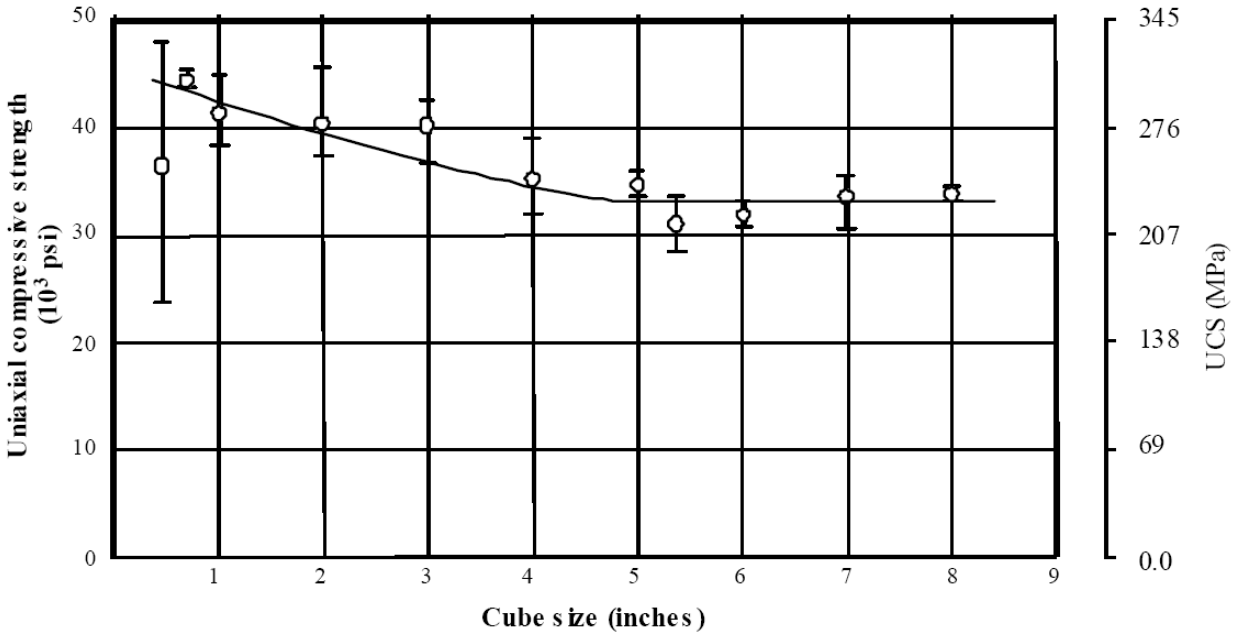

Figure 3.4: Relationship between pillar strength and pillar size for norite rock (Bieniawski, 1968b)

3.2.1.3 Discontinuities

Many attributes of discontinuities have to be considered in assessing pillar strength. Different geological structures may exist in the ore seam in which pillars are established. These have intense influence on the behaviour of pillars. The structural discontinuities which may be encountered in an ore seam include joints, fractures, striation lineation, fold axis, faults, fractured zones and shear zones. A pillar may have a high safety factor and width to height ratio which gives an impression that it is strong but the presence of intense discontinuities makes it to fail soon after mining. Generally the strength of a pillar decreases with the increasing frequency of these structures however a better picture of the relationship between the two can be obtained by numerical modelling. Numerical modelling packages like phase2, FLAC3D and MAP3D with several modelling capabilities can be utilised as they can model these structures.

3.2.1.4 Fractured zones

Some of the portions of the ore body can be affected by strong fracturing leading to fracture zones in pillars. The fracture zone consists of disintegrated pillar material with little load bearing capacity. Fracturing normally happens when rock is exposed to sudden change of stresses from high to low as excavations are made underground. Fracturing also takes place if the stresses increase due to mining. It may also be as a result of sudden release of energy by rocks under seismicity. Hudson (1992) points out that the intensity of fracturing of a pillar depends on vertical stresses and horizontal confining stresses. He confirms the fact that the edge of a pillar is under uniaxial loading state and further into the pillar a triaxial state of loading is observed. Fracturing happens in or at the edge of the pillars if the stress acting on the pillar exceeds its strength.

3.2.1.5 Geology

The geological minerals constituting a pillar also dictate its strength. Water absorbing minerals like phosphates swell when they absorb water setting the grain boundaries of the pillar material apart. The water makes the contact between the grain boundaries slippery reducing the frictional strength of these boundaries and the overall strength of the pillar. The infill material between joints in the pillar material also affects pillar strength. Slippery infill material like serpentine reduces frictional strength of the grain boundaries while infill minerals like calcite and feldspar increase the frictional strength of the grain boundaries. The increase in frictional strength at the grain boundary level is accompanied by an overall

increase in pillar strength taking other variables to be constant. A decrease in frictional strength at grain boundary level has the opposite effect when other variables are taken to be constant.

3.2.1.6 Pillar contacts with roof strata and floor strata

Like testing specimens in the laboratory, the contact of the pillar with the roof strata and floor strata has a great influence on the pillar strength. When the contact is not uniform, because of adversely oriented discontinuities or other factors, stress concentrations exist and they lessen the pillar strength. The smoothness or roughness of the contact surface dictates the pillar strength and load transfer. Rough surfaces encourage much friction thereby making the pillar stronger by preventing pillar failure through sliding over a smooth surface. However the rough surfaces bring about non uniform contact such that the contact surfaces do not allow smooth transfer of load to the pillar causing more stress to be transferred to other pillars with uniform contact surfaces.

3.2.1.7 Roof and floor stability

Despite having knowledge of the contacts, the condition and stability of the surrounding strata both in the roof and the floor have a bearing on the strength of the pillar. Pillars punch into the foundations and fail in tension if the bearing capacity of the foundation is not high enough. The lesser the stability of the foundation the more likely pillar failure is to be witnessed. Overall weaknesses in the floor and roof contribute to pillar system instability. Also note that the failure of roof and floor strata may cause bords failure while pillars remain intact.

3.2.1.8 K-ratio

K-ratio is the ratio of horizontal virgin stress to vertical virgin stress. K-ratio, as can be deduced from its definition, decreases with depth. At shallower depth there are high horizontal stresses acting on the pillar thereby confining it. The high confinement increases the pillar strength. The reverse holds for greater depth. Yilmaz (2007) points out that the resistance of stabilising pillars can be reduced by low values of k-ratio. He points out that high horizontal stresses cause bord failure in coal mines and also cause damage to tunnels located below mined out areas in shallow mining situations in the Bushveld Igneous

Complex. Figure 3.5 shows the variation of k-ratio with depth for underground stress measurements in South African Mines.

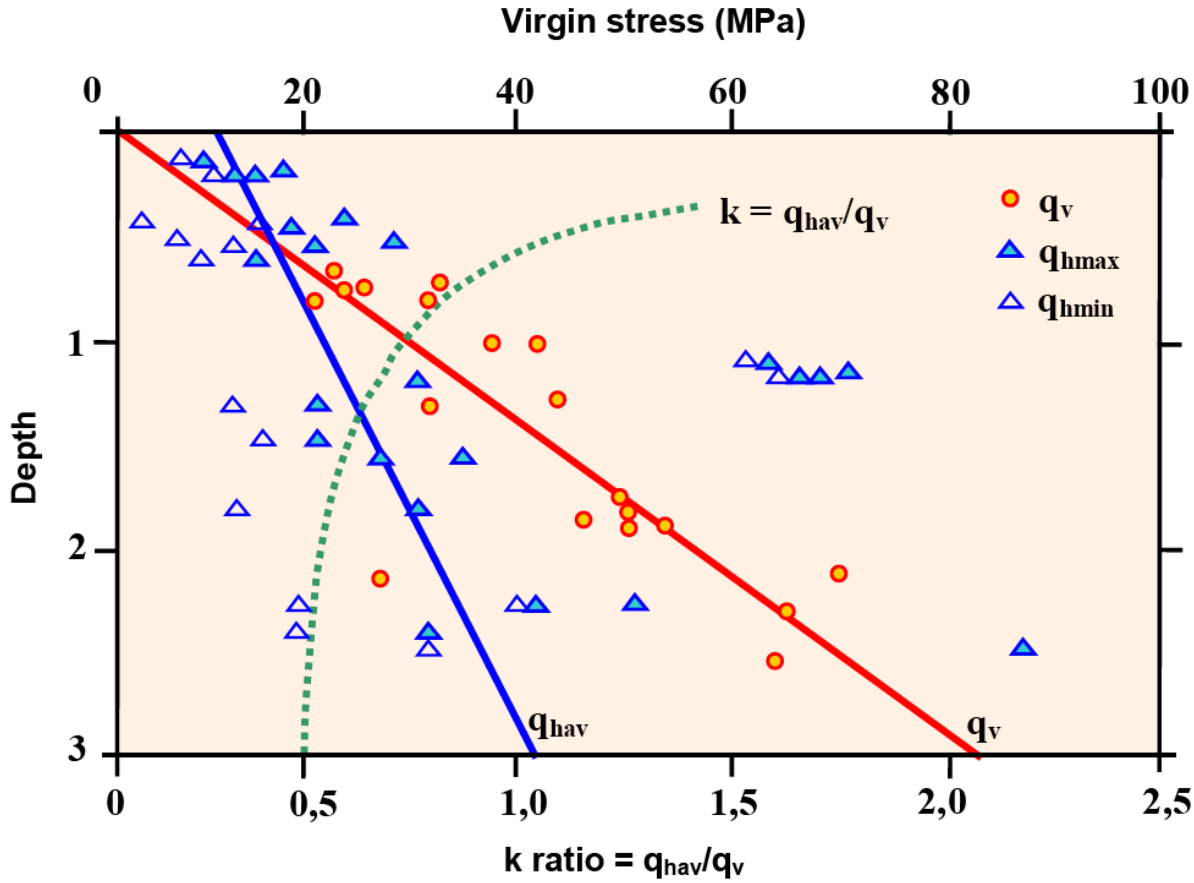

Figure 3.5: State of virgin stress as obtained from underground measurements (Wesseloo and Stacey, 2006)

3.2.1.9 Pillar confinement

It can be proved by laboratory triaxial tests that material strength is a function of confinement. As the confinement increases the material strength increases. However excessive confinement may result in the disking of the confined material. Practically, pillar confinement can be achieved by backfilling the area surrounding the pillar, cable anchoring, wire-meshing, applying thin spray-on liners or shotcreting the pillar.

3.2.1.10 Time dependent effects

Creep is the time dependent deformation of material under the influence of stress. When rock material is exposed to high stresses and temperature over a period of time it weakens thereby weakening the strength of the pillar. It is advisable to continue mining once started so that the projected life span of the mine is not exceeded much since the extra stand up time for pillars

encourages pillar creeping. The time between development and production must be optimal in order to reduce pillar stand up time.

3.2.1.11 Pillar loading condition

It is an arduous task to comprehend the complex loading environment of a pillar system in order to get its influence on the overall pillar strength. When the bord in a bord and pillar mining method is established there is a redistribution of stresses to attain force equilibrium. The acting forces try to close the void. The ability of the pillar to resist the load trying to close in the opening depends on its stiffness. The stiffer the pillar is the more it can resist the load. The hangingwall strata ability to move in to the void likewise depends on its stiffness; the less stiff it is the easier it closes in. The mechanism of load transfer to pillars is such that the load is more concentrated to the sides of pillar. Pillar sides are under less or no confinement so they easily fail as the load is transferred to them since they lack confinement which increases material strength. Load transfer to pillars in the loading system is affected by breaks in the rock characterised by geological and geotechnical structures.

3.2.1.12 Blasting effects

When pillars are established they experience blast damage due to the blasting activity in the immediate panels near them. The blast damage decreases as the excavations advance away from the pillars. Given this reality pillar strength determination methods have to take account of this as the pillar strength decreases with blast damage. The depth to which a pillar is destroyed due to blasting effects has to be quantified and this parameter accounted for in the strength formulae. Coupled to the blast damage is the pillar weakening effect of released gases pressure and concussion. The gas pressure and concussion exert stress on the pillar and induce sidewall slabbing.

3.2.1.13 Spalling and side scaling effects

The chance of a pillar to survive over a predicted life span is reduced by the action of side scaling, buckling and spalling. Pritchard and Hedley (1993) made an investigation into these factors at Denson Mine and illustrated the effects of these factors as shown in Figure 3.6. The investigation was done on dipping seams but also holds for flat or gently dipping seams in Bord and Pillar mining, since these effects are encountered in both environments. Spalling

and side scaling of a pillar can be as a result of stress and temperature changes in the pillar leading to pillar expansion and contraction.

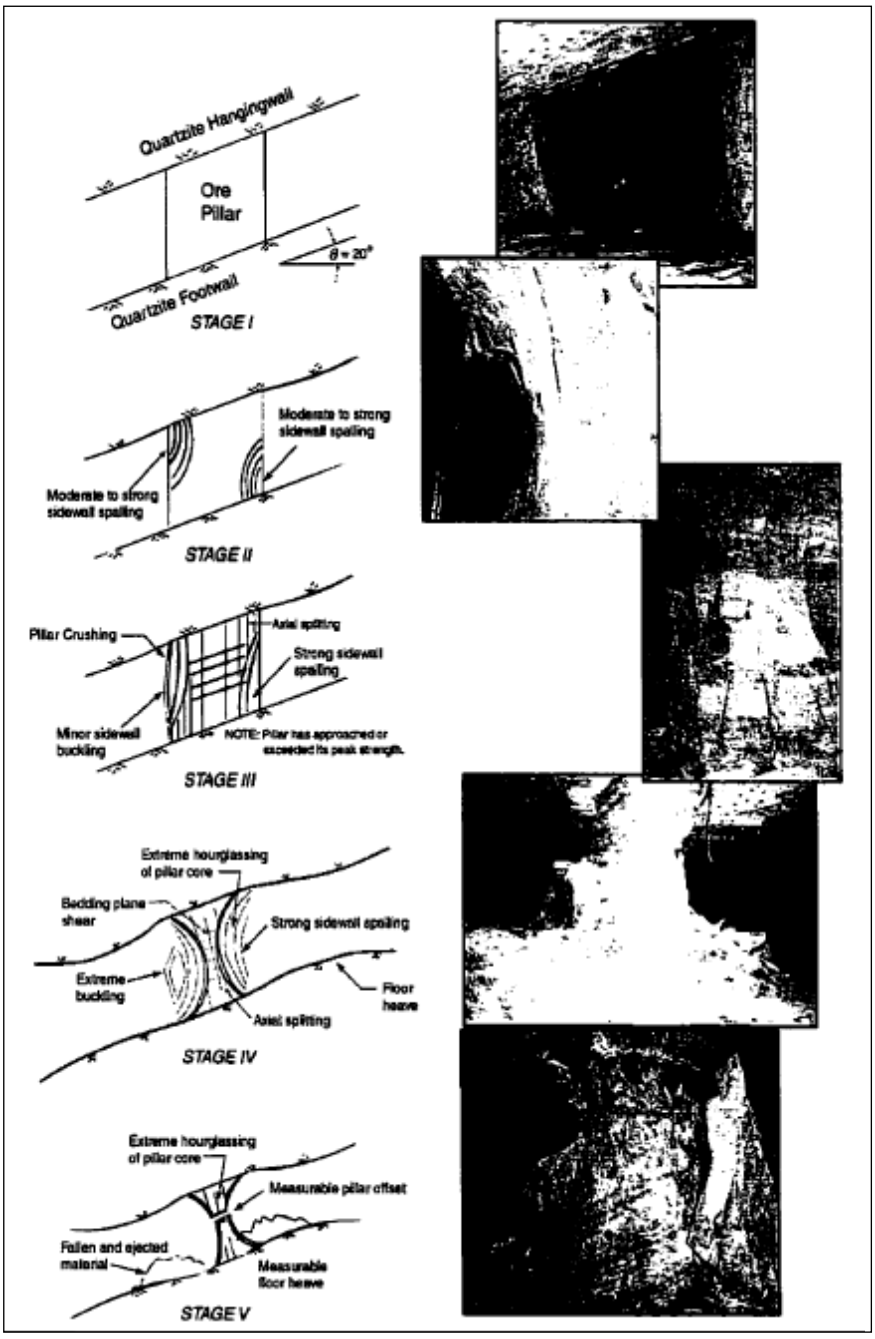

Figure 3.6: Effects of scaling, buckling and spalling on pillars (Pritchard and Hedley, 1993)

3.2.1.14 Influence of weak layers and weathering

Weathering in form of mechanical or chemical reduces the strength of a pillar. Pillar materials which are soluble like calcite are dissolved through chemical weathering thereby

disintegrating the composition of the pillar. Physical weathering occurs when pillars are exposed to high temperatures and low temperatures such that the outer surfaces peel of due to exfoliation. The weathering effect decreases pillar strength by reducing the material constituting the pillar. A study by Madden et al (1998) shows that the effects of blast damage, geological discontinuities, weathering, or weak layers within the pillar influence the strength of small pillars more dramatically than they do larger pillars. Weak layers have an overall effect of reducing pillar strength since weak material have a lower load bearing capacity compared to stronger layers. Failure would initiate at the weakest link.

3.2.1.15 Human error

Accuracy and precision are important in pillar design. Human error can have disastrous consequences. It may lead to overestimation of pillar strength due to inadequate quantification of factors affecting pillar strength. This way pillars are assigned higher loads which overpower their strength. In the same vein when pillar strength is underestimated larger pillars are left behind meaning that more resources than necessary are left behind. Human error may be eliminated or minimised by employing QA/QC (Quality Assurance/Quality Control) programmes to ensure checks and balances at every stage of the design process.

3.2.2 Comment on the factors affecting pillar strength

While it can be a challenge to account for all the discussed factors, it is imperative to build some conservatism in the pillar strength formulae in order to indirectly account for those factors which are difficult to quantify. Quantification of the fore discussed factors makes it easier to reliably account for them in the pillar strength adjustments.

3.3 Consequences of unstable pillar designs

Despite posing danger to workers, loss of profitable mining sections and entrapping expensive mining machinery pillar failure can have far reaching devastating consequences. One of the main problems of concern is surface subsidence due to the failure of underground workings. Subsidence causes damage to civil structures and the environment. Subsidence due to pillar failure is normally fast and causes wide cracks on the surface. Van der Merwe (2010) mentions that more subsidence, greater tilt and higher strain values are experienced at shallow

depth while the reverse is true for greater depth. This can actually severely cost a nation. Some highlights of the results of subsidence are outlined below:

- Damaging of roads, conveyors, conveyor belts, pipes, power pylons and houses.
- Agricultural effects such as shearing off of tree roots thereby killing the trees, severe ponding.
- Long term effects such as sinking of surface structures as a result of pillar failure and formation of sink-holes.
- Subsurface erosion which has a severe impact on agriculture.
- Interruption of both surface and underground water supplies.

Disastrous effects of subsidence as a result of pillar failure include tilting of houses on the surface above the area of underground failure as illustrated in Figure 3.7.

Figure 3.7: Illustration of the damaging effects of subsidence (Van der Merwe, 2010)

Several disheartening consequences of unstable pillar designs have occurred in the past and the photo presented in Figure 3.7 is for illustrative purposes only. These consequences can be

minimised or curbed at all by a comprehensive bord and pillar design and layout which considers all factors affecting pillar stability. Mines may go at logger heads with the government when law is enforced and risk being forced to close, the closure imposes poverty and economic haemorrhage on the nation as it lowers its GDP and increase unemployment rate.

Pillar design can be made much easier if the geotechnical zones in the study area in which the discussed factors have caused failure are identified. This helps in giving the most appropriate factors to concentrate on in each zone when doing the designs.

3.4 Pillar failure modes

Pillars fail when their strength is overpowered by the stress acting on them. The failure of pillars as generally encountered in mining is through either, stress induced progressive failure, structurally controlled failure or pillar bursts.

3.4.1 Stress induced progressive failure

When a pillar is established it is intact and have requisite load bearing capacity. As time progresses stresses build up acting on the pillar making the pillar material weak leading to the cracking, spalling and buckling of it. Factors like reduced confinement and high tangential (in circular geometries) stress also contribute to pillar failure. While there is no way of accommodating depth of failure in a pillar in calculating pillar strength there exists a linear relationship proposed by Kaiser et al (1996) which base on the approach built up by Martin (1997) for estimating the depth of pillar failure which is:

$$\frac{d_f}{a} = 1.34\frac{\sigma_{max}}{\sigma_c} - 0.57 \pm 0.05 \quad \text{----------37}$$

Where:

d_f is depth of pillar failure

a is an empirical constant

σ_{max} is maximum stress acting on pillar

σ_c is uniaxial compressive strength

Hour glass effect failure is suggested by Kaiser et al (1996) as the first stage of stress induced failure commonly encountered in hard rock mining. The graphical representation of the equation used by Kaiser et al (1996) to define stress induced failure is shown in Figure 3.8.

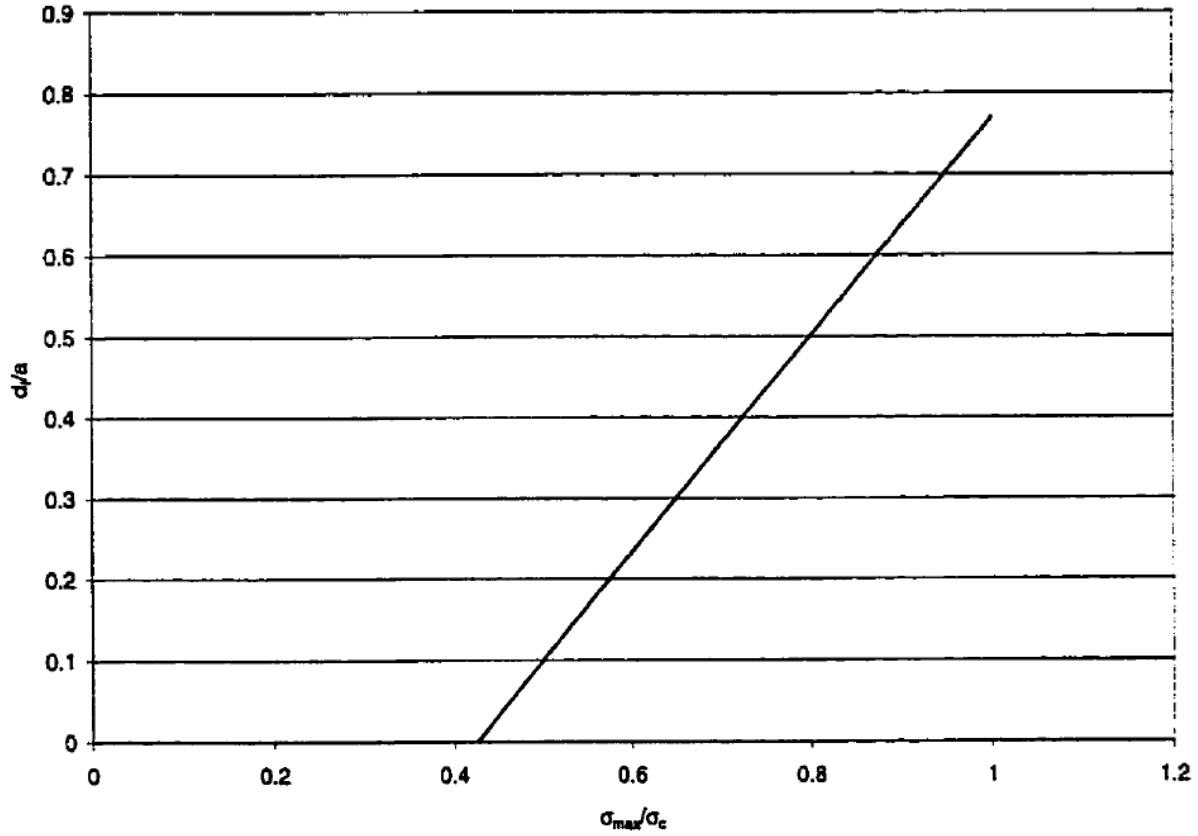

Figure 3.8: Plot of the equation to define depth of stress induced failure (Kaiser et al, 1996)

3.4.2 Structurally controlled failure

Structural defects in pillar material weaken it. Adversely oriented structural discontinuities may cause sliding to occur along these planes leading to shear failure of the pillar. Structural failure results from all structures, whether geological or geotechnical, which compromise the strength of the pillar.

3.4.3 Pillar bursts

The violent release of energy by a pillar is known as pillar burst. The pillar burst may result in complete failure of the pillar or mere ejection of rock from pillar skins while the core is left intact. Martin (1997) mentions that two conditions need to be satisfied before a pillar can burst. These conditions are:

1. The stress in the pillar must exceed the strength and,

2. The local mine stiffness must be less than that of the pillar.

With their work based on that of Martin (1997); Kaiser et al (1996) show that the first condition is satisfied when pillar stress exceeds 1/3 of the UCS. Mah et al (1995)'s data was used by Martin et al (1998) to illustrate this point as seen in Figure 3.9.

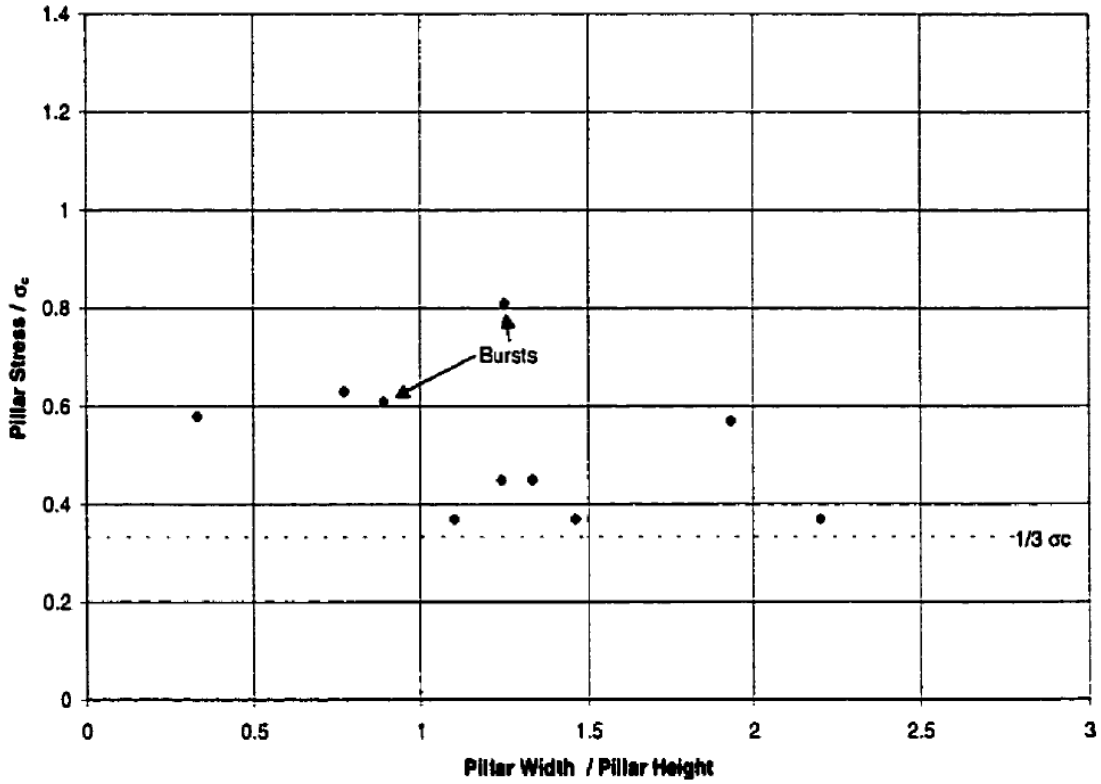

Figure 3.9 Rockburst potential in pillars, data from Mah et al (1995) (Martin et al, 1998)

3.5 Pillar failure curves

As a pillar fails, it follows the path shown in Figure 3.10 however the exact shape of the path taken by each pillar may differ. Brittle pillars normally experience a sudden failure when they experience peak stress while ductile pillars fail gradually when the magnitude of stress acting on them is high enough to fail them. The study of probability of failure done by Brady and Brown (2005) showed that pillars with safety factors below 1.3 are prone to high chances of failure. This is illustrated in Figure 3.11.

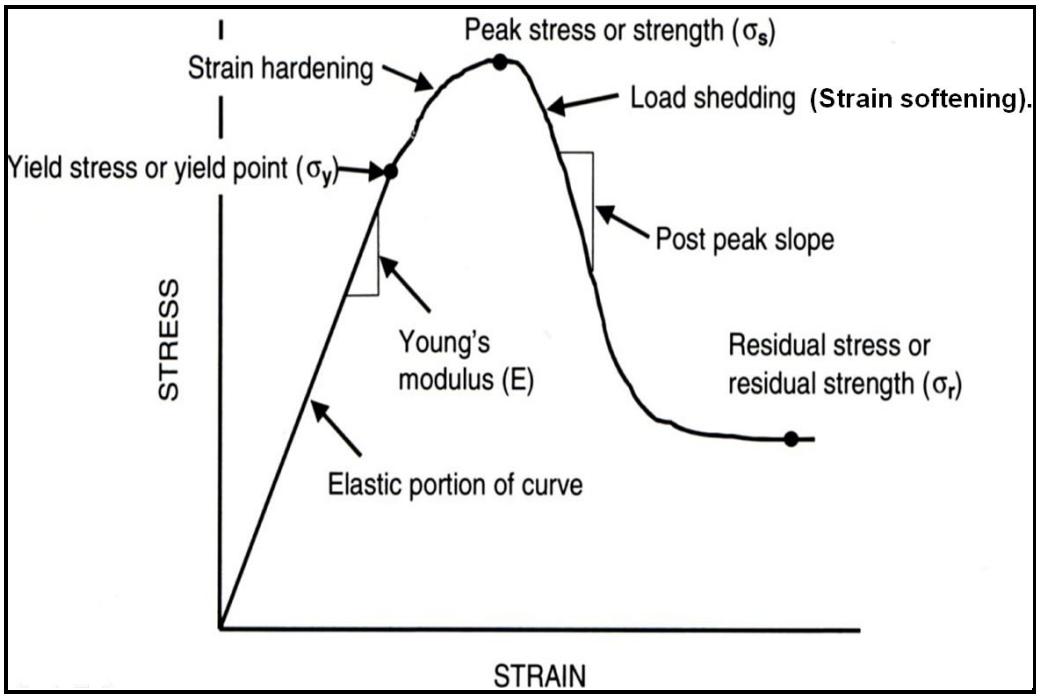

Figure 3.10: Stress strain curve for a typical pillar (Ryder and Jager, 2002)

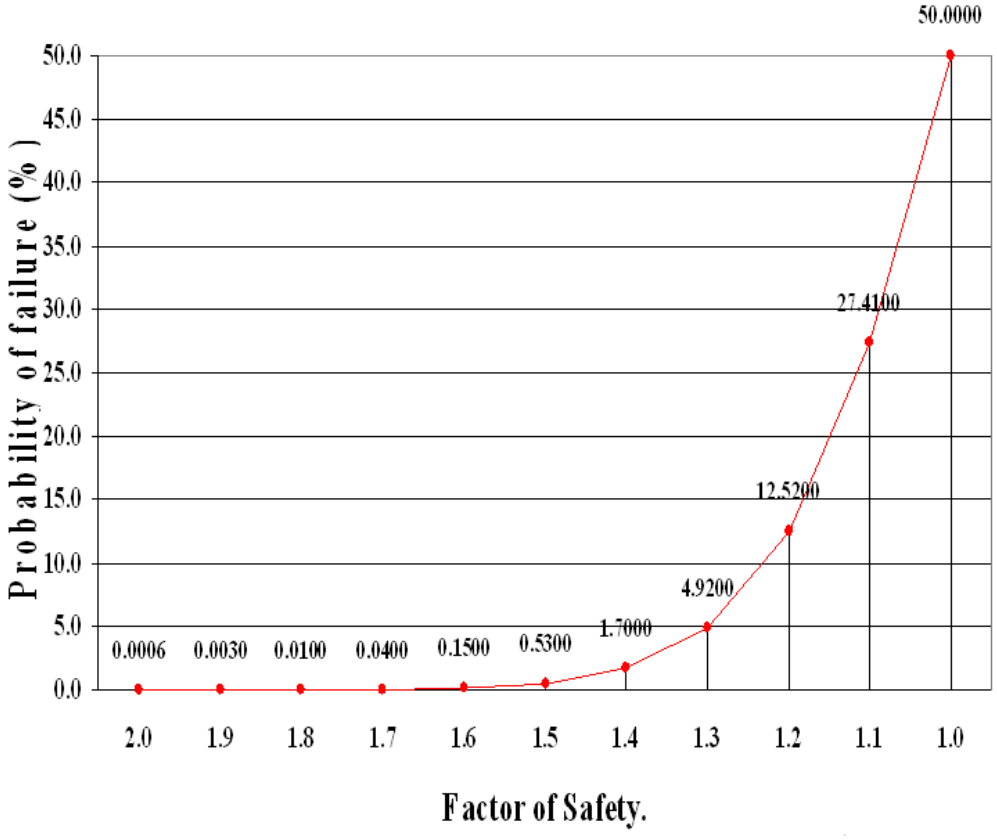

Figure 3.11: Relationship between Probability of failure and Factor of Safety (Brady and Brown, 2005)

3.6 Pillar Strength Determination combinations that can be used

3.6.1 Use of failure criteria to predict failure

Prediction of failure in pillars can also be done using failure criteria in rock engineering. These indicate situations in which failure is experienced. Failure criteria can be used as raw as they are or most usefully when they are used in numerical modelling packages. Some of the failure criteria which can be used to predict failure in pillars are as outlined below.

3.6.1.1 Mohr Coulomb Failure Criterion

This criterion describes the response to shear stress and normal stress by materials. This criterion is used in most numerical modelling programmes due to its ability to predict failure to a high degree of accuracy for conditions lying within its assumptions. It is also a powerful tool for determining cohesion and friction angle of rocks which are important parameters to determine for reliable prediction and design of structures in rock masses. However the Mohr Coulomb failure criterion has its own draw backs and these are given by Stacey (2010) as follows:

1. It implies that a major shear fracture occurs at peak strength,
2. It implies a direction of shear failure which often does not agree with observations, particularly in brittle rock,
3. It is linear, and peak strength envelopes determined experimentally are usually non-linear,
4. It assumes that cohesion and friction act fully in unison which is rarely so,
5. The criterion is likely to give incorrect results if the failure mechanism is not shear.

The criterion ignores σ_2 and only uses σ_1 and σ_3 but σ_2 has influence on the failure of rocks. The Mohr Coulomb Failure Criterion is represented by equation 38.

$$\tau = C + \sigma_n \tan\phi \quad \text{---------- 38}$$

Where:

τ = shear stress along the shear plane at failure

σ_n = normal stress acting on the shear plane

C = initial cohesive strength

ϕ = angle of internal friction

The orientation of the predicted failure plane is given as $45 + \frac{\phi}{2}$ degrees measured in the σ_1 – σ_3 plane from the σ_3 axis.

A plot of the Mohr circles in the shear stress against normal stress can be used to determine the cohesion and friction angle by plotting a Mohr envelope which is tangential to the Mohr circles. The angle of friction can be read off from the gradient of the Mohr envelope while the cohesion is the vertical intercept of the Mohr envelope. The Mohr envelope is as illustrated in Figure 3.12.

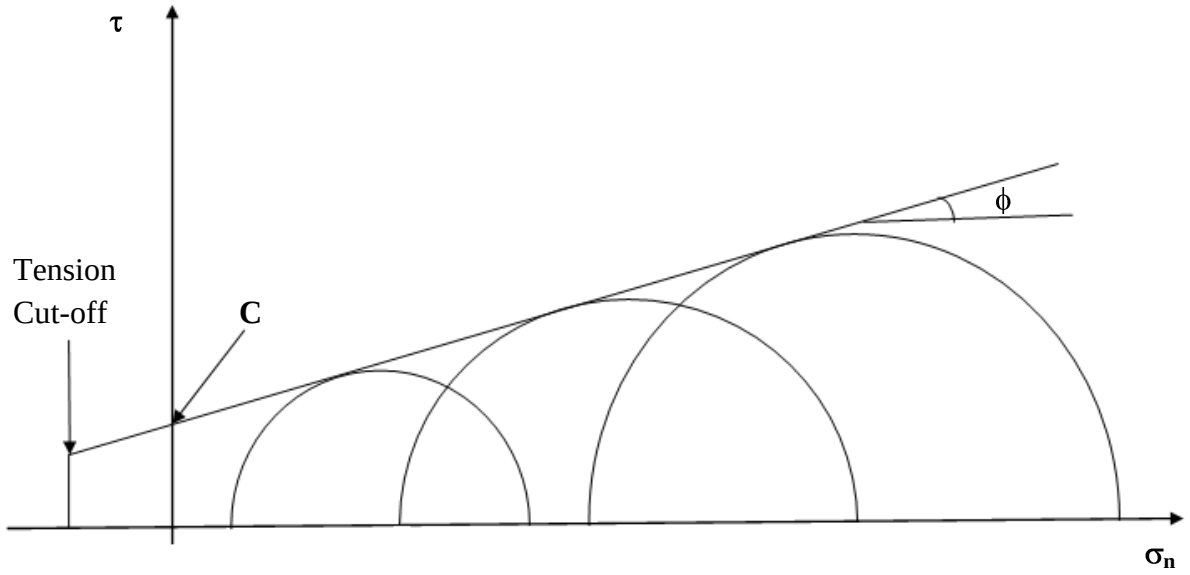

Figure 3.12: Graphical representation of the Mohr Coulomb Failure Criteria: Shear Stress against Normal Stress space

Other methods like the plot of σ_1 against σ_3 and the Apex point plot can also be used to determine cohesion (C) and the angle of internal friction (ϕ)

The Mohr Coulomb Failure criterion can be represented in the principal stresses plane using equation 39.

$$\sigma_1 = \sigma_c + \beta_o \sigma_3 \quad \text{----------39}$$

Where:

σ_1 is the major principal stress at failure.

σ_3 is the minor principal stress at failure.

$$\beta_o = \frac{1+\sin\varphi}{1-\sin\varphi} \quad \text{----------40}$$

$$\sigma_c = 2C \ \overline{\beta_O} \quad \text{----------41}$$

A set of σ_1 and σ_3 results from Tri-axial Compressive Strength tests are used to plot a line of best fit in the σ_1 against σ_3 space. The gradient of this line is β_o while its vertical intercept is σ_c. The given equation for β_o is then used to solve for internal angle of friction of the rock (ϕ). The determined β_o and σ_c can also be used in the equation for σ_c to calculate the cohesion of the rock (C). The principal stresses space representing the Mohr Coulomb Failure criterion is as given in Figure 13.

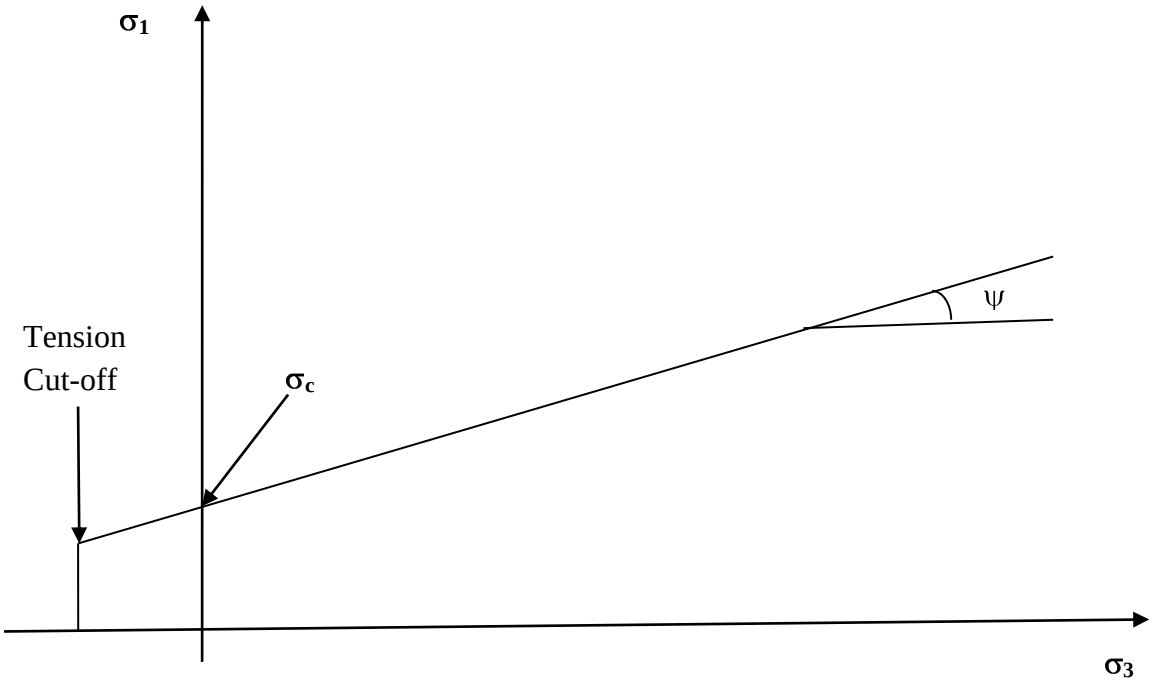

Figure 3.13: Graphical representation of the Mohr Coulomb Failure Criteria: Major Principal Stress against Minor Principal Stress space

Note that rock is weak in tension and therefore a tension cut-off is given in both space representations to show that the rock cannot sustain tension larger than that cut off.

The apex point method is another quick method of determining Mohr Coulomb parameters. This is done by calculating the apex of each Mohr Circle from the set of Tri-axial Compressive Strength test results and then drawing a line of best fit through these apex points. One does not need to draw the Mohr circles to determine the apex but simply use

simple equations to determine the x; y coordinates values of each point. The x-coordinate of each apex point is $(\sigma_1 - \sigma_3)/2$ while the y-coordinate is $(\sigma_1 + \sigma_3)/2$.

The equation of the line of best fit in the apex point method is written as:

$$\tau = K + \sigma_n \tan\theta \quad ----------42$$

Where:

K is the y intercept

θ is the slope

The Mohr Coulomb parameters can then be calculated using equations 43 and 44.

$$\phi = \sin^{-1} \tan \theta \quad ----------43$$

$$C = K\sec \phi \quad ----------44$$

Equations 43 and 44 are driven using linear regression between the Mohr envelope and the apex points line of best fit which is beyond the scope of this research report. Figure 3.14 gives a combined diagram for determining Mohr-Coulomb parameters using direct construction of Mohr-Coulomb failure envelope and the apex point method.

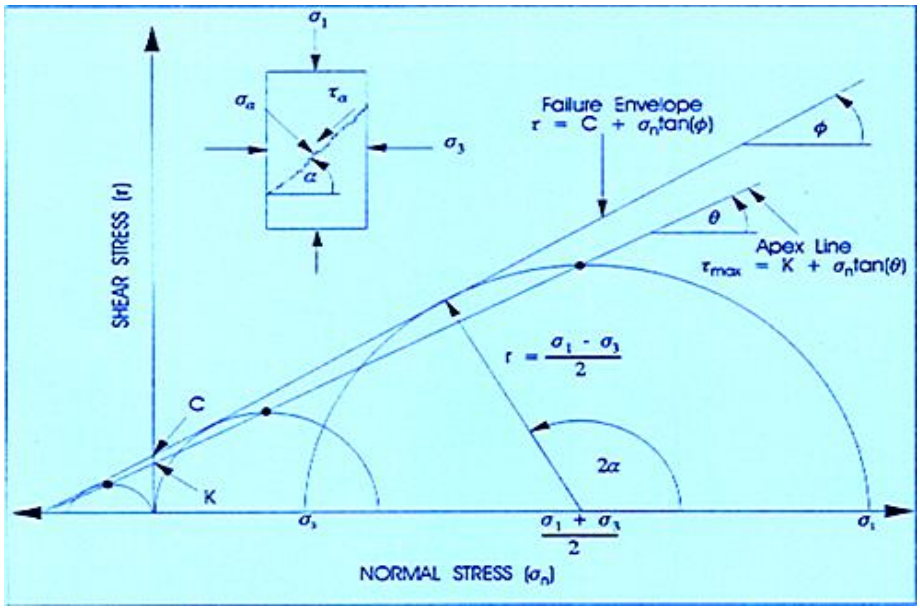

Figure 3.14: Determination of Mohr-Coulomb Parameters (Stacey, 2010)

3.6.1.2 Hoek Brown Failure Criterion

Basically the results of modelling using this failure criterion are almost the same as those numerical modelling results obtained using Mohr Coulomb failure criterion. This is because most of the formulation assumptions of the two criteria are the same. Like Mohr Coulomb failure criterion, Hoek Brown failure criterion is used to describe the response to shear stress and normal stress by materials. This criterion can be used to verify the results from numerical modelling using Mohr Coulomb failure criterion. Any major difference would mean a modelling error somewhere in the process.

Hoek – Brown failure criterion is represented by the following equation:

$$\sigma_1 = \sigma_3 + \sigma_{ci}\ m_b \cdot \frac{\sigma_3}{\sigma_{ci}} + s^{a} \quad \text{---------- 45}$$

Where:

m_b	is the Hoek – Brown constant m for the rock mass,
s and a	are constants which depend on the rock mass characteristics,
σ_{ci}	is the UCS of the intact rock,
σ_1	is the major principal stress and
σ_3	is the minor principal stress.

For intact rock, Hoek – Brown equation reduces to

$$\sigma_1 = \sigma_3 + \sigma_{ci}\ m_i \cdot \frac{\sigma_3}{\sigma_{ci}} + 1^{0.5} \quad \text{---------- 46}$$

Where:

m_i is the Hoek – Brown constant for the intact rock mass

The draw backs of Hoek – Brown failure criterion are similar to Mohr Coulomb failure criterion since it is also shear based. Stacey (2010) mentions that Hoek – Brown failure criteria applies to the “central” range of rock masses, that is, well – jointed rock masses in which the joints control behaviour rather than the rock material or individual significant planes of weakness.

3.6.1.3 Extension Strain Fracture Criterion

This is another failure criterion which can be used to model failure of rocks. This criterion works very well for predicting failure in brittle rocks and estimating the spalling of underground cavities in circumstances where rock failure occurs under stress levels not considered to be critical. In intact rock the criterion also works very well. Stacey (1981) states the criterion as follows: 'Fracture of brittle rock will initiate when the total extension strain in the rock exceeds a critical value which is characteristic of that rock type.' The criterion can be expressed using a mathematical expression as follows:

$$e \geq e_c \quad \text{----------47}$$

Where:

e_c is the critical value of the extension strain. The stress strain relationship which can be used to calculate the minimum principal strain is given as follows,

$$e_3 = \frac{1}{E}\left[\sigma_3 - \nu(\sigma_1 + \sigma_2)\right] \quad \text{----------48}$$

Where:

σ_1, σ_2, σ_3 are the principal stresses, E is the modulus of elasticity and ν is Poisson's ratio. Stacey (1981) pointed out that an extension strain occurs when $\nu(\sigma_1 + \sigma_2) > \sigma_3$.

The Extension Strain Fracture criterion is laudable as it automatically accommodates all the three dimensional stresses. It is also in agreement with most fracturing observed in brittle rock failures. While researchers like Martin (1997), Martin et al (1997), Wesseloo (2000), Diederichs (2003) and Eberhardt et al (2004) agree with the use of this criterion in estimating the spalling of underground cavities, Kuijpers (2000) pointed out that the criterion fails to address the physics involved in the formation of fractures in compressive stress environment.

3.7 Pillar design recommendations arising from the evaluation done

Little information on comprehensive pillar design for low reef platinum mining is available to the production personnel including the managers, planers and operators. It is then suggested that a simple, easy to disseminate pillar design system has to be established for safe, profitable platinum resource exploitation. The system should endeavour to account for the

mentioned factors affecting pillar strength. The decision makers at a mine are then pointed to all the critical considerations to be addressed as they design and operate the mine to uphold stability in the bord and pillar layout.

Geotechnical mapping and classification of pillars is quite important. One would realise that there are cases of early pillar collapse for pillars with high safety factors. Geotechnical variables in the pillar may also account for this trend. This criterion of classifying pillars allow designers to allocate different design criterion for each class and resist the temptation of using the same method of design for all the pillars. As such with this knowledge pillar strength formula can be adjusted accordingly. Geotechnical site investigation, even before pillars are formed, can be used to classify the site into different zones depending on geotechnical characteristics. This sheds more light on the expected behaviour of pillars in the different zones and therefore enables the application of the most appropriate pillar design approach for each zone.

A back analysis of the failed pillars can provide an empirical basis for designing pillars lying within the same empirical data base. This is useful since failure has already occurred. The actual performance for pillars designed within the same empirical range can then be comprehended by the back analysis such that the chances of failure are greatly reduced. For breaking new grounds a non-empirically determined design system has to be used to avoid dependence on pillar failure as a design approach.

A method of determining the effects of discontinuities on pillar strength have to be developed. Rock mass classification tools are most relevant in this case. For this purpose the platinum rock mass can be classified using Bieniawski (1989)'s RMR and the Q system developed by Barton et al (1974). These classification systems account for the discontinuity properties affecting pillar strength. The RMR considers the following six parameters.

1. Uniaxial compressive strength of rock material.
2. Rock Quality Designation (*RQD*).
3. Spacing of discontinuities.
4. Condition of discontinuities.
5. Groundwater conditions.

6. Orientation of discontinuities.

Bieniawski (1989) provided a table for the classification parameters and their ratings which can be used in calculating the classification of the rock mass under consideration. The table is as given in Appendix 1. A rating is given for each of the six parameters and the resultant classification value is obtained by summing the ratings.

The Q system calculates rock mass rating using the formula developed by Barton et al (1974) as follows:

$$Q = \frac{RQD}{J_n} \times \frac{J_r}{J_a} \times \frac{J_w}{SRF} \quad ----------49$$

Where:

RQD is the Rock Quality Designation

Jn is the joint set number

Jr is the joint roughness number

Ja is the joint alteration number

Jw is the joint water reduction factor

SRF is the Stress Reduction Factor

What each quotient represents is as outlined below:

1. Block size (RQD/Jn)

2. Inter-block shear strength (Jr/ Ja)

3. Active stress (Jw/SRF)

The outlined parameters accounted for by these rockmass classification systems confirms their relevance in determining rockmass strength which include pillar strength for the purpose of this study. This relevance is further confirmed by a research done by Arora (1987) which found out that joint frequency, joint frictional strength and the inclination of joints with

respect to major principal stress are the important factors affecting the strength and modulus of jointed rock samples.

It can be also noted that the bord and pillar layout has to be convenient and compatible with the mining machinery to be used, however it is recommended that machinery which suit the design should be procured.

The equations for determining jointing effects on pillar strength developed by Ramamurthy et al (1988) can be utilised together with the rock mass classification systems in assessing pillar strength by factoring in jointing effects. Joint frequency, orientation and strength are the parameters used in the equations. The equations developed by Ramamurthy et al (1988) are as given below:

$$\frac{\sigma_{cj}}{\sigma_{ci}} = e^{-0.017F} \quad \text{---------- 50}$$

$$F = \frac{J_f}{nr}$$

Where

σ_{cj} is the jointed rock strength

σ_{ci} is the intact rock strength

J_f is the joint frequency

n is an orientation parameter

r is a joint strength parameter

3.7.1 How to measure the discontinuity parameters

Jointed pillar strength is calculated using input values of joint frequency, joint dip and the base joint friction angle. The first two can be measured using a tape measure and clino rule while the base friction angle can be calculated using Barton and Choubey (1977)'s equation, which is:

$$\tau = \sigma_n \tan \phi + JRC \log_{10} \frac{JCS}{\sigma_n} \quad \text{---------- 51}$$

Where:

JRC is the joint roughness coefficient measurable on a scale from 1 (smoothest joints) to 20 (roughest joints)

JCS is the joint wall compressive strength

σ_n is the stress normal to the joint

ϕ is the base friction angle

Joint roughness coefficient can be determined using the standard profiles published by Barton and Choubey (1977) as shown in Figure 3.15.

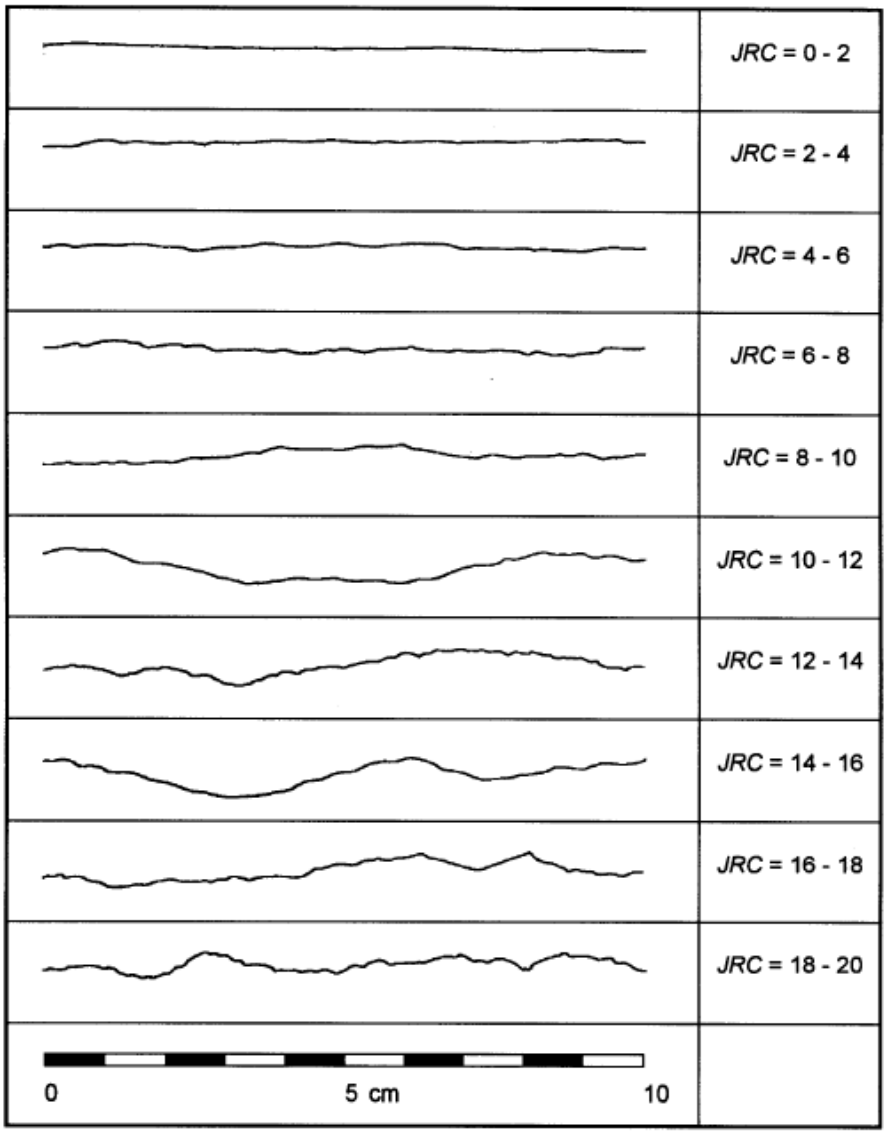

Figure 3.15: Roughness profiles and corresponding JRC values (Barton and Choubey, 1977)

The field joint profile is analysed and given a roughness coefficient of the profile it best approximates on the published profiles.

The joint wall compressive strength can be determined using a Schmidt hammer. The Schmidt hammer is pressed on the joint wall using an orientation of choice, normally a vertically downward orientation is used where possible, and a rebound number on the Schmidt hammer is recorded. 20 readings are taken this way and the values are arranged in ascending order. The first 50% of the values are discarded while the average of the last 50% is used to calculate the Schmidt rebound number. Knowing the density of the rock tested and the rebound number Figure 3.16 can then be used to determine the joint wall compressive strength.

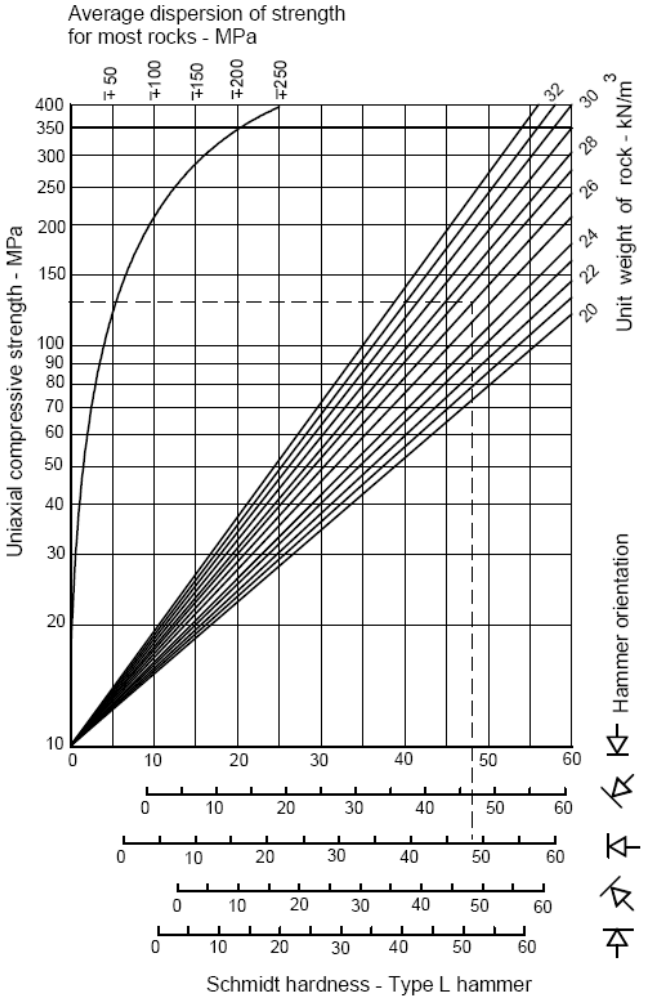

Figure 3.16: Schmidt Hammer Test JCS estimation chart showing Correlation between Schmidt hammer rebound number, hammer orientation, UCS and Rock density (Deere and Miller, 1966)

Above all it is always recommended that failures of pillars arising outside the known causes should be investigated as early as possible. This helps in finding an earlier solution before much loss is incurred. It cannot also be ignored that the traditional formulae which did not consider the factors discussed worked, at times, very well within their empirical range, hence after accounting for these factors in the adjustments it is quite appropriate to only use them in environments in which the factors are of effect.

3.8 Future work to be done

It can be realised from the preceding evaluation that further detailed research need to be done if a stable pillar design system for low reef platinum mining is to be achieved. The design has to consider all the factors affecting stability of the pillar system. The roof, pillar and the floor should be all accounted for as the components of the system.

Cases of collapse of those pillars with high safety factors within a short period of mining have to be investigated to get the finer details of the factors behind this trend. This knowledge will help in bringing long term stability to these pillars. Attaining stability in the pillar designs comes with the benefit of arresting the discussed negative consequences of instability in pillar designs.

Pillar deterioration has to be examined to have knowledge on how it affects strength so that this variable can be accounted for in the pillar design system. Foundation stability influence on pillar strength is another factor to be analysed so that pillars of appropriate strength and size are designed.

Back analysis can save time when designing those pillars lying within the empirical range of the assessed collapses. A data base of pillar collapse for the platinum mines situated on the Great Dyke helps the analysis. The key result areas for the analysis are as outlined below:

- To get some understanding of the relationship between pillar collapse frequency and design safety factor. This easily clarifies those circumstances in which pillars with high safety factors experience failure within the data base. This trend can then be compared with data bases used to establish the discussed formulae currently being used for pillar design.

- To assess the nature of the relationship between pillar collapse frequency and the width to height ratio. This gives an indication on the effect of mining width to height ratio on the strength of pillars. The information can then be compared against the data bases used with current formulae so that necessary adjustments can be done.
- For the pillars in the established data base the relationship between pillar life and frequency of pillars with such pillar life can also be examined. This gives a picture of how much the majority of pillars within the data base are expected to live.
- For each depth the frequency of pillar collapse can be measured so that an appropriate design which considers variation of strength and loading conditions with depth can be developed.
- For the new data base and the other data bases for other pillar design formulae, a relationship between the frequency of collapse and a given number of pillars can be compared in order to come up with the most appropriate representative statistical number of pillars to be involved in the data base.

Pillar scaling is one of the main factors affecting pillar strength. A high safety factor pillar may live short due to this. As such there is need to study pillar scaling rates. Numerical modelling packages with strong modelling capabilities can be used to get a clear picture on the relationship between pillar failure and scaling. It can be noticed that safety factor of pillars decrease with time as they are being affected by pillar scaling. It is then necessary to determine the period which lapse between pillar formation and collapse. Field observations can be done over a period of time to calculate scaling rates in the area of study. Scaling rate can be calculated using the following simple equation:

Scaling rate = Scaling depth (Sd) / Time taken to scale to that depth

Once the scaling rate is determined Monte Carlo simulations can then be used to calculate pillar life or the probability of survival of a pillar up to a particular number of years. For those pillars which were scaled before the commencement of the scaling study survey information on them can be utilised in calculating the depth of scaling. The old pillar offset data and the current can be used for this purpose. The same technique can be utilised for the present study.

The extent to which pillars can be affected by scaling can be assessed by determining the chemical composition of the pillar rock material. It can be noticed that clay material is more prone to scaling that harder material like quartz.

3.9 Conclusions

The evaluation of the current pillar design systems showed that there are shortcomings which need to be addressed to come up with a competent pillar design system. The success of a bord and pillar mining method in the exploitation of platinum heavily depends on a comprehensive and competent pillar design method. Pillars need to be large enough to contain load and to be small enough to avoid loss of resource. The TAT remains the simplest method of calculating pillar load however not all pillars in the mining layout will carry equal load since, as observed by Ozbay et al (1995), pillars near permanent abutments or lines of regional pillars carry low stresses than the TAT predicts, regardless of the extent of mining. Ozbay et al (1995) point out that while these deviations are small at shallow depths and low extraction ratios and in fact negligible in most aspects of coal design, they can be quite significant in hard rock mines which adopt much higher extraction ratios. Numerical models can be used in calculating pillar load for complicated mining layouts with different pillar sizes and great depth/span. Failure can be detected in the numerical models by incorporating failure criteria like Mohr Coulomb, Hoek Brown and Extension Strain.

While the current pillar strength formulae mainly consider w/h ratio and pillar material strength, it was shown in this evaluation that several unaccounted for factors have a bearing on the strength of a pillar. Some of the unaccounted for factors discovered during the evaluation are contact of the pillar with the roof and floor, roof and floor conditions, effects of adversely oriented joints, spalling and side scaling effects, influence of pillar loading conditions, blasting damage effects, influence of weak layers and weathering, impact of k-ratio, time dependent effects, geology, fractured zones and effects of different types of discontinuities within the rock strata.

The current pillar design systems are empirically determined. To calibrate the pillar design curve in empirical designs, pillar failure has to occur. While this may work for the mines lying within the empirical limits of the data used to develop the formulae, it is prudent for engineers to utilise tools which do not rely on failures. For the new mines which are to be established a tool should be availed with the power and capacity to design the pillars without waiting for failure to take place. It is crucial to note that empirical pillar design do not

embrace the fact that pillar design system is a system. As a system, considerations of the roof, the pillar and the floor is mandatory since neglecting one component of the system will affect all system components. Geotechnical mapping and classification of pillars as well as assessing the effects of discontinuities on pillar strength using rockmass classification systems need to be considered in the design process. These considerations help combat cases of early pillar collapse for pillars with apparently high safety factors due to non-consideration of these factors.

CHAPTER.4 CASE STUDY 1: REFLECTIONS ON GEOTECHNICAL WORK UNDERTAKEN AT A LARGE SCALE PLATINUM MINING EXPLORATION PROJECT: SOME LESSONS

4.0 Introduction.

The geotechnical work undertaken by the author at this exploration project gives an insight into areas of particular attention if we are to come up with reasonably reliable pillar design parameters. It suffices to say the quality of input into the pillar design system influences the quality of the result we get from it. Amongst the Geotechnical work discussed in this chapter are oriented core drilling, logging practice, core sampling procedure, laboratory tests and rock mass classifications. Pillar design results for the large scale platinum exploration project using different pillar design formulae presented in Chapter 2 are also discussed.

4.1 Oriented Core drilling.

To get a true picture of the insitu rock, core is oriented. Core orientation is the determination of the topmost point or bottommost point of the top face of a drill run which is then linked to the next run. The geotechnical holes were drilled using an ATC orientation tool. This way an orientation line was drawn along the topmost of the core. This makes it easier to make a unique orientation of the core in space. This reference line is the one used to determine the trend and plunge of the joints.

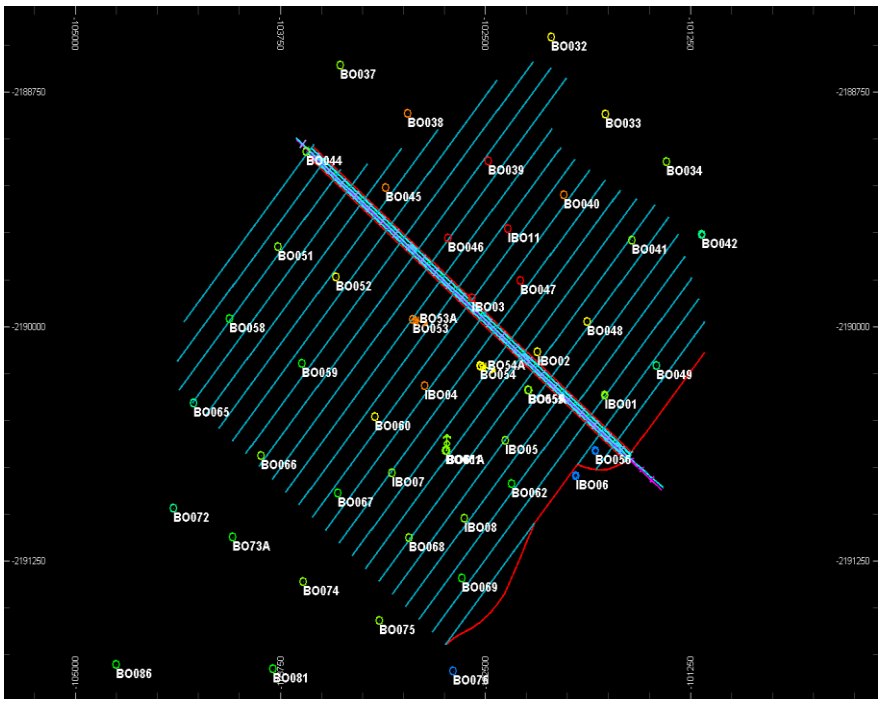

Figure 4.1: Exploration boreholes (Todal Mining Geotechnical data base, 2009)

Several Exploration boreholes were drilled on the site. These are shown in Figure 4.1 above. For the sake of this discussion the author chooses BO53A for illustrative purposes.

4.1.1 Downhole survey

Downhole Survey was carried out to pick any deviations from the supposed drilling axis.

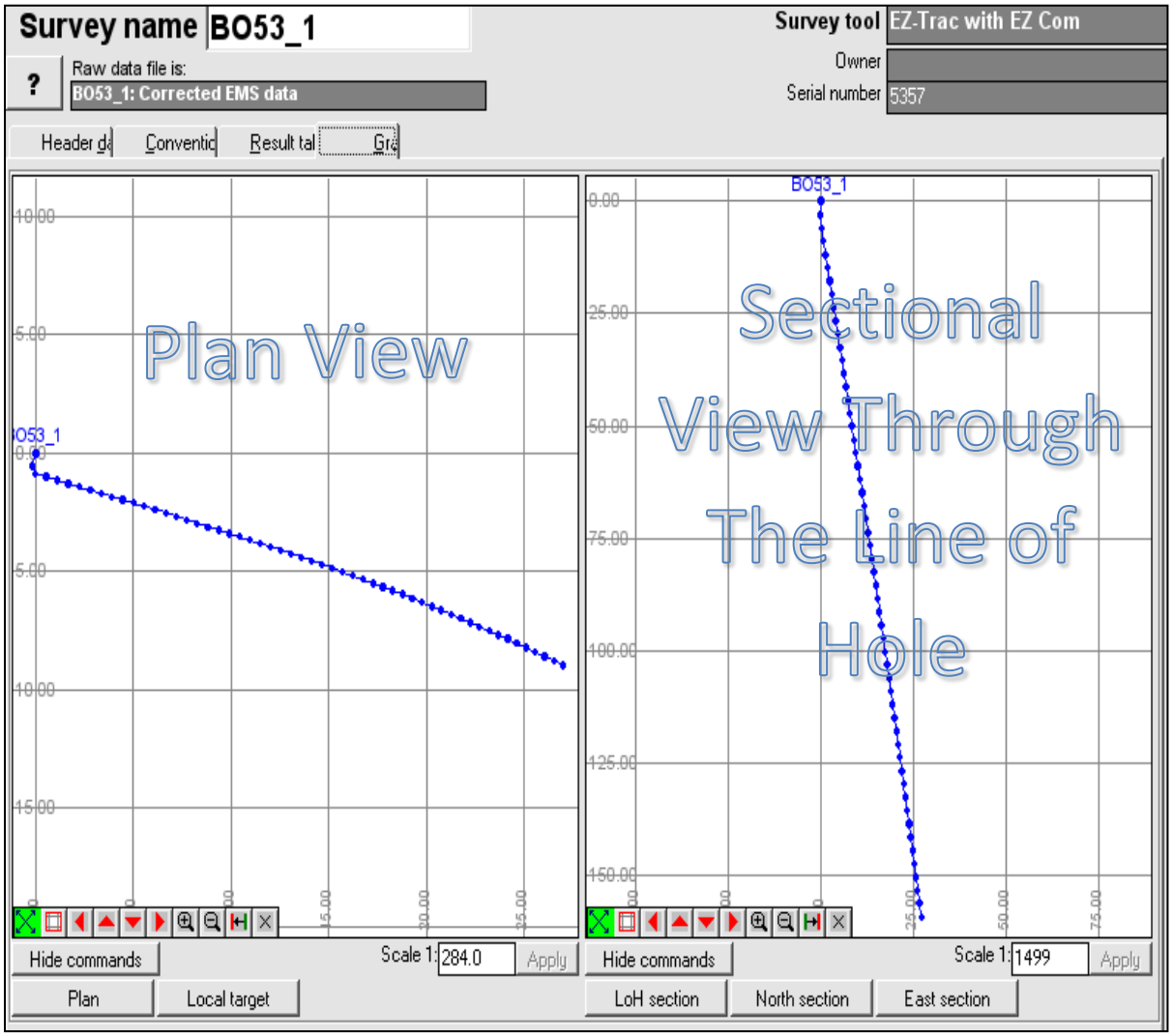

Figure 4.2: Downhole Survey Plan and Section of Borehole BO53A (Todal Mining Geotechnical Data Base, 2009).

No deviation from the drilling axis was picked. The deviation witnessed on the top minor potion of the hole was due to casing interference and is not an indication of true deviation. Table 4.1 shows the computerised logging details from the downhole survey instrument. The high precision instrument helps to minimise human error once set appropriately.

Table 4.1: Downhole survey results for borehole BO53A

African Mining & Exploration

Survey of Hole BO53A
For Todal Mining Private Limited
Surveyed 18/12/08 08:38
Hole size NQ
Surveyed By Darren Muirhead

Magnetic Reference Data
Magnetic Strength 29570 nT
Magnetic Dip 58.3 degrees
"MD"= Magnetic Dip Deviation > 0.5 degrees
"MT"= Magnetic Strenth Deviation > 1000 nT

Station	Quality	Dip	Azimuth	East	North	Elevation	Mag.Dip	Mag.Str.	Mag.Y	Mag.Z	Roll Angle	DLS	Comment
Metres	*	Degrees	Degrees	Metres	Metres	Metres	Degrees	nT	nT	nT	Degrees	deg./30m	
8	MD+MT	78.9	190.3	0.0	0.0	0.0	66.0	27565	0	25186	155.5	0.0	Casing interference
11	MD+MT	79.2	203.6	0.6	2.0	0.0	78.9	36496	0	35810	211.2	1581.9	Casing interference
14	MD+MT	79.2	104.1	0.5	2.4	3.0	59.7	30872	0	26658	59.6	164.9	Casing interference
17	OK+OK	78.8	102.8	0.1	2.5	5.9	58.3	29480	0	25094	0.7	4.4	
20	OK+OK	78.9	104.1	0.7	2.6	8.9	58.0	29417	0	24961	55.9	2.6	
23	OK+OK	79.0	105.0	1.2	2.8	11.8	57.9	29395	0	24890	116.5	2.3	
26	OK+OK	78.8	104.8	1.8	2.9	14.8	58.0	29377	0	24908	49.6	2.3	
29	OK+OK	78.9	103.4	2.3	3.1	17.7	58.2	29385	0	24972	349.4	2.9	
32	OK+OK	79.0	103.3	2.9	3.2	20.6	58.2	29381	0	24973	310.7	0.7	
35	OK+OK	79.0	103.4	3.5	3.3	23.6	58.2	29395	0	24985	298.0	0.9	
38	OK+OK	79.1	103.3	4.0	3.5	26.5	58.2	29385	0	24962	290.5	0.4	
41	OK+OK	79.1	103.8	4.6	3.6	29.5	58.2	29386	0	24964	268.7	1.0	
44	OK+OK	79.1	103.9	5.1	3.7	32.4	58.2	29381	0	24970	354.6	0.6	
47	OK+OK	79.3	104.7	5.7	3.9	35.4	58.0	29397	0	24943	150.4	2.6	
50	OK+OK	79.3	105.3	6.2	4.0	38.3	58.0	29387	0	24914	112.9	1.1	
53	OK+OK	79.3	105.2	6.7	4.2	41.3	58.0	29361	0	24888	123.3	0.6	
56	OK+OK	79.2	105.2	7.3	4.3	44.2	58.0	29385	0	24912	67.4	1.5	
59	OK+OK	79.2	105.8	7.8	4.5	47.2	58.0	29392	0	24919	71.4	1.4	
62	OK+OK	79.2	104.6	8.4	4.6	50.1	58.2	29393	0	24968	329.7	2.2	
65	OK+OK	79.4	104.5	8.9	4.8	53.1	58.1	29403	0	24972	248.5	1.5	
68	OK+OK	79.4	104.7	9.4	4.9	56.0	58.2	29434	0	25003	233.1	0.7	
71	OK+OK	79.3	105.0	10.0	5.0	59.0	58.1	29399	0	24971	356.7	1.6	
74	OK+OK	79.3	105.1	10.5	5.2	61.9	58.2	29425	0	24999	337.6	0.0	
77	OK+OK	79.4	104.6	11.0	5.3	64.8	58.2	29410	0	24999	283.1	1.7	
80	OK+OK	79.6	105.0	11.6	5.5	67.8	58.1	29420	0	24974	191.0	2.0	
83	OK+OK	79.6	104.6	12.1	5.6	70.7	58.2	29413	0	24989	232.7	0.7	
86	OK+OK	79.5	105.4	12.6	5.7	73.7	58.1	29404	0	24966	229.0	1.6	
89	OK+OK	79.4	106.0	13.2	5.9	76.6	58.1	29404	0	24963	356.6	2.0	
92	OK+OK	79.5	106.6	13.7	6.0	79.6	58.0	29391	0	24923	49.9	1.2	
95	OK+OK	79.5	106.0	14.2	6.2	82.5	58.2	29426	0	24999	358.1	0.9	
98	OK+OK	79.5	107.0	14.7	6.4	85.5	58.1	29430	0	24973	28.3	1.8	
101	OK+OK	79.7	107.8	15.3	6.5	88.4	57.9	29428	0	24935	91.4	2.2	
104	OK+OK	79.6	107.1	15.8	6.7	91.4	58.0	29403	0	24937	41.3	1.2	
107	OK+OK	79.6	107.1	16.3	6.8	94.3	58.1	29402	0	24971	359.2	0.0	
110	OK+OK	79.7	106.7	16.8	7.0	97.3	58.2	29393	0	24976	319.8	1.2	
113	OK+OK	79.9	107.2	17.3	7.2	100.3	58.1	29420	0	24981	207.4	2.4	
116	OK+OK	79.9	107.1	17.8	7.3	103.2	58.2	29401	0	24978	272.0	0.8	
119	OK+OK	80.0	108.7	18.3	7.5	106.2	58.0	29401	0	24926	129.4	3.0	
122	OK+OK	79.8	108.7	18.8	7.6	109.1	58.0	29422	0	24955	33.4	2.0	
125	OK+OK	80.0	108.0	19.3	7.8	112.1	58.0	29400	0	24946	177.2	2.8	
128	OK+OK	79.9	109.8	19.8	8.0	115.0	58.0	29420	0	24937	97.3	3.2	
131	OK+OK	80.0	108.3	20.3	8.1	118.0	58.1	29408	0	24968	233.8	2.8	
134	OK+OK	80.0	108.5	20.8	8.3	120.9	58.1	29388	0	24957	215.6	0.6	
137	OK+OK	80.1	109.6	21.3	8.5	123.9	58.0	29386	0	24924	166.7	1.9	
140	OK+OK	80.0	110.0	21.8	8.7	126.8	58.0	29362	0	24893	71.4	1.1	
143	OK+OK	80.1	110.7	22.2	8.8	129.8	57.9	29376	0	24892	108.4	1.9	
146	OK+OK	80.3	109.3	22.7	9.0	132.8	58.1	29386	0	24935	179.3	2.7	
149	OK+OK	80.2	109.3	23.2	9.2	135.7	57.9	29207	0	24752	216.2	0.3	
152	OK+OK	80.3	109.9	23.7	9.3	138.7	58.0	29371	0	24910	179.8	1.4	
155	MD+MT	80.4	112.3	24.2	9.5	141.6	57.7	28472	0	24075	187.0	4.1	
158	MD+MT	80.3	113.9	24.6	9.7	144.6	56.4	26765	0	22302	240.6	2.7	
161	OK+MT	80.2	108.3	25.1	9.9	147.5	58.3	28565	0	24303	339.7	9.6	
164	OK+OK	80.1	111.8	25.6	10.1	150.5	58.1	29137	0	24736	20.0	6.0	
167	MD+OK	80.2	111.9	26.0	10.3	153.4	57.7	29097	0	24599	77.9	0.7	
170	OK+OK	80.4	111.5	26.5	10.5	156.4	57.9	29078	0	24643	172.5	2.1	

4.1.2 Possible errors to be avoided in orienting core

It is crucial to note that insitu rock quality determination plays a pivotal role in pillar design as such sources of error must be addressed from the onset. The orientation mark has to be correct and precise and this largely depends on the driller's technique and expertise. An emphasis on the need of precision and accuracy has to be made. There is need to extend the orientation mark precisely. Normally there is a tendency to drill holes in one particular orientation. It is crucial to vary drilling orientation if we are to ensure all joint sets are intersected. Surface mappings done at an earlier stage has to be reconciled with multiple orientation results to ascertain if enough orientations have been done to pick all the joint sets. This has a bearing in RQD determination.

4.2 Logging Practice

After core has been oriented it is then logged as a way to determine the geotechnical parameters influencing pillar design. When logging core, particular attention has to be given to Quality Analysis and Quality Control (QA/QC) issues. A step by step guidance has to be in place to prevent concentration on unnecessary detail and there has to be a system in place to ensure compliance. The system has to ensure that all the particular geotechnical characteristics are determined to a reliable level of accuracy. Geotechnical logging was done to pave way for rock mass classification. Rock mass classification schemes can be used to build up a picture of the composition and characteristics of a rock mass, therefore providing estimates of the strength and deformation properties of the rock mass. It is these parameters which are necessary when calculating pillar strength.

The following is a discussion on the logging practice undertaken at the exploration site. A total of 50 boreholes were geotechnically logged by the author of which 4 were oriented (BO53A, BO54A, BO55A and BO61A). The oriented boreholes are used in this discussion as they capture much geotechnical detail of the rockmass compared to the unoriented boreholes. BO53A is used for illustrative purposes in the text while geotechnical logs for BO54A and BO55A are given in Appendices 3 and 4 respectively for the reader's reference. Photos for BO53A, BO54A and BO55A are presented in Appendix 2. The logging was done in three stages. Three meter runs were used for the assessment. Although geotechnical assessments were done throughout each drill hole, the main zone of interest is the reef horizon and immediate upper and lower positions surrounding it. As such these are the areas presented for the sake of this discussion to maintain brevity and clarity.

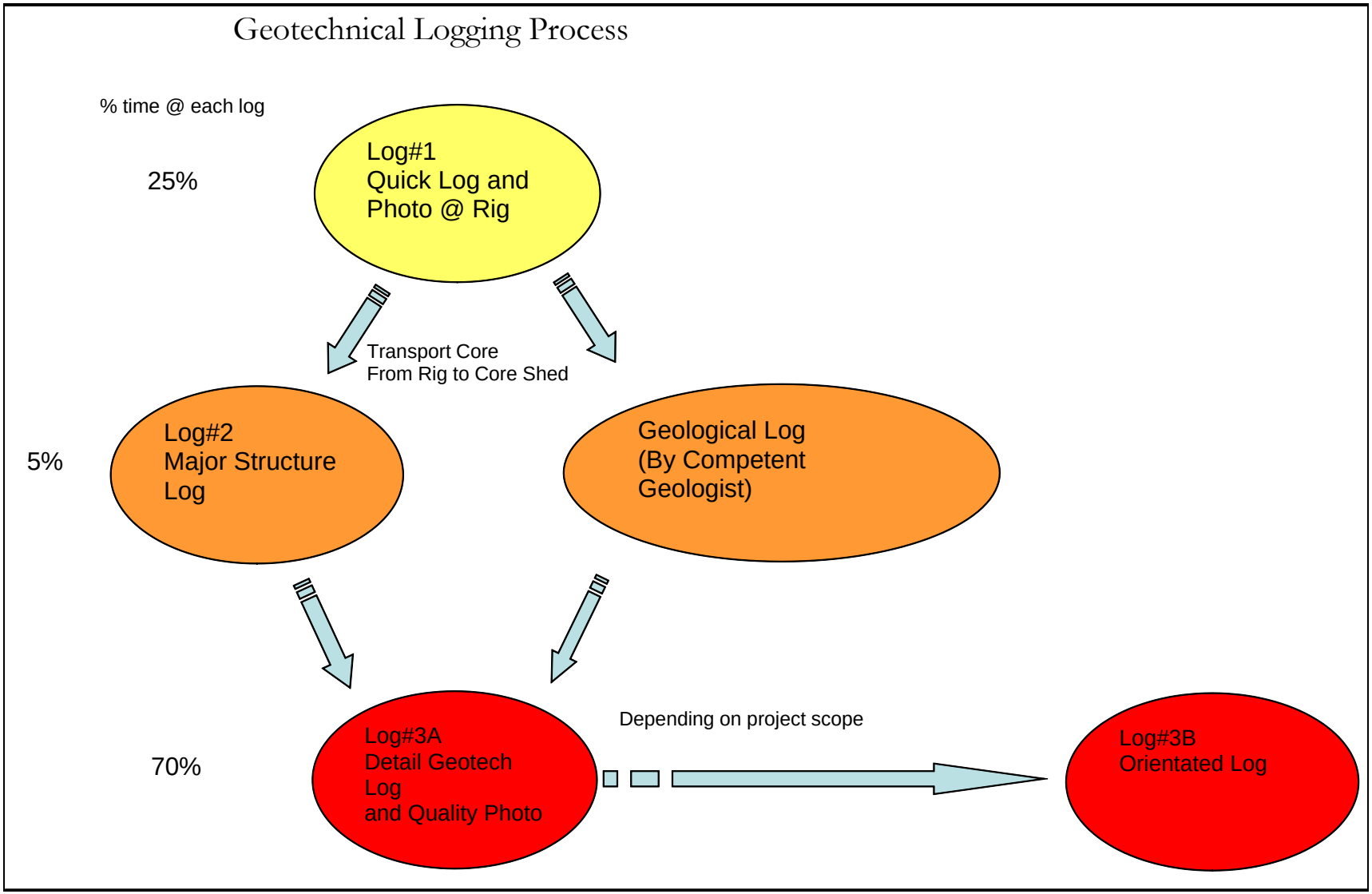

Figure 4.3: Logging process adopted at the Exploration Site (SRK Logging Manual, 2006)

Figure 4.3 presents a flow chart of how geotechnical logging was done on the site. The detailed description of the logging process is given in the following discussions.

4.2.1 Quick Log Per Run - Log 1

Log1 was a quick log per run capturing rock type, Total Core Recovery (TCR), Solid Core Recovery (SCR), Rock Quality Designation (RQD) as well as photos and short comments per run. The quick log per run is shown in Table 4.2. Total Core Recovery is the sum of all measurable core recovered in one drill run while SCR is defined as the sum of all sections of the core run that are greater than 1 core diameter. Sections of core with multiple mechanical breaks and handling breaks need to be considered as solid core. RQD is the ratio of the core recovered counting pieces greater than 100 mm to the total length of the run expressed as a percentage. It is imperative to note that breakages due to handling and drilling have to be ignored and core taken to be continuous at these points when calculating RQD. There has to be a guideline which enables the logger to pick these mechanical breaks. RQD is used for qualitative analysis of rock strength. Weak rock types like kimberlite may have low joint counts and thereby record high RQD. This RQD, when used in Rock Mass Classification gives an unrepresentative high value. Due to this, rock samples are send to the laboratory for quantitative rock mass strength analysis.

Table 4.2: Quick Log per run for borehole BO53A

Log#1 - Quick Log Per Run

TODAL MINING - GEOTECHNICAL

Site: Bokai | Hole Number: BO53A | Hole Position | **PC Input**

Bearing: 102 | x: 30 01 03.3 | By: Tawanda

Logged by: Tawanda | Plunge: -80 | y: 19 47 47.9 | Checked: Tawanda

z: 1 155 | Page no: 2 of 10

From (m)	To (m)	Rock Type	TCR (m)	SCR (m)	[RQD] Length >100mm	Photo Number	Comments
83.45	86.45	Anothositic norite	3.00	3.00	3.00	BO53A-14,15	Wholely intact rock
86.45	89.45	Anothositic norite	3.02	3.02	3.02	BO53A-15	OCJ @ 87.04, RIR
89.45	92.45	Anothositic norite	2.99	2.99	2.99	BO53A-15,16	Wholely intact rock
92.45	95.45	Anothositic norite	3.00	3.00	3.00	BO53A-16	Wholely intact rock
95.45	98.45	Anothositic norite	2.95	2.95	2.95	BO53A-16,17	Wholely intact rock
98.45	101.45	Anothositic norite	3.00	3.00	2.95	BO53A-17	OCJs @ 100.11, 100.73,100.78, 101.14, RIR
101.45	104.45	Anothositic norite	3.00	3.00	2.96	BO53A-17,18	FZ btwn 102.21 & 102.25, RIR
104.45	107.45	Anothositic norite	3.00	3.00	3.00	BO53A-18	Wholely intact rock
107.45	110.45	Anothositic norite	3.00	3.00	3.00	BO53A-18,19	OCJ @ 109.43, RIR
110.45	113.45	Anothositic norite	3.00	3.00	3.00	BO53A-19,20	OCJ @ 111.92
113.45	116.45	Anothositic norite	2.98	2.98	2.98	BO53A-20	Wholely intact rock
116.45	119.45	Anothositic norite	3.04	3.04	3.04	BO53A-20,21	Wholely intact rock
119.45	122.45	Anothositic norite	2.99	2.99	2.99	BO53A-21	Wholely intact rock
122.45	125.45	Anothositic norite	3.01	3.01	3.01	BO53A-21,22	Wholely intact rock
125.45	128.45	Anothositic norite	2.96	2.96	2.96	BO53A-22	OCJ @ 126.34, RIR
128.45	131.45	Anothositic norite	2.98	2.98	2.73	BO53A-22,23	FZ btwn 130.79 & 131, FZ btwn 131.41 & 131.45, RIR
131.45	134.45	Anothositic norite	2.91	2.91	2.77	BO53A-23	OCJs @ 132.03, 132.23, FZ btwn 133.04 & 133.18, OCJs @ 133.42, 134.19, RIR
134.45	137.45	Anothositic norite	2.94	2.94	2.94	BO53A-23,24	OCJs @ 135.44, 135.95, RIR
137.45	140.45	Anothositic norite	3.00	3.00	3.00	BO53A-24	OCJs @ 138.65, 138.71,RIR
140.45	143.45	Anothositic norite	2.80	2.80	2.80	BO53A-24,25	OCJs @ 140.79, 140.99, 142.59, 142.72, RIR
143.45	146.45	Anothositic norite	2.75	2.75	2.75	BO53A-25	OCJs @ 144.98, RIR
146.45	149.45	Anothositic norite & Websterite @ 148.31	3.02	3.02	2.75	BO53A-25,26	OCJs @ 146.93, 147.38, 147.99,148.11, FZ btwn 148.95 & 149.22, RIR
149.45	152.45	Websterite	3.04	3.04	3.04	BO53A-26,27	OCJs @ 149.45, 149.69, 150.26, 150.99, 151.51, 151.97, RIR
152.45	155.45	Websterite	3.00	3.00	3.00	BO53A-27	OCJs @ 154.19, 154.39, RIR
155.45	158.45	Websterite & Bronzitite @ 155.46	2.97	2.97	2.97	BO53A-27,28	OCJs @ 157.13, 158.45, RIR
158.45	161.45	Bronzitite	3.05	3.05	2.46	BO53A-28	OCJ @ 159.22, CJ @ 159.97, FZ btwn 160.86 & 161.45, RIR
161.45	164.45	Bronzitite	2.95	2.95	2.89	BO53A-28,29	FZ btwn 161.45 & 161.51, OCJs @ 162.06, 162.42, FZ btwn 163.57 & 163.62, RIR
164.45	167.45	Bronzitite	3.00	1.89	0.93	BO53A-29	FZ btwn 165.26 & 167.45, RIR
167.45	170.45	Bronzitite	3.01	3.01	2.82	BO53A-29,30	FZ btwn 167.45 & 167.64, OCJs @ 168.83, 168.98, CJ @ 169.23, OCJ @ 169.51, CJs @ 170.17, 170.21, OCJ @ 170.37, RIR

Table 4.3: Major structures log for borehole BO53A

Log#2 - Major Structures

TODAL MINING - GEOTECHNICAL

Site: Bokai | Hole Number: BO53A | Hole Position | **PC Input**

Bearing: 102 | **X:** 30 01 03.3 | By: Tawanda

Logged by: Tawanda | Plunge: -80 | **Y:** 19 47 47.9 | Checked by: Tawanda

Z: 1 155 | Page no: 6 of 10

Distance or Interval		Visual Log	Structure Type		Typical Orientation			Brittle Structure Properties			Water Staining	Description
From	To		Code	Class	Alpha	Beta	Stick (T)op or (B)ottom	Micro-scale Geometry	Infill	Alteration		
83.45	86.45											Wholely intact rock
86.45	87.04		J	2	30	60	B	8	SP	1	√	1OCJ, faulted with displacement, RIR
87.04	89.45											Wholely intact rock
89.45	92.45											Wholely intact rock
92.45	95.45											Wholely intact rock
95.45	98.45											Wholely intact rock
98.45	100.11		J	2	35	316.8	B	8	SP	1	√	1OCJ, faulted with displacement, RIR
100.11	100.73		J	2	60	180	B	8	SP	1	√	1OCJ, faulted with displacement, RIR
100.73	100.78		J	2	60	180	B	8	SP	1	√	1OCJ, faulted with displacement, RIR
100.78	101.14		J	2	60	180	B	8	SP	1	√	1OCJ, faulted with displacement, RIR
101.14	102.21											Wholely intact rock
102.21	102.25		FZ	3					SP	3	√	Rock mass weakened by strong fracturing
102.25	104.45											Wholely intact rock
104.45	107.45											Wholely intact rock
107.45	109.43		J	2	85	278.4	B	8	SP	1	√	1OCJ, faulted with displacement, RIR
109.43	111.92		J	2	45	316.8	B	8	SP	1	√	1OCJ, faulted with displacement, RIR
111.92	113.45											Wholely intact rock
113.45	116.45											Wholely intact rock
116.45	119.45											Wholely intact rock
119.45	122.45											Wholely intact rock
122.45	125.45											Wholely intact rock
125.45	126.34		J	2	55	213.6	B	8	SP	1	√	1OCJ, faulted with displacement, RIR
126.34	130.79											Wholely intact rock
130.79	131.00		FZ	3					SP	3	√	Rock mass weakened by strong fracturing
131.00	131.41											Wholely intact rock
131.41	131.45		FZ	3					SP	3	√	Rock mass weakened by strong fracturing
131.45	132.03		J	2	25	276	B	8	SP	1	√	1OCJ, faulted with displacement, RIR
132.03	132.23		J	2	25	276	B	8	SP	1	√	1OCJ, faulted with displacement, RIR
132.23	133.04											Wholely intact rock
133.04	133.18		FZ	3					SP	3	√	Rock mass weakened by strong fracturing
133.18	133.42		J	2	25	276	B	8	SP	1	√	1OCJ, faulted with displacement, RIR
133.42	134.19		J	2	25	276	B	8	SP	1	√	1OCJ, faulted with displacement, RIR
134.19	135.44		J	2	15	276	B	8	SP	1	√	1OCJ, faulted with displacement, RIR
135.44	135.95		J	2	15	276	B	8	SP	1	√	1OCJ, faulted with displacement, RIR
135.95	138.65		J	2	15	0	B	8	SP	1	√	1OCJ, faulted with displacement, RIR
138.65	138.71		J	2	15	0	B	8	SP	1	√	1OCJ, faulted with displacement, RIR
138.71	140.79		J	2	60	67.2	B	8	SP	1	√	1OCJ, faulted with displacement, RIR
140.79	140.99		J	2	60	67.2	B	8	SP	1	√	1OCJ, faulted with displacement, RIR
140.99	142.59		J	2	45	213.6	B	7	SP	1	√	1OCJ, faulted with displacement, RIR
142.59	142.72		J	2	45	213.6	B	7	SP	1	√	1OCJ, faulted with displacement, RIR
142.72	144.98		J	2	20	180	B	8	SP	1	√	1OCJ, faulted with displacement, RIR
144.98	146.33		J	2	20	180	B	8	SP	1	√	1OCJ, faulted with displacement, RIR
146.33	146.93		J	2	30	180	B	8	SP	1	√	1OCJ, faulted with displacement, RIR
146.93	147.38		J	2	30	180	T	8	SP	1	√	1OCJ, faulted with displacement, RIR

Structure Code Table

Structure		Code
Shear Zone		SZ
Fracture Zone		FZ
Fault		F
Fracture		Fr
Joint		J
Striation lineation		L
Fold Axis		FA
Vein		V
Dyke		D

Structure Class Table

Class	Description
1	Strongly sheared (cataclasite/mylonite), or brecciated
2	Clearly faulted with displacement or striations
3	The rock mass is weakened by alteration or strong fracturing, a nearby major structure is likely.
4	The core is completely broken because of poor core recovery. Possibly structure related
5	Core is strongly or completely altered/weathered to residual soil/mud.

Wall Alteration

1 - wall=rock hardness

2 - wall>rock hardness

3 - wall<rock hardness

Fill Type

Q - Quartz	G - Gouge
C - Calcite	M - Magnesium
FE - Iron oxide	H - Haematite
CL - Clay	S - Sulphide
B - Breccia	O - Other

Micro/Small Scale Joint Expression

Rough/Stepped/Irregular - 1

Smooth Stepped - 2

Slickensided Stepped - 3

Rough Undulating - 4

Smooth Undulating - 5

Slickensided Undulating - 6

Rough Planar - 7

Smooth Planar - 8

Polished - 9

Table 4.4: Major structures log for borehole BO53A (Continuation)

Log#2 - Major Structures

TODAL MINING - GEOTECHNICAL

Site: Bokai | Hole Number: BO53A | Hole Position | **PC Input**

Bearing: 102 | **X:** 30 01 03.3 | By: Tawanda

Logged by: Tawanda | Plunge: -80 | **Y:** 19 47 47.9 | Checked by: Tawanda

Z: 1 155 | Page no: 7 of 10

Distance or Interval		Visual Log	Structure Type		Typical Orientation			Brittle Structure Properties			Water Staining	Description
From	To		Code	Class	Alpha	Beta	Stick (T)op or (B)ottom	Micro-scale Geometry	Infill	Alteration		
147.38	147.99		J	2	30	180	T	8	SP	1	√	1OCJ, faulted with displacement, RIR
147.99	148.11		J	2	30	180	T	8	SP	1	√	1OCJ, faulted with displacement, RIR
148.11	148.95		_	_	_	_	_	_	_	_	_	Wholely intact rock
148.95	149.22		FZ	3	_	_	_	_	SP	3	√	Rock mass weakened by strong fracturing
149.22	149.45		J	2	85	336	B	8	SP	1	√	1OCJ, faulted with displacement, RIR
149.45	149.69		J	2	85	336	B	8	SP	1	√	1OCJ, faulted with displacement, RIR
149.69	150.26		J	2	85	336	B	8	SP	1	√	1OCJ, faulted with displacement, RIR
150.26	150.99		J	2	15	108	T	8	SP	1	√	1OCJ, faulted with displacement, RIR
150.99	151.51		J	2	15	108	B	8	SP	1	√	1OCJ, faulted with displacement, RIR
151.51	151.97		J	2	40	96	B	8	SP	1	√	1OCJ, faulted with displacement, RIR
151.97	154.19		J	2	15	0	B	8	SP	1	√	1OCJ, faulted with displacement, RIR
154.19	154.39		J	2	15	0	B	8	SP	1	√	1OCJ, faulted with displacement, RIR
154.39	157.13		J	2	45	84	B	8	SP	1	√	1OCJ, faulted with displacement, RIR
157.13	158.45		J	2	85	312	B	8	SP	1	√	1OCJ, faulted with displacement, RIR
158.45	159.22		J	2	15	0	B	8	SP	3	√	1OCJ, faulted with displacement, RIR
159.22	159.97		J	2	15	_	_	8	SP	1	√	1OCJ, faulted with displacement, RIR
159.97	160.86		_	_	_	_	_	_	_	_	_	Wholely intact rock
160.86	161.45		FZ	3	_	_	_	_	SP	3	√	Rock mass weakened by strong fracturing
161.45	161.51		FZ	3	_	_	_	_	SP	3	√	Rock mass weakened by strong fracturing
161.51	162.06		J	2	45	223.2	B	7	SP	1	√	1OCJ, faulted with displacement, RIR
162.06	162.42		J	2	45	223.2	B	7	SP	1	√	1OCJ, faulted with displacement, RIR
162.42	163.57		_	_	_	_	_	_	_	_	_	Wholely intact rock
163.57	163.62		FZ	3	_	_	_	_	SP	3	√	Rock mass weakened by strong fracturing
163.62	165.26		_	_	_	_	_	_	_	_	_	Wholely intact rock
165.26	167.45		FZ	3	_	_	_	_	SP	3	√	Rock mass weakened by strong fracturing
167.45	167.64		FZ	3	_	_	_	_	SP	3	√	Rock mass weakened by strong fracturing
167.64	168.83		J	2	75	180	B	7	SP	1	√	1OCJ, faulted with displacement, RIR
168.83	168.98		J	2	75	180	B	7	SP	1	√	1OCJ, faulted with displacement, RIR
168.98	169.23		J	2	75	180	B	7	SP	1	√	1OCJ, faulted with displacement, RIR
169.23	169.51		J	2	15	120	B	7	SP	1	√	1OCJ, faulted with displacement, RIR
169.51	170.17		J	2	60	_	_	_	SP	1	√	1CJ, faulted with displacement, RIR
170.17	170.21		J	2	60	_	_	_	SP	1	√	1CJ, faulted with displacement, RIR
170.21	170.37		J	2	70	28.8	B	4	SP	1	√	1OCJ, faulted with displacement, RIR
170.37	170.45		_	_	_	_	_	_	_	_	_	Wholely intact rock

Structure Code Table

Structure		Code
Shear Zone		SZ
Fracture Zone		FZ
Fault		F
Fracture		Fr
Joint		J
Striation lineation		L
Fold Axis		FA
Vein		V
Dyke		D

Structure Class Table

Class	Description
1	Strongly sheared (cataclasite/mylonite), or brecciated
2	Clearly faulted with displacement or striations
3	The rock mass is weakened by alteration or strong fracturing, a nearby major structure is likely.
4	The core is completely broken because of poor core recovery. Possibly structure related
5	Core is strongly or completely altered/weathered to residual soil/mud.

Wall Alteration

1 - wall=rock hardness
2 - wall>rock hardness
3 - wall<rock hardness

Fill Type

Q - Quartz	G - Gouge
C - Calcite	M - Magnesium
FE - Iron oxide	H - Haematite
CL - Clay	S - Sulphide
B - Breccia	O - Other

Micro/Small Scale Joint Expression

Rough/Stepped/Irregular - 1
Smooth Stepped - 2
Slickensided Stepped - 3
Rough Undulating - 4
Smooth Undulating - 5
Slickensided Undulating - 6
Rough Planar - 7
Smooth Planar - 8
Polished - 9

Table 4.5: Detailed Geotechnical Log for borehole BO53A

Log#3 - Detail Geotech Log

TODAL MINING- GEOTECHNICAL

Site: Bokai

Logged by: Tawanda

Hole Number: BO53A
Bearing: 102
Plunge: -80

Hole Position
X: 30 01 03.3
Y: 19 47 47.9
Z: 1 155

PC Input
By: Tawanda
Checked: Tawanda
Page no: 10 of 10

From	To	Rock Type	Intact Rock Strength			Fracture Frequency						Joint Condition (Micro/Filling/Alteration)						Cemented Joints		Micro Fractures	
												Set 1		Set 2		Set 3					
			Strong Mpa	Weak Mpa	% Weak	Total	Natural	Foliation	Set 1	Set 2	Set 3	α/β	MFA	α/β	MFA	α/β	MFA	Count	Fill Type	Intensity Count/m	Fill Type (if any)
83.45	86.45	Anothositic norite	R5																		
86.45	89.45	Anothositic norite	R5			1	1		1			0.5	8SP1					1	SP		
89.45	92.45	Anothositic norite	R5																		
92.45	95.45	Anothositic norite	R5																		
95.45	98.45	Anothositic norite	R5																		
98.45	101.45	Anothositic norite	R5			4	4		1	3		0.11	8SP1	0.333	8SP1			4	SP		
101.45	104.45	Anothositic norite	R5	R4	1.0133	3	3		3				SP3								
104.45	107.45	Anothositic norite	R5																		
107.45	110.45	Anothositic norite	R5			1	1		1			0.305	8SP1					1	SP		
110.45	113.45	Anothositic norite	R5			1	1		1			0.142	8SP1					1	SP		
113.45	116.45	Anothositic norite	R5																		
116.45	119.45	Anothositic norite	R5																		
119.45	122.45	Anothositic norite	R5																		
122.45	125.45	Anothositic norite	R5																		
125.45	128.45	Anothositic norite	R5			1	1		1			0.257	8SP1					1	SP		
128.45	131.45	Anothositic norite	R5	R4	8.39	5	5		3	2			SP3		SP3						
131.45	134.45	Anothositic norite	R5	R4	4.81	8	8		2	4	2	0.0906	8SP1		SP3	0.0906	8SP1	4	SP		
134.45	137.45	Anothositic norite	R5			2	2		2			0.054	8SP1					2	SP		
137.45	140.45	Anothositic norite	R5			2	2		2			∞	8SP1					2	SP		
140.45	143.45	Anothositic norite	R5			4	4		2	2		0.893	8SP1	0.211	8SP1			4	SP		
143.45	146.45	Anothositic norite	R5			2	2		2			0.111	8SP1					2	SP		
146.45	149.45	Anothositic norite & Websterite @ 148.31	R5	R3	8.94	8	8		4	3		0.167	8SP1		SP3			4	SP		
149.45	152.45	Websterite	R5			6	6		3	2	1	0.253	8SP1	0.139	8SP1	0.4167	8SP1	6	SP		
152.45	155.45	Websterite	R5			2	2		2			∞	8SP1					2	SP		
155.45	158.45	Websterite & Bronzitite @ 155.46	R5			2	2		1	1		0.536	8SP1	0.272	8SP1			2	SP		
158.45	161.45	Bronzitite	R4	R3	19.34	8	8		2	6		∞	8SP1		SP3			2	SP		
161.45	164.45	Bronzitite	R4	R2	7.32	10	10		5	2	3		SP3	0.202	7SP1		SP3	2	SP		
164.45	167.45	Bronzitite	R4	R2	31	23	23		23				SP3								
167.45	170.45	Bronzitite	R4			10	10		3	3	2		SP3	0.417	7SP1		SP1	7	SP		

Micro/Small Scale Joint Expression

Rough/Stepped/Irregular - 1
Smooth Stepped - 2
Slickensided Stepped - 3
Rough Undulating - 4
Smooth Undulating - 5
Slickensided Undulating - 6
Rough Planar - 7
Smooth Planar - 8
Polished - 9

Fill Type	
Q - Quartz	G - Gouge
C - Calcite	M - Magnesium
FE - Iron oxide	H - Haematite
CL - Clay	S - Sulphide
B - Breccia	O - Other

Wall Alteration
1 - wall=rock hardness
2 - wall>rock hardness
3 - wall<rock hardness

4.2.2 Major Structures - Log 2

The evaluation key for these structures is as given in Table 4.3 and Table 4.4. At this stage all major structures which have a bearing on the rock mass quality are logged and evaluated. The structures include Shear Zones, Fracture Zones, Faults, Fractures, Joints, Striation Lineations, Fold Axis, Veins and Dykes. Also logged at this stage are Typical Orientations and Brittle properties of these structures. Water staining properties of the discontinuities were evaluated. When water pressure is present in a rock mass, the surfaces of the discontinuities are forced apart and the normal stress on the discontinuity is reduced. This in turn reduces the shear strength of the discontinuities. For the typical orientations, angles α and β were measured. A graduated strip and a carpenter's angle were used to measure these orientation parameters. SRK Geotechnical Core Logging Manual (2006) was used as a guide. Alpha angle (α): the carpenter angle is used to measure the maximum dip (α) of the feature relative to the core axis. Beta angle (β): The plastic calibrated strip is placed with the "0" on the orientation line of the same piece of core and the tape is wrapped clockwise around the core so that the 360º point returns to the orientation line. The angle (β) is then measured, clockwise, to the bottom of the ellipse. In this convention, only the upper part of the feature is used for the measurement. The measured angles are as illustrated in Figure 4.4.

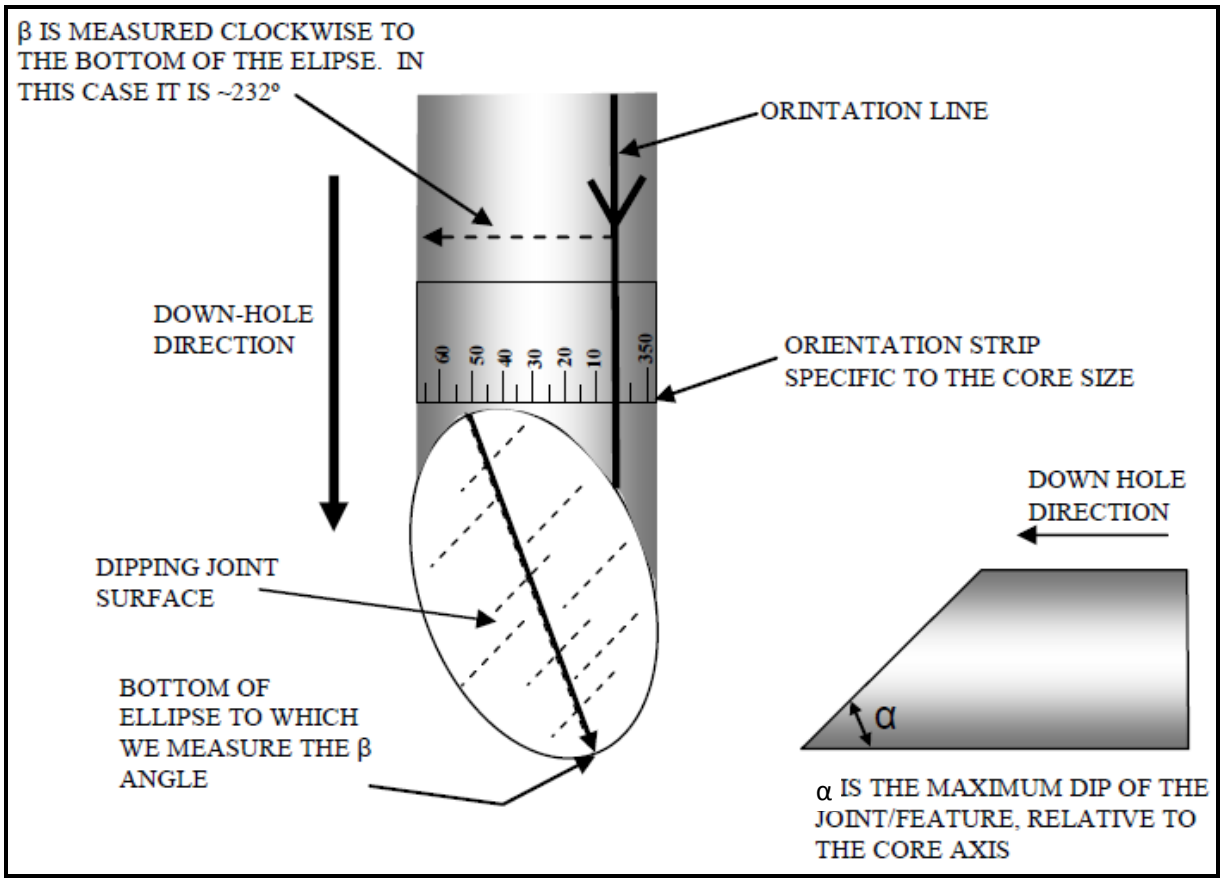

Figure 4.4: Illustration of how Beta (β) and Alpha (α) angles were determined in the project (SRK Logging Manual, 2006)

4.2.3 Error Concern Areas for Major Structures Logging

There is often a challenge in differentiating between cemented joints and open joints from the discontinuities which exist in the drill core. For this reason it is rational to consider an open cemented joint in the drill core as an open joint fracture since the joint is weak hence why it easily opens up. Joint infill type has an influence on the strength of joints so expertise is required to differentiate the various infill types. Joint strength is also affected by alteration so alteration analysis knowledge is critical. Estimation or averaging of joint parameters can also be a challenge. The influence of a joint set on excavation stability is dependent on the joint set orientation. It follows that it is advisable to assess joint conditions for individual sets as this enables us to clearly pick the joint set with the most effect on pillar stability and adjust our design appropriately.

4.3 Detailed Geotechnical Log – Log 3

At this stage initial estimate of rock strength was done using a geological hammer. Rock strength was measured on a scale of R1 to R6 depending on its response to a knock by the

geological hammer. R1 signifies highest strength while R6 is for weakest rock. A reconciliation of the geological hammer results was done by sending samples of the rock for laboratory strength tests, the results of which are shown in Table 4.6.

For more accurate results the author observed that it is necessary to adopt an evaluation scale for weak rock which quantifies the level of weakness. A scale of S1 to S6 can be used lest we lose much detail. It was also observed that IRS is affected by elements such as microdefects, foliation and schistocity so for representative samples sampling has to be done in multiple orientations. Detailed Geotechnical logging was done on a domain basis so as to pick sections of the core with the same geotechnical characteristics. The domains were kept to less than 3 m to preserve accuracy by avoiding over averaging. In addition to IRS, other parameters evaluated were fracture frequency, joint conditions, cemented joint count and micro fractures. For more detail see Table 4.5.

4.4 Overall Considerations in geotechnical logging

The geotechnical logging should suite the rockmass classification system to be used. It is imperative for the geotechnical logging sheet to accommodate all the parameters which will be used in the calculation of pillar strength. The logging sheet and instructions should be presented in a way which is easy to understand to minimise human errors and increase accuracy and precision.

Table 4.6: Results of Uniaxial Compressive Strength Tests

RESULTS OF UNIAXIAL COMPRESSIVE STRENGTH TESTS WITH MODULUS & POISSON'S RATIO MEASUREMENTS BY MEANS OF STRAIN GAUGES

ROCKLAB
DIVISION OF SOILLAB (PTY) LTD
Tel: 012 481 3894
Fax: 012 481 3812
E-mail: Chenj@rocklab.co.za

Client: Badger Mining Sampling Location: Zimbabwe

19-Mar-09

SPECIMEN PARTICULARS				SPECIMEN DIMENSIONS					SPECIMEN TEST RESULTS								
Rocklab Specimen No 3569-	Sample No	Sample Depth From.. To.. (m)	Rock Type	Diameter mm	Height mm	Ratio of Height to Diameter	Mass g	Density g/cm³	Failure Load kN	Strength (UCS) MPa	Tangent Elastic Modulus @ 50% UCS GPa	Secant Elastic Modulus @ 50% UCS GPa	Poisson's Ratio Tangent @ 50% UCS	Poisson's Ratio Secant @ 50% UCS	Linear Axial Strain at Failure mm/mm	Failure Code	Note
UCM-01A	GT53/1	146.00 - 146.16		47.12	111.8	2.4	560.6	2.88	388.1	222.6	105.0	107.0	0.21	0.20	0.002267	XB	
UCM-01B	GT53/4	146.50 - 146.70	Gabbro - Norite	47.11	120.9	2.6	605.8	2.87	226.4	129.9	116.0	103.0	0.34	0.26	0.001244	2B	
UCM-01C	GT53/10	147.38 - 147.61		47.14	80.2	1.7	393.7	2.81	203.6	116.7	94.9	95.9	0.27	0.24	0.001334	5B	
UCM-02A	TM2014	158.54 - 158.69		47.33	114.4	2.4	639.3	3.18	241.1	137.0	100.0	107.0	0.31	0.27	0.001671	XA	
UCM-02B	TM2016	158.84 - 158.99	Bronzitite	47.30	116.0	2.5	654.2	3.21	260.1	148.0	99.4	101.0	0.30	0.21	0.001921	XA	
UCM-02C	TM2018	159.29 - 159.44		47.29	118.9	2.5	675.8	3.24	301.7	171.8	134.0	142.0	0.30	0.31	0.001546	XB	

Note: All tests were conducted according to the ISRM's specfications.

Table 4.7: Results of Triaxial Compressive Strength Tests

RESULTS OF TRIAXIAL COMPRESSIVE STRENGTH TESTS WITH ELASTIC MODULUS AND POISSON'S RATIO MEASUREMENTS BY MEANS OF STRAIN GAUGES

ROCKLAB
DIVISION OF SOILLAB (PTY) LTD
Tel: 012 481 3894
Fax: 012 481 3812
E-mail: Chenj@rocklab.co.za

Client: Badger Mining (Pty) Ltd. Samping Location: Zimbabwe

31-Mar-09

SPECIMEN PARTICULARS				SPECIMEN DIMENSIONS					SPECIMEN TEST RESULTS									
Rocklab Specimen No 3569-	Sample No.	Sample Depth From.. To (m)	Rock Type	Diameter mm	Height mm	Ratio of Height to Diameter	Mass g	Density g/cm³	Confining Pressure σ_3 Mpa	Failure Load P kN	Strength (TCS) σ_1 MPa	Tangent Elastic Modulus @ 50% TCS GPa	Secant Elastic Modulus @ 50% TCS GPa	Tangent Poisson's Ratio @ 50% TCS	Secant Poisson's Ratio @ 50% TCS	Linear Axial Strain at Failure mm/mm	Failure Code	Note
TCM-01A	GT53/2	146.16 - 146.33	Gabbro - Norite	47.09	99.2	2.1	499.6	2.89	10	475.7	273.1	99.1	101.0	0.34	0.27	0.002790	XA	
TCM-01B	GT53/3	146.33 - 146.5		47.12	98.0	2.1	491.8	2.88	20	608.1	348.7	89.8	102.0	0.30	0.33	0.003977	XA	
TCM-01C	GT53/5	146.70 - 146.85		47.11	96.6	2.1	478.9	2.84	30	394.1	226.1	97.9	126.0	0.18	0.23	0.002138	XA	
TCM-01D	GT53/6	146.85 - 146.93		47.12	94.3	2.0	467.7	2.84	40	555.1	318.3	93.4	103.0	0.30	0.33	0.003067	8B	
TCM-01E	GT53/7	146.93 - 147.08		47.12	100.1	2.1	495.6	2.84	10	489.7	280.8	89.2	100.0	0.33	0.28	0.003681	6B	
TCM-01F	GT53/8	147.08 - 147.23		47.12	101.0	2.1	496.9	2.82	20	584.5	335.2	89.7	105.0	0.31	0.34	0.003607	XA	
TCM-01G	GT53/9	147.23 - 147.38		47.12	97.7	2.1	480.2	2.82	30	591.9	339.4	87.4	92.1	0.31	0.29	0.003847	4B	
TCM-01H	GT53/10	147.38 - 147.61		47.14	93.5	2.0	458.0	2.81	40	625.7	358.5	90.7	94.5	0.34	0.32	0.003469	3B	
TCM-02A	TM2007	157.49 - 157.64	Bronzitite	47.29	99.8	2.1	570.0	3.25	10	315.4	179.6	87.3	97.0	0.27	0.26	0.002244	XA	
TCM-02B	TM2008	157.64 - 157.79		47.30	97.6	2.1	548.1	3.19	20	402.9	229.3	85.8	104.0	0.31	0.37	0.002436	XA	
TCM-02C	TM2009	157.79 - 157.94		47.30	94.9	2.0	526.3	3.16	30	328.0	186.7	74.3	89.6	0.25	0.27	0.002953	XA	
TCM-02D	TM2010	157.94 - 158.09		47.27	98.3	2.1	540.2	3.13	40	357.3	203.6	72.6	88.7	0.26	0.32	0.003662	XA	
TCM-02E	TM2011	158.09 - 158.24		47.30	97.8	2.1	541.4	3.15	10	261.0	148.5	87.3	107.0	0.32	0.40	0.001569	XA	
TCM-02F	TM2012	158.24 - 158.39		47.29	100.8	2.1	560.6	3.17	20	291.2	165.8	89.1	101.0	0.25	0.26	0.001807	XA	
TCM-02G	TM2015	158.69 - 158.84		47.30	94.9	2.0	526.7	3.16	30	366.2	208.4	74.7	90.9	0.26	0.30	0.003648	XA	
TCM-02H	TM2017	158.99 - 159.14		47.29	99.8	2.1	566.5	3.23	40	469.1	267.1	92.5	119.0	0.24	0.27	0.002691	XA	

Note: All tests were conducted according to the ISRM's Specification. TCS - stands for Triaxial Compressive Strength.

Table 4.8: Results of rock specific gravity measurements

RESULTS OF ROCK SPECIFIC GRAVITY MEASUREMENTS

ROCKLAB
DIVISION OF SOILLAB (PTY) LTD
Tel: 012 481 3894
Fax: 012 481 3812
E-mail: Chenj@rocklab.co.za

Client: Badger Mining — Sampling site: Zimbabwe — 19-Mar-09

SPECIMEN PARTICULARS				SPECIFIC GRAVITY MEASUREMENTS				
Rocklab Specimen No 3569-	Sample No.	Borehole Depth From.. To.. m	Rock Type	Mass after OD 105ºc gram	Water Relative Density g/cc	Volume of the material cm^3	Bulk Specific Gravity g/cc	Note
SG-01	GT 53/1	146.00 - 146.16	Gabbro - Norite	49.29	0.998	17.1	2.870	
SG-03	GT 53/3	146.33 - 146.5		69.89	0.997	24.3	2.864	
SG-05	GT 53/5	146.70 - 146.85		66.33	0.997	23.1	2.864	
SG-07	GT 53/7	146.93 - 147.08		63.99	0.998	22.4	2.851	
SG-09	GT 53/9	147.23 - 147.38		66.75	0.998	23.8	2.803	
SG-11	GT 53/11	149.45 - 149.57	Websterite	51.01	0.998	16.2	3.141	
SG-13	GT 53/13	149.69 - 149.81		80.09	0.997	25.3	3.160	
SG-15	GT 53/15	149.93 - 150.05		49.37	0.998	15.3	3.225	
SG-17	TM 2007	157.49 - 157.64	Bronzitite	37.95	0.998	11.8	3.207	
SG-20	TM 2010	157.94 - 158.09		54.57	0.998	17.3	3.148	
SG-23	TM 2013	158.39 - 158.54		39.51	0.998	12.5	3.160	
SG-26	TM 2016	158.84 - 158.99		49.76	0.998	15.5	3.196	
SG-29	TM 2019	159.29 - 159.44		69.88	0.997	21.8	3.200	

4.5 Rock Characterisations for the geotechnical work done at the site.

Rock mass classification systems were used to estimate the strength of the rock mass which is an important parameter for determining pillar strength. The classification systems adopted for the project were Bieniawski's RMR, Barton's Q-system, and Laubscher's MRMR.

4.5.1 RMR

Rock Mass Rating is a Geomechanical Classification System introduced by Bieniawski in 1976. As more case records were examined he continuously refined it such that the ratings assigned to the different parameters have significantly changed. The latest Bieniawski's version of 1989 was used for the project. Beniawski makes use of 6 parameters to classify a rock mass. The parameters are:

1. Uniaxial compressive strength of rock material.
2. Rock Quality Designation (*RQD*).
3. Spacing of discontinuities.
4. Condition of discontinuities.
5. Groundwater conditions.
6. Orientation of discontinuities.

It can be noted all these parameters were catered for on the project logging atlas. Bieniawski (1989) developed a table for the classification parameters and their ratings as shown in Table AI, Appendix 1. The RMR value is calculated by picking the corresponding ratings for the parameters from the table and then summing them up. Bieniawski divides the rock mass into 5 classes as shown in Table 4.9.

Table 4.9: RMR classification table (Bieniawski, 1989)

CLASS	RMR	DESCRIPTION
I	81 – 100	Very good rock
II	61 – 80	Good rock
III	41 – 60	Fair rock
IV	21 – 40	Poor rock
V	<21	Very poor rock

4.5.2 Q-System

Barton et al, 1974 came up with the Tunnelling Quality Index (Q) after evaluating numerous underground excavations case histories. The index Q varies on a logarithmic scale and is measured from a minimum of 0.001 to a maximum of 1000 as described in Table 4.10.

Table 4.10: Q System classification (Barton et al, 1974)

Q INDEX VALUE	ROCK MASS CLASS
0.0001 – 0.01	Exceptionally poor
0.01 – 0.1	Extremely poor
0.1 – 1.0	Very poor
1 – 4	Poor
4 – 10	Fair
10 – 40	Good
40 - 100	Very good
100 – 400	Extremely good
400 - 1000	Exceptionally good

In this Classification System, Q is calculated as follows:

$$Q = \frac{RQD}{J_n} \times \frac{J_r}{J_a} \times \frac{J_w}{SRF} \quad \text{----------} \quad 52$$

Where:

RQD is the Rock Quality Designation

J_n is the joint set number

J_r is the joint roughness number

J_a is the joint alteration number

J_w is the joint water reduction factor

SRF is the stress reduction factor

4.5.3 Link between RMR and Q System

To make a comparison between the Bieniawski's RMR and the calculated RMR, transformation equations given below were used.

1. RMR = 9lnQ + 44 (Bieniawski, 1976)
2. RMR = 5lnQ + 60.8 (South African tunnels - Choquet and Hadjigeorgiou, 1993)

It was noted that results got using formula 1 deviated much from the Bieniawski RMR so formula 2 was used as it gave a closer correlation. Tables 4.11 gives the RMR values calculated from Q using formula 2.

4.5.4 Laubscher' MRMR

This system was developed based on caving operations witnessed by Laubscher in several countries in Africa. However, of late other case histories for mining operations have been captured in the data base.The Modified Rock Mass Rating system was brought about by Laubscher (1977, 1984), Laubscher and Taylor (1976) and Laubscher and Page (1990) to address the shortfalls of Bieniawski's RMR system. The MRMR system takes the RMR system and adjusts it for stress changes, insitu and induced stresses and the effects for blasting and weathering. The resultant MRMR value is accompanied with a set of support recommendations suitable for it. Table 4.11 gives the MRMR classification System results for the project.

Table 4.11: Bokai On-Reef Zone Rock Mass Classification – MRMR (Laubscher, 1990)

BOKAI ON-REEF ZONE ROCK MASS CLASSIFICATION – MRMR (LAUBSCHER, 1990)				
Bore Hole	**Zone (m)**	**RMR**	**Cumulative Adjustments**	**MRMR**
BO 56	45 – 53	59		40
IBO 01	114 – 122	74	Weathering	50
BO55A	119 - 127	72	96%	49
IBO 02	138 - 146	69		47
BO 54A	142– 150	75		51
IBO 03	171 – 179	63		43
BO 53A	150 – 158	70	Induced stress	47
IBO 11	182 - 190	77	100%	52
BO 052	143 – 151	69		47
BO 045	158 – 166	74		50
BO 051	115 - 123	81		55
BO 58	100 – 108	85	Joint orientation	58
BO 59	114 – 122	79	75%	53
BO 60	135 – 143	74		50
BO 61A	132 – 140	70		47
BO 62	94 – 102	72		49
BO 66	101 – 109	72	Blasting	49
BO 68	120 – 128	84	94%	57
BO 39	189 – 197	77		52
BO 41	130 – 138	57		39

4.6 Rock Mass Characterisation

For a realistic pillar design criterion rock mass properties were determined using laboratory tests. The laboratory tests were done at RockLab Laboratory in Pretoria, South Africa. The tests carried out at the Laboratory were Uniaxial and Triaxial Compression. The parameters determined were UCS, Poisson's ratio, Young's modulus and Specific gravity. The laboratory triaxial test results together with rockmass classification results were used in the RocLab Rocscience software to determine the Mohr-Coulomb and Hoek-Brown parameters of the hanging wall and the mineralised zone. A summary of the laboratory tests results together with RockLab results is given in Table 4.12.

Table 4.12: Laboratory Rock Tests Results and RockLab Results Summary

ROCK PROPERTY	HANGING WALL	MINERALIZED ZONE
Triaxial Compressive Strength (MPa)	310.1	198.6
Uniaxial Compressive Strength (MPa)	156.4	152.3
Density (t/m^3)	2.84	3.18
Elastic Modulus (GPa)	97.6	91.4
Poisson's Ratio	0.31	0.29
Geological Strength Index	80.0	70.0
Disturbance Factor	0.0	0.0
Hoek-Brown: m_i	18	15
Hoek-Brown: m_b	8.8	5.1
Hoek-Brown: s	0.11	0.04
Hoek-Brown: a	0.50	0.50
Mohr-Coulomb: C (MPa)	15.2	11.7
Mohr-Coulomb: ϕ (Deg)	44.3	40.0

4.7 Pillar Design Considerations

The detailed logging data was processed to give some input into the pillar design at exploration stage. For calculating strength DRMS was used instead of the strength of a unit cube of platinum rock. This approach was adopted since DRMS considers all the parameters which were assessed in the logging programme which have a bearing on the pillar strength. In determining DRMS, RMS is first calculated using the following equation suggested by Laubscher (1990):

$RMS = UCS \times (RMR - R_{UCS})/100$

Where: RMR is the total of the Rock Mass Rating

R_{UCS} is the Uniaxial Compressive Strength rating

To obtain the DRMR needed for calculating pillar strength, the RMS was then adjusted for the effects of blasting, weathering and joint orientation which were 95%, 96% and 74% respectively. Hedley and Grant (1972) power formula was used for calculating pillar strength however their suggestion of using strength of a unit cube of rock as input was replaced by DRMR which is more representative of pillar experience. The formula used is as follows:

$$P_s = DRMS.\frac{W_e^{0.5}}{h^{0.7}} \quad \text{---------- 53}$$

Where:

DRMS is the design rock mass strength

W_e is the effective pillar width given by 4xPillar Area/Pillar Perimeter

h is the pillar height

Since the maximum depth of ore at the exploration site is less than 300 m the mine to be established is considered to be shallow so the Tributary Area Theory was applied, however the setbacks of this theory as discussed earlier are still valid and further research work need to be undertaken to account for these shortfalls.

Pillar Stress = $\sigma_v/(1 - e)$

Where: σ_v is the vertical insitu stress

e is the areal extraction ratio as determined by the Tributary Area Theory

For calculating the square pillar width at different depth for a constant SF of 1.6 the following values were used for the parameters in the SF equation (SF = Pillar Strength/Pillar Load):

Mining height	1.8 m
Pillar Centres	18 m
Rock density	2 700 kg/m3
UCS of intact pillar rock	152.3 MPa
DRMS	48.4 MPa

The resultant square pillar widths at various depth for a constant SF of 1.6 are as given in Table 4.13.

Table 4.13: Variation of square pillar width with depth at a constant SF of 1.6

Depth Below Surface (m)	Pillar Width (m)	SF
100	4.53	1.6
120	4.88	1.6
140	5.19	1.6
160	5.47	1.6
180	5.73	1.6
200	5.98	1.6

Note that the same approach was adopted to determine pillar width at different depths for a constant SF of 1.6 for the different pillar design formulae discussed in Chapter 2 as applied to the large scale platinum exploration project data base. This was meant to illustrate the uncertainty brought about by these formulae in the pillar design process. The results are as presented under section 4.9

The Rock Mass Classification data used for this research is presented in Tables 4.14 to 4.17.

Table 4.14: Bokai On-Reef Zone Rock Mass Classification – Q System (Barton)

BOKAI ON-REEF ZONE ROCK MASS CLASSIFICATION – Q SYSTEM (Barton)											
Bore Hole	**Zone (m)**	**RQD**	**Joint Condition**					**RQD/J_n**	**J_r/J_a**	**J_w/SRF**	**Q**
			Set No. (J_n)	**Roughness No. (J_r)**	**Alteration No. (J_a)**	**Water Reduction Fact. (J_w)**	**Stress Reduction Fact. (J_s)**				
BO 56	45 – 53	76	3	1.5	6	1	2.5	25.3	0.25	0.4	2.5
IBO 01	114 – 122	98	3	1.5	1.5	1	2.5	32.7	1	0.4	13.1
BO55A	119 – 127	99	4	1	0.75	1	2.5	24.8	1.3	0.4	12.9
IBO 02	138 – 146	89	4	3	3	1	2.5	22.3	1	0.4	8.9
BO 54A	142– 150	98	4	1	1	1	2.5	24.5	1	0.4	9.8
IBO 03	171 – 179	57	9	3	1	1	2.5	6.3	3	0.4	7.6
BO 53A	150 – 158	100	4	1	1	1	2.5	25.0	1	0.4	6.3
IBO 11	182 – 190	100	2	1.5	0.75	1	2.5	50.0	2	0.4	40.0
BO 52	143 – 151	75	9	3	1	1	2.5	8.3	3	0.4	10.0
BO 45	158 – 166	96	3	1.5	0.75	1	2.5	32.1	2	0.4	25.7
BO 51	115 – 123	99	4	3	1	1	2.5	24.8	3	0.4	29.7
BO 58	100 – 108	100	1	1	1	1	2.5	100.0	1	0.4	40.0
BO 59	114 – 122	95	4	3	2	1	2.5	23.8	1.5	0.4	14.3
BO 60	135 – 143	96	6	1.5	1	1	2.5	16.0	1.5	0.4	9.6
BO 61A	132 – 140	99	6	1	1	1	2.5	16.5	1	0.4	6.6
BO 62	94 – 102	95	9	1.5	1	1	2.5	10.6	1.5	0.4	6.4
BO 66	101 – 109	100	4	1	1	1	2.5	25.0	1	0.4	10.0
BO 68	120 – 128	100	1	1	1	1	2.5	100.0	1	0.4	40.0
BO 39	189 – 197	98	2	1.5	1	1	2.5	49.0	1.5	0.4	29.4
BO 41	130 – 138	77	15	4	4	1	2.5	5.1	1	0.4	2.0

Table 4.15: Bokai On-Reef Zone Rock Mass Classification – RMR (Bieniawski)

BOKAI ON-REEF ZONE ROCK MASS CLASSIFICATION – RMR (Bieniawski)									
Bore Hole	**Zone (m)**	**RQD**	**UCS**	**Joint Spacing**	**Joint Condition**	**Groundwater**	**Joint Orientation**	**RMR**	**Calculated RMR from Q***
BO 56	45 – 53	17	12	8	12	15	-5	59	65
IBO 01	114 – 122	20	12	10	22	15	-5	74	74
BO55A	119 - 127	20	12	10	20	15	-5	72	74
IBO 02	138 - 146	17	12	10	20	15	-5	69	72
BO 54A	142– 150	20	12	15	18	15	-5	75	72
IBO 03	171 – 179	13	12	8	20	15	-5	63	71
BO 53A	150 – 158	20	12	10	18	15	-5	70	70
IBO 11	182 - 190	20	12	15	20	15	-5	77	79
BO 052	143 – 151	17	12	8	22	15	-5	69	72
BO 045	158 – 166	20	12	10	22	15	-5	74	77
BO 051	115 - 123	20	12	15	24	15	-5	81	78
BO 58	100 – 108	20	12	20	23	15	-5	85	79
BO 59	114 – 122	20	12	15	22	15	-5	79	74
BO 60	135 – 143	20	12	10	22	15	-5	74	72
BO 61A	132 – 140	20	12	10	18	15	-5	70	70
BO 62	94 – 102	20	12	10	20	15	-5	72	70
BO 66	101 – 109	20	12	10	20	15	-5	72	69
BO 68	120 – 128	20	12	20	22	15	-5	84	79
BO 39	189 – 197	20	12	15	20	15	-5	77	78
BO 41	130 – 138	17	12	8	10	15	-5	57	64

*RMR = 5lnQ + 60.8

Table 4.16: Bokai Decline Zones Rock Mass Classification – Q System (Barton)

BOKAI DECLINE ZONES ROCK MASS CLASSIFICATION – Q SYSTEM (Barton)											
Bore Hole	**Zone (m)**	**RQD**	**Joint Condition**					**RQD/J_n**	**J_r/J_a**	**J_w/SRF**	**Q**
			Set No. (J_n)	**Roughness No. (J_r)**	**Alteration No. (J_a)**	**Water Reduction Factor (J_w)**	**Stress Reduction Factor (J_s)**				
On-Reef											
BO 56	45 – 53	76	3	1.5	6	1	2.5	25.3	0.25	0.4	2.5
IBO 01	114 – 122	98	3	1.5	1.5	1	2.5	32.7	1	0.4	13.1
BO55A	119 - 127	99	4	1	0.75	1	2.5	24.8	1.3	0.4	12.9
IBO 02	138 - 146	89	4	3	3	1	2.5	22.3	1	0.4	8.9
BO 54A	142– 150	98	4	1	1	1	2.5	24.5	1	0.4	9.8
IBO 03	171 – 179	57	9	3	1	1	2.5	6.3	3	0.4	7.6
BO 53A	150 – 158	100	4	1	1	1	2.5	25.0	1	0.4	6.3
IBO 11	182 - 190	100	2	1.5	0.75	1	2.5	50.0	2	0.4	40.0
BO 52	143 – 151	75	9	3	1	1	2.5	8.3	3	0.4	10.0
BO 45	158 – 166	96	3	1.5	0.75	1	2.5	32.1	2	0.4	25.7
BO 51	115 - 123	99	4	3	1	1	2.5	24.8	3	0.4	29.7
Off-Reef											
IBO 01	132 - 137	100	1	1.5	0.75	1	2.5	100	2	0.4	80.0
IBO 02	153 - 158	100	1	1.5	1	1	2.5	100	1.5	0.4	60.0
BO 53A	165 - 170	63	9	1.5	1	1	2.5	7.0	1.5	0.4	4.2
IBO 11	199 - 204	96	6	3	2	1	2.5	16.0	1.3	0.4	8.3
BO 54A	156 - 161	100	1	1	1	1	2.5	100	1	0.4	40.0

Table 4.17: Bokai Decline Zones Rock Mass Classification – RMR (Bieniawski)

BOKAI DECLINE ZONES ROCK MASS CLASSIFICATION – RMR (Bieniawski)									
Bore Hole	**Zone (m)**	**RQD**	**UCS**	**Joint Spacing**	**Joint Condition**	**Groundwater**	**Joint Orientation**	**RMR**	**Calculated RMR from Q***
On-Reef									
BO 56	45 – 53	17	12	8	12	15	-5	59	65
IBO 01	114 – 122	20	12	10	22	15	-5	74	74
BO55A	119 - 127	20	12	10	20	15	-5	72	74
IBO 02	138 - 146	17	12	10	20	15	-5	69	72
BO 54A	142– 150	20	12	15	18	15	-5	75	72
IBO 03	171 – 179	13	12	8	20	15	-5	63	71
BO 53A	150 – 158	20	12	10	18	15	-5	70	70
IBO 11	182 - 190	20	12	15	20	15	-5	77	79
BO 052	143 – 151	17	12	8	22	15	-5	69	72
BO 045	158 – 166	20	12	10	22	15	-5	74	77
BO 051	115 - 123	20	12	15	24	15	-5	81	78
Off-Reef									
IBO 01	132 - 137	20	12	15	26	15	-5	83	83
IBO 02	153 - 158	20	12	15	22	15	-5	79	81
BO 53A	165 - 170	13	12	8	20	15	-5	63	68
IBO 11	199- 204	17	12	10	20	15	-5	69	71
BO 54A	156 - 161	20	12	20	18	15	-5	80	79

*RMR = 5 ln Q + 60.8

4.8 Pillar Numerical Modelling using Examine 2D

An analysis of stress distribution around a pillar line running through pillar centres was done using Examine 2D modelling software and the results are as given in Figure 4.5 and Figure 4.6. Examine 2D is a simplistic software package which can be utilised to get an initial picture of stress distribution. It was noticed that pillar stress is high on the centres of the pillars and decreases going away from the centres to the edge of pillars. This is evidenced by the zero strength factor at the centres of the pillars and gradual increase of the strength factor to 4 going towards the edge of the pillars. Examine 2D is used for elastic analysis and cannot be used to model failure as it has no ability to model plasticity. Where detailed numerical modelling analysis is required complex modelling packages with numerous capacities like modelling failure and joints should be used. These modelling packages include Phase 2, FLAC3D, UDEC and MAP3D.

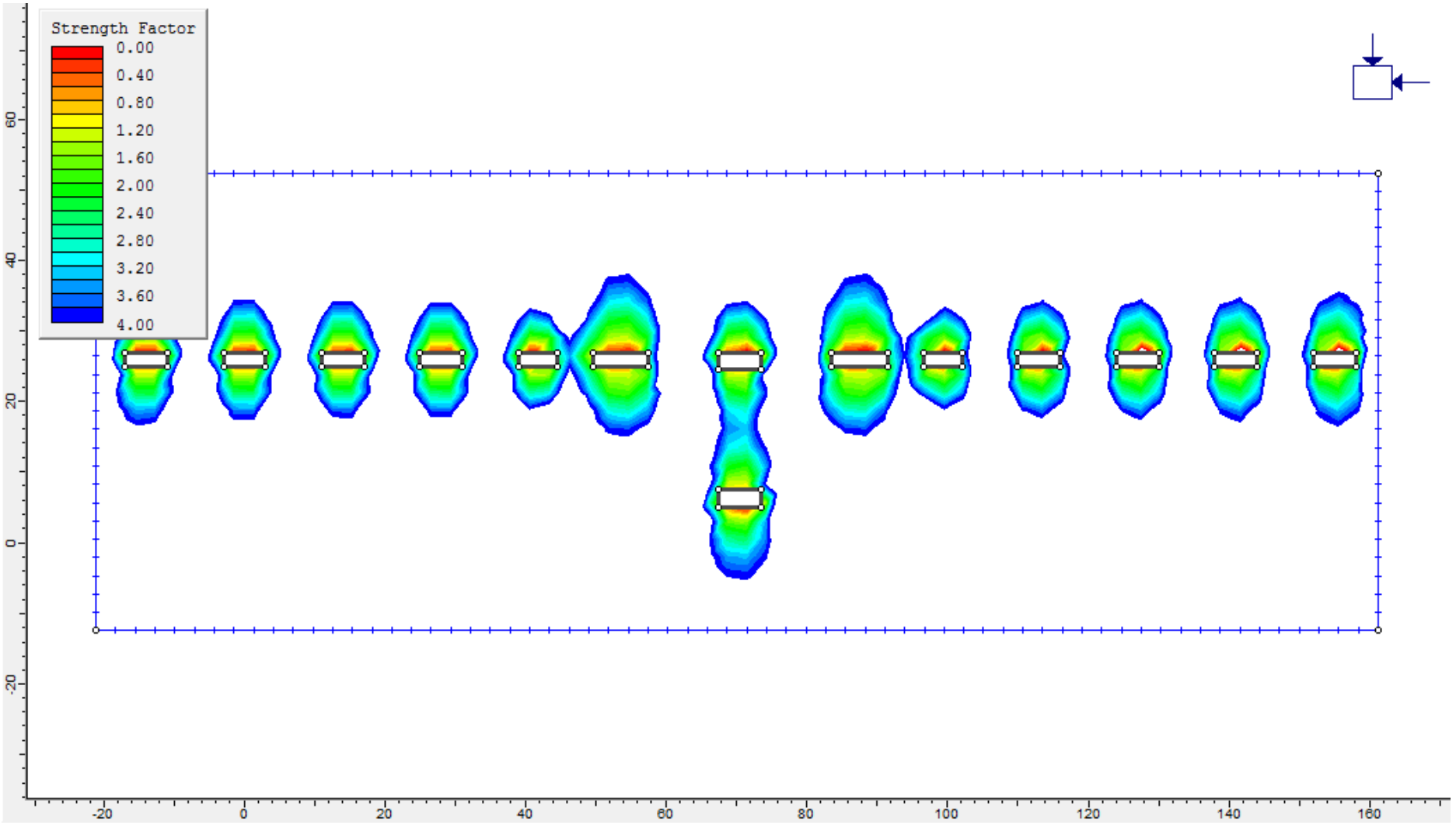

Figure 4.5: Section through pillar line

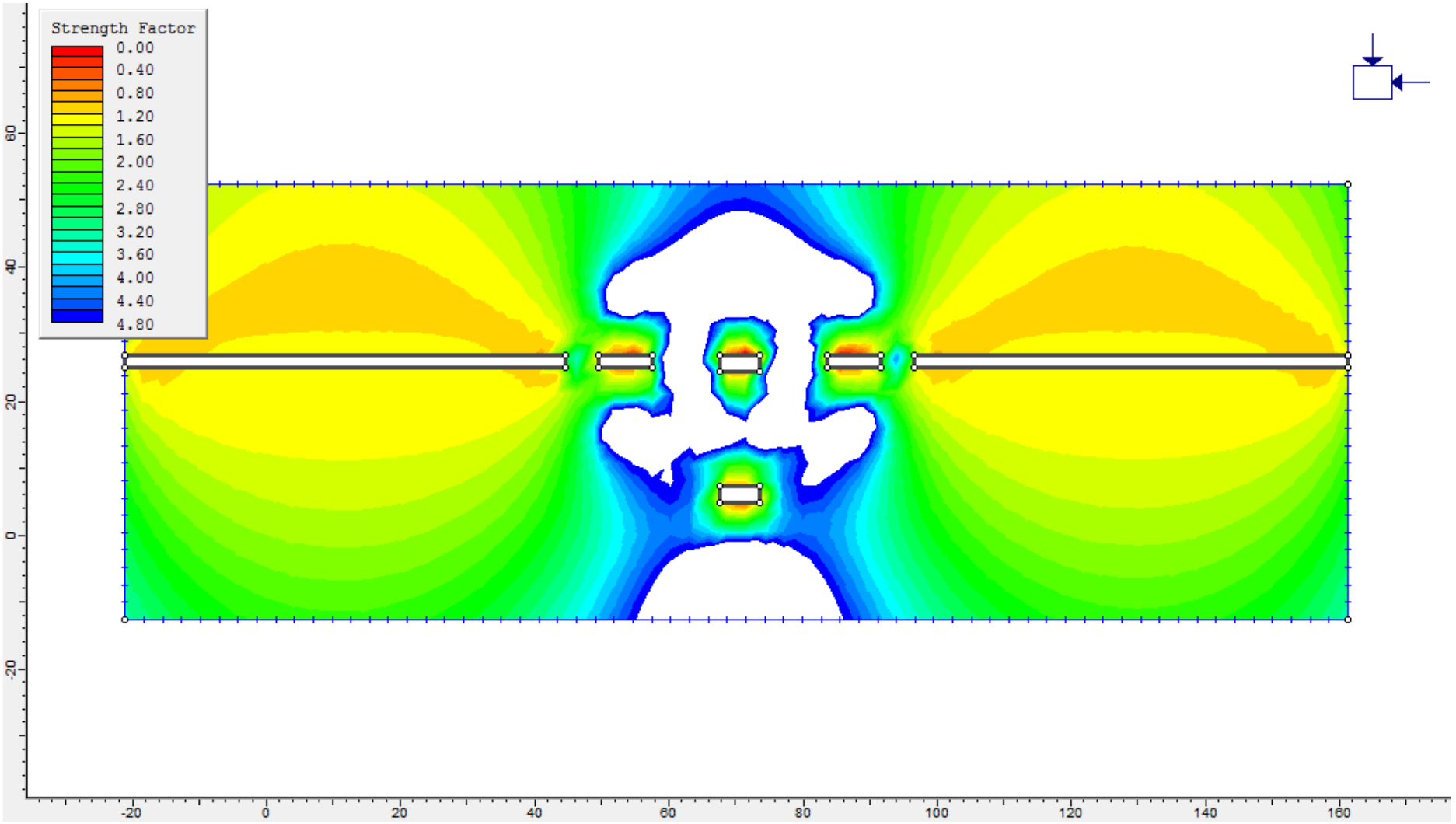

Figure 4.6: Section between pillar lines

4.9 Pillar Design Results for the large scale platinum exploration project using the different pillar design formulae discussed in Chapter 2

To highlight the current uncertainty in the pillar design process, the pillar design formulae presented in Chapter 2 were used to determine square pillar sizes at different depth using the Platinum Exploration Data. A constant SF of 1.6 was used in the calculations since it is the minimum permitted SF for the project. The TAT was used to determine the stresses at different depth since the mining layout is of large lateral extent, several times greater than the mining depth and regular with same size pillars. It is important to note that the Coates' method reduces to the usual TAT under these conditions (large width of extraction span, L) so only the TAT was used for the assessment.

Since there is no straight forward way of calculating pillar width from the SF equation, several iterations were performed in excel to find the pillar width corresponding to a SF of 1.6 for each pillar strength formula. For the sake of clarity and brevity, the formulae presented in Chapter 2 are not repeated here but the values of the parameters as applied to the platinum exploration data base are given and the results summarised in Table 4.18. The Parameters used in the pillar design exercise for the large scale platinum exploration project are as follows:

Mining height	1.8 m
Pillar Centres	18 m
Rock density	2 700 kg/m3
UCS of intact pillar rock	152.3 MPa
DRMS	48.4 MPa

The other parameters values for each of the formulae are as presented in Chapter 2.

The results of the pillar design exercise are as summarised in Table 4.18.

Table 4.18: Pillar Design Results for the different pillar design formulae

Strength Formula	Strength (MPa)	Stress (TAT) (MPa)	Depth (m)	Pillar Width (m)	w/h Ratio	SF
Hedley and Grant (1972)	149.71	93.43	100	3.06	1.70	1.6
Von Kimmelmann et al (1984)	84.20	52.55	100	4.08	2.27	1.6
Krauland and Soder (1987)	50.41	31.50	100	5.27	2.93	1.6
Potvin et al (1989)	120.44	74.79	100	3.42	1.90	1.6
DRMS Approach (Laubscher, 1990)	68.27	42.63	100	4.53	2.52	1.6
Sjoberg (1992)	92.90	57.81	100	3.89	2.16	1.6
Lunder and Pakalnis (1997)	96.75	60.26	100	3.81	2.12	1.6
Hedley and Grant (1972)	155.24	96.98	120	3.29	1.83	1.6
Von Kimmelmann et al (1984)	87.18	54.22	120	4.40	2.44	1.6
Krauland and Soder (1987)	52.19	32.54	120	5.68	3.16	1.6
Potvin et al (1989)	127.83	79.67	120	3.63	2.02	1.6
DRMS Approach (Laubscher, 1990)	70.85	44.08	120	4.88	2.71	1.6
Sjoberg (1992)	95.71	59.51	120	4.20	2.33	1.6
Lunder and Pakalnis (1997)	100.01	62.45	120	4.10	2.28	1.6
Hedley and Grant (1972)	160.11	99.98	140	3.50	1.94	1.6
Von Kimmelmann et al (1984)	89.69	55.92	140	4.68	2.60	1.6
Krauland and Soder (1987)	53.75	33.57	140	6.04	3.36	1.6
Potvin et al (1989)	134.52	83.93	140	3.82	2.12	1.6
DRMS Approach (Laubscher, 1990)	73.07	45.47	140	5.19	2.88	1.6
Sjoberg (1992)	98.15	61.29	140	4.47	2.48	1.6
Lunder and Pakalnis (1997)	102.60	63.84	140	4.38	2.43	1.6
Hedley and Grant (1972)	164.63	102.24	160	3.70	2.06	1.6
Von Kimmelmann et al (1984)	91.95	57.36	160	4.94	2.74	1.6
Krauland and Soder (1987)	55.22	34.39	160	6.38	3.54	1.6
Potvin et al (1989)	140.86	87.48	160	4.00	2.22	1.6
DRMS Approach (Laubscher, 1990)	75.02	46.78	160	5.47	3.04	1.6
Sjoberg (1992)	100.50	62.56	160	4.73	2.63	1.6
Lunder and Pakalnis (1997)	104.88	65.29	160	4.63	2.57	1.6
Hedley and Grant (1972)	168.37	105.14	180	3.87	2.15	1.6
Von Kimmelmann et al (1984)	93.98	58.68	180	5.18	2.88	1.6
Krauland and Soder (1987)	56.51	35.29	180	6.68	3.71	1.6
Potvin et al (1989)	146.50	90.99	180	4.16	2.31	1.6
DRMS Approach (Laubscher, 1990)	76.78	47.96	180	5.73	3.18	1.6
Sjoberg (1992)	102.58	64.01	180	4.96	2.76	1.6
Lunder and Pakalnis (1997)	106.75	66.67	180	4.86	2.70	1.6
Hedley and Grant (1972)	172.02	107.20	200	4.04	2.24	1.6
Von Kimmelmann et al (1984)	95.87	59.78	200	5.41	3.01	1.6
Krauland and Soder (1987)	57.77	36.01	200	6.97	3.87	1.6
Potvin et al (1989)	151.43	94.62	200	4.30	2.39	1.6
DRMS Approach (Laubscher, 1990)	78.43	48.93	200	5.98	3.32	1.6
Sjoberg (1992)	104.57	65.20	200	5.18	2.88	1.6
Lunder and Pakalnis (1997)	108.41	67.53	200	5.09	2.83	1.6

4.9.1 Comments on Pillar Design Results from the different design formulae

After exploration is completed one needs a clear method for designing pillars lest the uncertainty induces disastrous pillar failure. Looking at the results shows that one is faced with an arduous task of choosing which formulae to use as they all give different pillar sizes. The results clearly show that there is no clear way of solving the pillar design problem. This is a pure indication that further research has to be dedicated to pinning this problem and solve it once and for all. All the discussed factors influencing pillar design have to be considered and built into an effective procedure or formula which pillar design practioners for low reef platinum mining can use.

4.10 Conclusions

The work on the large scale platinum exploration project presented an excellent opportunity to map out areas of much care and consideration when collecting the geotechnical parameters used in designing pillars. The exploration work also highlighted how rockmass classification methods can be utilised in determining the overall strength of pillars. Geotechnical parameters important for pillar design were collected by means of geotechnical logging and laboratory tests. The geotechnical logging consisted of three stages: quick log per run, major structures log and detailed geotechnical log. Error concerns and areas of special attention for each logging stage were highlighted in this chapter. It is imperative for the geotechnical logging sheet to accommodate all the parameters which will be used in the calculation of pillar strength. The logging sheet and instructions should be presented in a way which is easy to understand to minimise human errors and increase accuracy and precision. It suffices to say the quality of input into the pillar design system influences the quality of the results gotten from it

The platinum exploration data was utilised to assess the variance of the results of square pillar sizes at different depth calculated using different pillar design formulae presented in Chapter 2 at a constant SF of 1.6. All the formulae gave different square pillar size results pointing to the fact that there is currently no clear way of solving the pillar design problem. It is important that all the discussed factors influencing pillar design be considered and lumped into an effective procedure or formula which pillar design practioners for low reef platinum mining can use.

CHAPTER 5: CASE STUDY 2: DESIGN OF SUPPORT PILLARS AT ESTABLISHED PLATINUM MINES GROUP X

5.0 Introduction

Having done the evaluations of pillar design systems, this chapter strives to give pillar design systems as practiced at Platinum Mines Group X and highlight the inadequacy of the design systems as currently practiced. The methods of load and pillar strength are assessed as part of the evaluations. The drawbacks of the current approach at these mines heavily borrow from the already discussed insufficiency of the current pillar design systems for low reef platinum mining, as such no much detail is discussed in this chapter but it is given for illustrative purposes only.

5.1 Pillar Design

5.1.1 Pillar Load Determination

Platinum Mines Group X does not go beyond 325 m in depth so the Tributary Area Theory is used. At these shallow depths the effects of horizontal stresses are significant such that the confinement imposed on the pillars strengthen them and enable them to carry load directly above them. However despite conformance with the requirements of the Tributary Area Theory at shallow depth, the drawbacks alluded to in the evaluations chapter are still valid. The variation of stress on a 5 m x 5 m pillar with depth is shown in Figure 5.1.

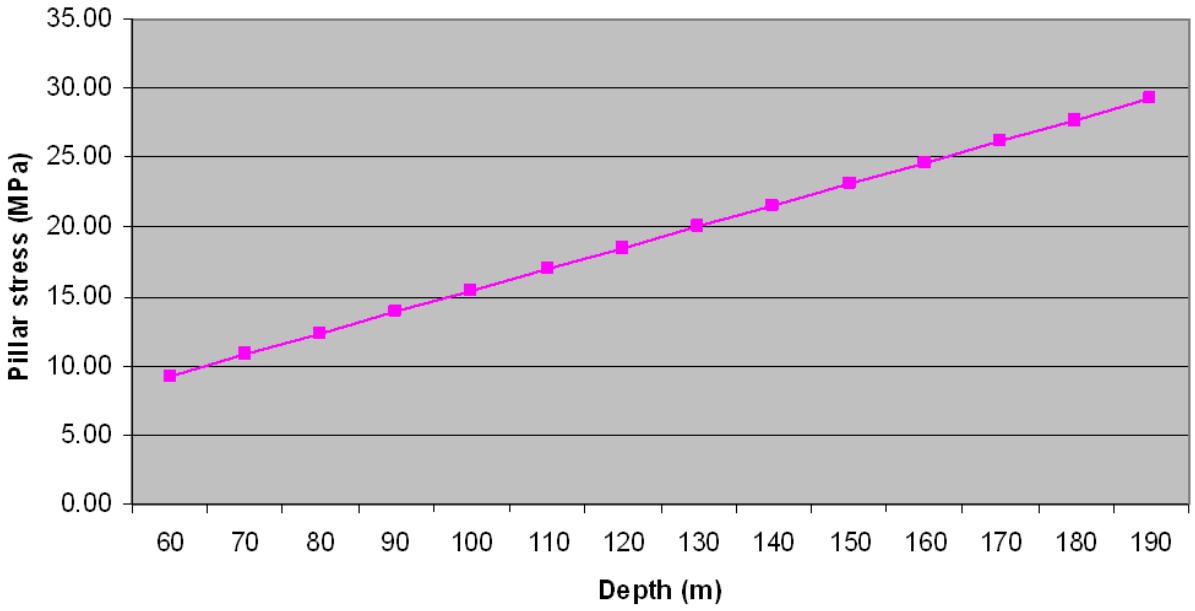

Figure 5.1: Variation of pillar stress with depth at Platinum Mines Group X

5.2 Pillar Strength Determination

Hedley and Grant (1972)'s power formula, equation 34, is used for the determination of pillar strength. Some sort of conservatism is built in this formula at these mines by considering only a 3rd of the Uniaxial Compressive Strength of a unit cube of platinum rock.

5.2.1 Inadequacy of the use of Hedley and Grant (1972)'s power formula

As alluded to in the evaluations presented in chapter 3, Hedley and Grant (1972)'s formula ignores many factors which influence pillar strength. This results in pillar failure due to over estimation of pillar strength. As mentioned earlier, no matter how the UCS of insitu rock material is adjusted downwards there is always a challenge in quantifying the influence of the other factors affecting pillar strength. Adversely oriented joints and geological and geotechnical discontinuities are some of the factors which highly influence overall pillar strength. The consideration of UCS and w/h ratio alone in calculating strength ignores the systematic concept of pillar design. The other two components of the system, roof-pillar contact condition and floor-pillar contact condition, are ignored resulting in the overestimation of pillar strength

The pillar safety factor used in the design is 1.6 which appears to be good and no pillar failure is expected. Nevertheless pillar failures continue to occur calling for the accommodation of the left out factors in the designs as discussed in chapter 3. Figure 5.2 illustrates one of the pillar failures experienced at Platinum Mines Group X.

Figure 5.2: Example of a pillar burst under the current pillar design practice at Platinum Mines Group X

Coupled to the mentioned left out factors in the designs are factors such as ignorance to the use of survey directives when forming pillars and substandard drilling, charging and blasting practice. Pillar failure can also arise from incorrect assessment of ground conditions which lead to overestimation of rockmass strength.

5.2.2 Influence of w/h ratio on Pillar strength

As the width to height ratio of a pillar increases its size also increases. The relationship between pillar strength and w/h ratio is as depicted in Figure 5.3.

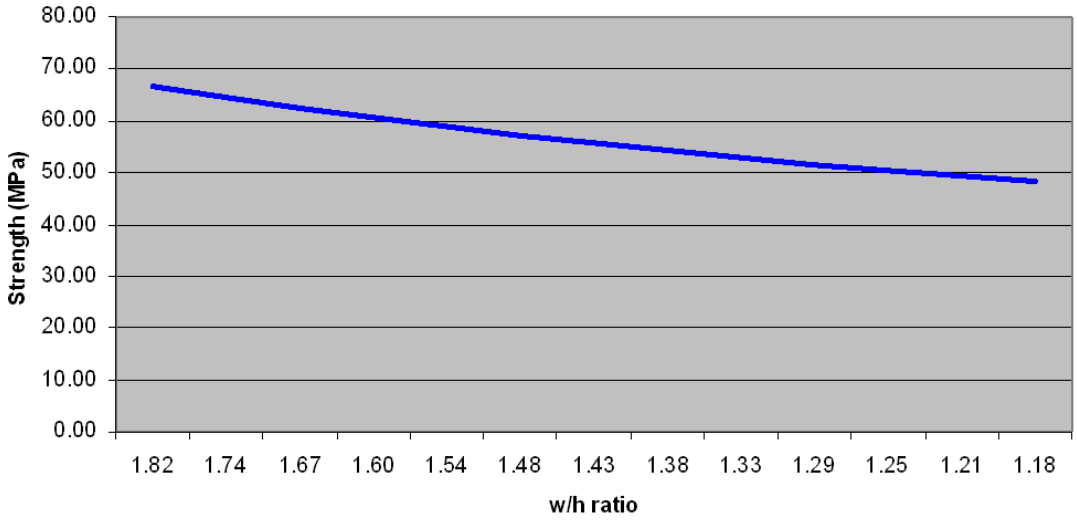

Figure 5.3: Variation of pillar strength with w/h ratio at Platinum Mines Group X

The strength of a pillar material decreases with size like any other material. The decrease in strength as specimen size increases does not drop to zero but to a residual value such that any further decrease in size is not accompanied by a decrease in specimen strength.

5.3 Support Pillar Design

Pillars are designed such that a safety factor of at least 1.6 is achieved. Pillar dimensions must be in such a way to achieve this requirement. Table 5.1 presents typical pillar dimensions and extraction ratios for instope pillars at different depth.

Table 5.1: Typical instope pillar dimensions and extraction ratios at Platinum Mines Group X

Average	Average	Pillar Dimensions			Effective	Areal	Pillar	Pillar	Safety
Depth	Virgin	Pillar	Pillar	Pillar	Pillar	Extraction	Strength	Stress	Factor
	Stress	Length	Width	Height	Width	(in panel)			
(m)	(MPa)	(m)	(m)	(m)	(m)	(%)	(MPa)	(MPa)	
150	4.8	4	4	2.5	4.00	86.8	60.3	36.1	1.67
160	5.1	4	4	2.5	4.00	86.8	60.3	33.6	1.57
170	5.4	5	4	2.5	4.44	84.8	63.6	35.7	1.78
180	5.7	5	4	2.5	4.44	84.8	63.6	37.8	1.68
190	6.0	5	4	2.5	4.44	84.8	63.6	39.9	1.60
200	6.4	5	5	2.5	5.00	82.6	67.4	36.6	1.84
210	6.7	5	5	2.5	5.00	82.6	67.4	38.5	1.76
220	7.0	5	5	2.5	5.00	82.6	67.4	40.3	1.68
230	7.3	5	5	2.5	5.00	82.6	67.4	42.1	1.60
240	7.6	6	5	2.5	5.45	80.8	70.4	39.7	1.78
250	7.9	6	5	2.5	5.45	80.8	70.4	41.3	1.71
260	8.3	6	5	2.5	5.45	80.8	70.4	43	1.64
270	8.6	7	5	2.5	5.83	79.2	72.8	41.2	1.77
280	8.9	7	5	2.5	5.83	79.2	72.8	42.7	1.71
290	9.2	7	5	2.5	5.83	79.2	72.8	44.2	1.65
300	9.5	7	5	2.5	5.83	79.2	72.8	45.8	1.59

5.4 Mining Layout

The adopted mining layout is as shown in Figure 5.4.

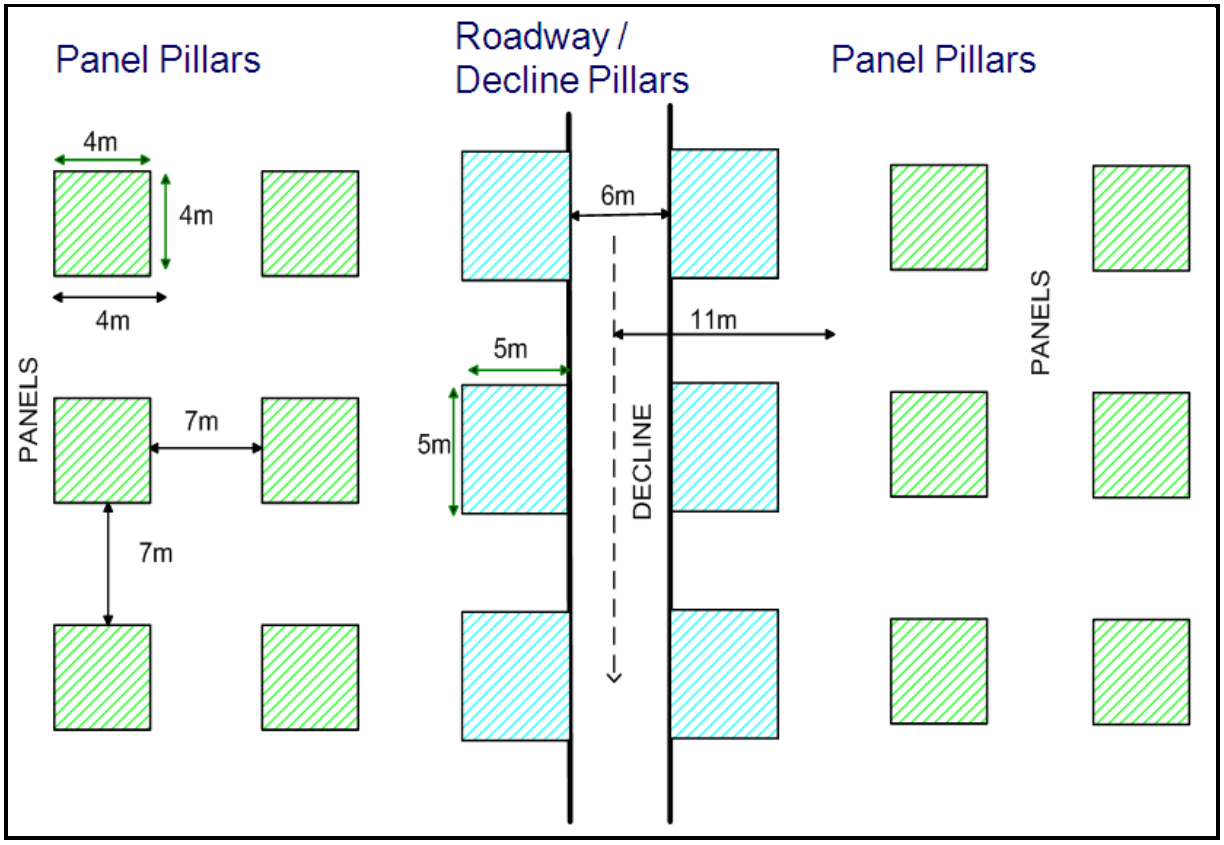

Figure 5.4: Mining Layout at Platinum Mines Group X

5.5 Conclusions

Platinum Mines Group X utilises the TAT and the Hedley and Grant (1972) formulae to determine pillar load and pillar strength respectively. These have been discussed together with other approaches earlier on and were found be insufficient as they do not take account of several factors influencing pillar stability. Platinum Mines Group X serves as a good illustration of mines faced with pillar design uncertainty due to the failure of current pillar design systems to account for discussed influential factors. As soon as the research into a pillar design system accounting for all influential factors is concluded, it will be recommended that Platinum Mines Group X migrates to the resultant effective pillar design procedure or formula to reduce uncertainty.

CHAPTER 6: CONCLUSIONS AND RECOMMENDATIONS

A reliable pillar design system spurs a mine to high levels of safety. It was the main objective of this research to make an evaluation of the current pillar design systems for low reef platinum mining with a main view to increase safety in the extraction of this invaluable resource. While much work has been done in the past with regards to the design of coal pillars after the CoalBrook disaster of 1960, not much research has been dedicated to the design of hard rock pillars. A disaster need not be the one prompting engineers to devise a solution; they should always stay put and ahead with solutions. In a bid to achieve this objective extensive literature review of the current practice was undertaken. The author's work with a large scale platinum exploration project and established platinum mines was also utilised in pointing out the inadequacies of the current pillar design systems. Appropriate recommendations were formulated in order to enhance safety practice in designing pillars. During the course of this research the following conclusions and observations were made:

- Pillar design results for the large scale platinum exploration project using different pillar design formulae discussed in chapter 2 were significantly different showing the uncertainty brought about by the current pillar design formulae in the pillar design process. These results clearly show that there is currently no clear way of solving the pillar design problem. Further research has to be dedicated to pinning this problem and solve it once and for all.
- Competent pillar design systems depend on the accurate determination of pillar load and pillar strength. There are many factors influencing these two variables unaccounted for by the current pillar design systems. The current systems consider pillar material strength and w/h ratio in determine pillar strength but the failure of even high safety factor pillars is an indication of overestimation of pillar strength due to leaving out other factors like contact of the pillar with the roof and floor, roof and floor conditions, effects of adversely oriented joints, spalling and side scaling effects, influence of pillar loading condition, blasting damage effects, influence of weak layers and weathering, impact of k-ratio, time dependent effects, geology, fractured zones, effects of different types of discontinuities within the rock strata, among others.
- The tributary area theory works well for shallow mining when the pillar layout is regular. The theory assumes that each pillar in the system carries an equal amount of load in the layout however pillars near permanent abutments carry lesser load. It is

imperative to note that mining potholes and fault losses often left out in practical mining reduces extraction ratios which in turn give a low APS than that planned for.

- The current pillar design systems for low reef platinum mining were empirically developed and require pillar failure to occur in order to calibrate the pillar design empirical curves. This approach works for the design of pillars in areas lying within the empirical range used to develop the empirical curves. However some pillars designed this way and meeting the definition of the empirical database fail showing that more parameters need to be considered in the empirical database when formulating the formulae.
- It was observed that most of the platinum mines are not quite aware of the significance of adjusting the K parameter in the power formula. They use 1/3rd strength of a unit cube of the platinum rock and believe this builds some conservatism in determining pillar strength. As mentioned, this approach leaves out many factors which influence pillar strength such that even a high safety factor pillar designed this way may collapse.

To bridge the knowledge gap in the current pillar design systems in order to gain some milestone achievements, more research still needs to be done. The evaluation done by this research has pointed researchers to the following recommendations:

- While it is fine to design pillars empirically, this has to be done only for the fields lying within the empirical range of the data base which also consider all the parameters affecting pillar stability. It is highly recommended that for those virgin areas which do not lie within the empirical range there should be a system in place to design the pillars which does not rely on pillar failure. A theoretical framework for such designs can be developed by utilising numerical modelling packages. All the geological and geotechnical information from the exploration crew can be inbuilt in the numerical modelling packages in order to come up with the theoretical framework for designing the pillars from the beginning.
- The pillar load and pillar strength formulae to be developed have to consider all the parameters affecting these variables. The pillar design formulae should adopt the systematic nature of pillar design so that all the components, roof-pillar contact, the pillar itself and the pillar-floor contact, are accounted for in the design. Excellence in the design of other components while one is ignored leads to disastrous consequences

like loss of machinery, life, highly productive sections and all the disastrous consequences of surface subsidence due to underground pillar failure.

- The tributary area theory needs to be revisited so that the mentioned factors like mining potholes, fault losses and the overall loading environment assessments can be done in order to build these factors in the formulation of the Tributary Area Theory.
- Numerical modelling techniques play a pivotal role in reliable determination of pillar stress and pillar strength. All what is needed is to collect all geological and geotechnical details and feed them in the numerical modelling packages. However for one to get a meaningful result from such packages they need to know their limitations.
- For those mines with already failed pillars, back analysis proves to be very useful in devising a pillar design system since failure would have already occurred. The back analysis can give a clear picture on the relationship between pillar collapse frequency and design safety factor, pillar collapse frequency and w/h ratio, pillar life and the frequency of pillars with that pillar life, depth and frequency of pillar collapse among others. The understanding of these relationships forms a solid base on which reliable pillar design systems can be developed.
- Discontinuities are amongst the major factors affecting pillar strength so it is vital to quantify their influence on pillar strength. Rockmass classification systems like the RMR, Q-System and Laubscher's MRMR system can be utilised in the quantification of pillar strength. These classification systems consider most of the factors influencing rockmass strength not currently accommodated by the current pillar design systems.
- Failure Criteria can be utilised in predicting pillar failure. These can be utilised as they are or when used in numerical modelling packages. Mohr Coulomb, Hoek Brown and the Extension Strain are some of the criteria which can be used. Mohr Coulomb and Hoek Brown Criteria's mode of failure prediction are similar while Extension Strain criterion goes further than these two by considering all the three principal stresses affecting pillar strength. Strain Extension Criterion predicts failure quite well in hard brittle rock.
- Where collapses of pillars occur within a short period of mining investigations have to be done promptly in order to establish the cause. This helps to solve the problem while it is in its early stages. Such investigations should never be shelved as the problem has the potential of developing into a pillar run.

- Knowing all the parameters needed for pillar design system, the geotechnical logging manual for those who capture them in the field should have these parameters included in its format. To minimise human error the logging personnel and the designers should get adequate training in the execution of their duties. Human error needs close attention since whether everything is captured and done, inaccuracy can render the pillar design unstable.

In the process of formulating a lasting solution for the design of platinum pillars, the main aim has to be coming up with a truly optimum pillar size. As noted smaller pillars puts the mine at risk of collapse since they offer inadequate support to the mine while bigger pillars becomes unsustainable since more platinum resources are left out in the ground. This wasteful exploitation of resources also impacts heavily on the general sustainable development of an economy. For sustainable development, as explained by Brundtland (1987), the current generation should be able to meet all its needs without compromising the future generation's ability to meet its own needs. Bigger pillars also make a mine not to realise its full economic capacity. Addressing the mentioned research areas is critical in coming up with a comprehensive pillar design system.

REFERENCES

Arora, V. (1987). *Strength and deformational behaviour of jointed rocks.* Delhi, India: Indian Institute of Technology.

Barton, N and Choubey, V. (1977). *The shear strength of rock joints in theory and practice*. Rock Mechanics, vol. 10.

Barton, N., Lien, R and Lunde, J. (1974). Engineering classification of rock masses for the design of tunnel support. *International Journal for Rock Mechanics ,* vol. 6, no. 4, pp. 189 – 236.

Besol-Manual. (1997). Boundary element solution user guidelines manual.

Bieniawski, Z.T. (1968a). *The compressive strength of hard rock,* vol. 8 , pp. 163 – 182.

Bieniawski, Z.T. (1968b). The effects of specimen size on the compressive strength of coal. *International Journal of Rock Mechanics and Mining Science,* vol. 5, pp. 325 – 335.

Bieniawski Z.T. 1976. Rock mass classification in rock engineering. In: *Proceedings of the Symposium on Exploration for Rock Engineering.* (Edited by Bieniawski Z.T.) vol. 1, pp. 97 – 106. Cape Town, A.A. Balkema.

Bieniawski, Z.T. (1989). Engineering rock mass classifications. New York: John Wiley and Sons.

Bowles, J. E. (2002). Foundation Analysis and Desisn. In Fifth-Edition (Ed.).

Brady, B.H.G and Brown, E.T. (1992). *Rock Mechanics For underground mining* (2nd ed.). Chaprnan and Hall.

Brady, B.H.G and Brown, E.T. (2005). *Rock Mechanics For underground mining* (Third Edition ed.). New york, United State of America: Springer Science and Business Media, Kluwer Academic Publishers.

Brady, B.H.G. (1977). An analysis of rock behaviour in an experimental stoping block at the Mount Isa Mine, Queensland, Australia. *International Journal of Rock Mechanics and Mining Science and Geornechanics Abstracts,* pp. 1459 – 1466.

Bruntland, G. (1987). Our common future: The World Commission on Environment and Development, *Oxford University Press*, Oxford.

Bunschinger, J. (1876) "Mitteilungen aus dem Mechanisch-Technishen Laboratorium der K, Technishen Hochschule inMunschen, 6.'' [Cited in Du et al (2008)]

Bunting, D. (1911). Chamber Pillars in Deep Anthracite Mines. *Transactions of the American Institute of Mining and Metallurgical Engineers (AIME),* vol. 42, pp. 236 – 245.

Cahnbley, H. (1993). Comment on pillar size determination. [Cited in Ozbay et al (1995).

Choquet, P and Hadjigeorgiou, J. (1993). Design of Support for Underground Excavations, Chapter 12. In: *Comprehensive Rock Engineering*. J. Hudson (Ed.), Pergamon Press, vol. 4, pp. 314 – 348.

Coates, D. (1981). Rock dynamics. In *Rock mechanics principles.* (p. 874p). Monography, Canada: Department of Energy, Mines and Resources.

Deere, D.U and Miller, R.P. (1966). *Engineering classification and index properties for intact rock.* Air Force Weapons Laboratory Technical Report (AFWL-TR).

Diederichs, M. S. (2003). Rock fracture and collapse under low confinement conditions. *The Journal of Rock Mechanics and Rock Engineering ,* vol. 35, no. 5, pp. 339 – 381.

Du, X., Lu, J., Morsy, K and Peng, S. (2008). Coal Pillar Design Formulae Review and Analysis. *27th International Conference on Ground Control in Mining (ICGCM),* pp. 254 – 261.

Eberhardt, E., Spillmann, T., Maurer, H., Willenberg, H., Loew, S and Stead, D. (2004). The Randa Rockslide Laboratory: Establishing brittle and ductile instability mechanisms using numerical modelling and microseismicity. *9th International Symposium of Landslides.* Rio de Janerio, June 28 – July 2, A. A Balkema, Leiden, pp. 481 – 487.

Free-Encyclopedia. (2010). *Definition of room and pillar mining method*. Retrieved March 28, 2010, from Wikipedia: http://en.wikipedia.org/wiki/Mining.

Google-maps. (2010). *The Zimbabwe Great Dyke Platinum Complexes*. Retrieved March 26, 2010, from http://maps.google.com/.

Hansen, J. (1970). A Revised and Extended Formula for Bearing Capacity. *Bulletin of the Danish Geotechnical Institute* (no. 28), pp. 5 – 11.

Hedley, D.G.F and Grant F. (1972). Stope-and-pillar design for the Elliot Lake Uranium Mines. *The Bulletin of the Canadian Institute of Mining and Metallurgy*, vol. 65, pp. 37 – 44.

Hedley, D.G.F. (1976). *Pillar Mechanics in Post-Pillar Mining.* Mineral Resources Laboratory. Ottawa, Canada: Canadian Institute of Mining and Energy Technology.

Hoek, E. and Brown, E.T. (1980). *Underground Excavations in Rock.* London.

Hoek, E., Kaiser, P.K and Bawden, W.F. (1997). *Support of Underground Excavations in Hard Rock.* (Balkema-A-A., Ed.) Rotterdam.

Holding, G. (2008). Training manual for production personnel in the principles of strata control. *Great dyke geological succession* .

Holland, C.T and Gaddy, F.L (1956). A study of the Ultimate Strength of Coal as Related to the Absolute Size of Cubical Specimens Tested. Bulletin No. 112, Virginia Polytechnic.

Holland, C.T. (1964). The Strength of Coal in Mine Pillars, *Proceedings of the 6th United States of America Symposium on Rock Mechanics*, University of Rolla.

Hudson, J.A. (1992). Rock Characterisation. *Rock Characterisation: International Society of Rock Mechanics, Eurock,* pp. 428 – 431. Chester: British Geotechnical Society.

Hudyrna, M.R. (1988). Rib pillar design in open stope mining. MSc. Thesis, University of British Columbia, Vancouver, Canada.

Hustrulid, W.A and Bullock, R.L. (2001). Underground Mining Methods: Engineering Fundamentals and International Case Studies. pp. 493 – 494, ISBN 0873351932.

Jager, A.J and Ryder J.A. (1999). *A Handbook on Rock Engineering Practice for Tabular Hard Rock Mines.* The Safety in Mines Research Advisory Committee (SIMRAC) Publications.

Jahns, H. I. (1966). Measuring the strength of rock in situ at an increasing scale. *Proceeding of the First International Society for Rock Mechanics (ISRM) Congress*, pp. 477 – 482, Lisbon.

Kaiser, P.K., McCreath, D.R and Tannant, D.D. (1996). *The Canadian Rockburst.* Canada.

Kersten, R. (1984). The design of pillars in the shrinkage stoping of a South African gold mine. *The Journal of The South African Institute of Mining and Metallurgy,* vol. 84, no. 11, pp. 365 – 368.

Krauland, N and Soder, P.E. (1987). Determining pillar strength from pillar failure observation. *Engineering and Mining Journal*, vol. 8, pp. 34 – 40.

Kuijpers, J. (2000). Fracturing around highly stressed excavations in brittle rock. *AITES-ITA 2000 World Tunnel Congress*. *South African Institute of Mining and Metallurgy.* Durban, Republic of South Africa.

Laubscher, D.H (1977). Geomechanics classification of jointed rock masses - mining applications. *Trans International Institute of Mining and Metallurgy,* vol. 86, pp. A1 – 8.

Laubscher, D.H and Taylor, H.W. (1976). The importance of geomechanics classification of jointed rock masses in mining operations. In Bieniawski-ZT (Ed.), *Exploration for rock engineering*, vol. 1, pp. 119 – 128. Cape Town: Balkema.

Laubscher, D.H. (1984). Design aspects and effectiveness of support systems in different mining conditions. *Transactions International Journal of Mining and Metallurgy*, vol. 93, A70 - A82.

Laubscher, D.H. (1990). A geomechanics classification system for the rating of rock mass in mine design. *The Journal of The Southern African Mining and Metallurgy,* vol. 90, no. 10, pp. 257 – 273.

Laubscher, D.M and Page, C.H. (1990). The design of rock support in high stress or weak rock environments. *Proceeding of the 92nd Canadian Institute of Mining and MetallurgyAnnual General Meeting,* vol. 91. Ottawa: Canadian Institute of Mining and Metallurgy.

Lunder, P.J and Pakalnis, R. (1997). Determination of the strength of hard-rock mine pillars. *The Bulletin of the Canadian Institute of Mining and Metallurgy*, vol. 90, no. 10, pp. 51 – 55.

Lunder, P.J. (1994). Hard rock pillar strength estimation: An applied empirical approach. MSc thesis, University of British Columbia, Vancouver, Canada.

Madden, B.J. (1991). A re-assessment of coal-pillar design. *Journal of The South African Institute of Mining and Metallurgy,* vol. 91, pp. 27 – 37.

Madden, B.J., Canbulat, I and York, G. (1998). Current South African coal pillar research. *The South African Institute of Mining and Metallurgy*, no. 11, pp. 7 – 10.

Mah, P., Pakalnis, R.C and Vongpaisd, S., 1995. Use of 3D numerical modelling & empirical design to develop mining strategies in burst prone ground. In H. Mitri (Ed.), *Canadian Conference on Computer Applications in the Mineral industry*. Montreal: McGill University.

Martin, C.D and Maybee, W.G. (2000). The strength of hard-rock pillars. *International Journal of Rock Mechanics and Mining Sciences,* vol. 37, no. 4, pp. 1239 – 1246.

Martin, C.D. (1997). Seventeenth Canadian Geotechnical Colloquium: The effect of cohesion loss and stress path on brittle rock strength. *Canadian Geotechnical Journal,* vol. 5, no. 34, pp. 698 – 725.

Martin, C.D., Kaiser, P.K and Maybee, G. (1998). A failure criterion for the stability of drifts and piliars. *CIM/AGM* . Montreal, Canada.

Martin, C.D., Read, R. S and Martino, J. B. (1997). Observation of brittle failure around a circular test tunnel. *International Journal of Rock Mechanics: Mining Science and Geomechanical Abstracts,* vol. 34, no. 7, pp. 1065 – 1073.

Meyerhof, G.G. (1951). The Ultimate Bearing Capacity of Foundations. *Canadian Geotechnical Journal,* vol. 2, no. 4, pp. 301 – 332.

Meyerhof, G.G. (1963). Some recent research on bearing capacity of foundations. *Canadian Geotechnical Journal,* vol. 1, pp. 16 – 26.

Obert, L and Duvall, W.I. (1967). *Rock Mechanics and the Design of Structures in Rock.* John Wiley and Sons.

Ozbay, M.U., Ryder, J.A and Jager, A.J.,. (1995). The design of pillar systems as practised in shallow hard-rock tabular mines in South Africa. *The Journal of The South African Institute of Mining and Metalurgy*, vol. 84, no. 8, pp. 7 – 18.

Ozbay, M.U and Roberts, M.K.C. (1988). Yield pillars in stope support. In: *Proceedings of the Symposium on Rock Mechanics in Africa, South African National Group on Rock Mechanics (SANGORM),* Swaziland, pp. 317 – 326.

Potvin, Y., Hudyma, M.R and Miller, H.D.S. (1989). Design guidelines for open stope support. *The Bulletin of Canadian Mining and Metallurgy*, vol. 82, pp. 53 – 62.

Pratt, H.R., Black, A.D., Brown, W.S and Brace, W.F. (1972). The effect of specimen size on the mechanical properties of unjointed diorite. *International Journal of Rock Mechanics and Mining Science*, vol. 9, pp. 513 – 529.

Prendergast, M.D. (1991). The Wedza - Mimosa platinum deposit, Great Dyke, Zimbabwe: layering and stratiform PGE mineralisation in a narrow mafic magma chamber. *Geological Magazine*, vol. 128, no. 8, pp. 235 – 249.

Prendergast, M.D. (2009). *Unpublished report on Bokai Platinum Mine Geology*.

Pritchard, C.J and Hedley, D.G.F. (1993). Progressive pillar failure and rock bursting at Denison Mine. In Young-RP (Ed.), *Proceedings of 3rd International Symposium on Rockbursts and Seismicity in Mines*. Kingston. Rotterdam: A.A. Balkema, pp. 111 – 116.

Ramamurthy, T., Rao, G.V and Singh J.A. (1988). A strength criterion for anisotropic rocks. *Proceeding of the 5th Australia-New Zealand Conference on geomechanics*, vol. 1, pp. 253 – 257. Sydney, Australia.

Roberts, D.P., Roberts, M.K.C., Jager, A.J and Coetzer, S. (2005). The determination of the residual strength of hard rock crush pillars with a width-to-height ratio of 2:1. *The Journal of The South African Institute of Mining and Metallurgy*, vol. 105, no. 7, pp 401 – 408.

Roberts, D.P., van der Merwe, J.N., Canbulat, I., Sellers, E.J and Coetzer, S. (2002). *Development of a Method to Estimate Coal Pillar Loading.* The Safety In Mines Research Advisory Committee (SIMRAC) Publications.

Ryder, J.A and Jager, A.J. (2002). *A text book on Rock Mechanics for tabular hard rock mines.* Johannesburg, South Africa: The Safety in Mines Research Advisory Committee (SIMRAC); in conjunction with CSIR Division of Mining Technology.

Ryder, J.A and Ozbay, M.U. (1990). A methodology for designing pillar layouts for shallow mining. *Proceedings of the International Society for Rock Mechanics (ISRM) International Symposium on Static and Dynamic Considerations in Rock Engineering* , pp. 273 – 286.

Salamon, M.D.G and Munro, A.H. (1967). A Study of the Strength of Coal Pillars. *The Journal of the South African Institute of Mining and Metalurgy,* vol. 68, no. 4, pp. 55 – 67.

Salamon, M.D.G and Wagner, H. (1985). Practical Experience in the Design of Coal Pillars. *Safety in Mines Research Proceedings of the 21st International Conference.* Sydney, October: Safety In Mines Research Advisory Committee.

Salamon, M.D.G. (1974). Rock mechanics of underground excavations. In: *Proceedings* of the *3rd Congress of the International Society for Rock Mechanics (ISRM),* Denver, vol. 2, pp. 951 – 1099.

Salamon, M.D.G. (1982). *Unpublished report to Wankie Colliery.* Wankie, Zimbabwe.

Salamon, M.D.G. (1983). The role of pillars in mining, Rock mechanics in mining practice. (S. Budavari, Ed.) *The South African Institute of Mining and Metallurgy*, pp. 173 – 200.

Salamon, M.D.G. (1999). Strength of coal pillars from back-calculation. In K. R. Amadei B (Ed.), *Proceedings of 37th US Rock Mechanics Symposium,* vol. 1, pp. 29 – 36. Vail: Rotterdam: A.A. Balkema.

Sjoberg, J. (1992a). *Failure modes and pillar behaviour in the Zinkgruvan mine. Rock Mechanics.* Lulea University, Department of Mining Engineering. Rotterdam: Balkemia.

Sjoberg, J. (1992b). *Stability and Design of Stope Roofs and Sill Pillars in Cut and Fill and Open Stope Mining with Application to Zinkgruvan Mines.* Licentiate Thesis, Lulea University of Technology, Lulea, Sweeden.

Smith, G.N and Smith I.G.N. (1998). *Elements of Soil Mechanics* (7th ed.). Blackwell Science.

Spencer, D.A. (2010). Hard Rock Tabular Mining: Regional and Support Pillars. *A lecture delivered to GDE (rock engineering) students class of 2010* . Witwatersrand University, Johannesburg, South Africa.

SRK Logging Manual. (2006). *Geotechnical Core Logging Generic Training Manual.* Training Mannual, SRK Consulting Engineers and Scientists, Geotechnical Engineering Department, Vancouver, Canada.

Stacey, T. (2010). *MINN7008 Numerical Modelling Techniques in Rock Engineering Course Notes.* University of the Witwatersrand, Department of Mining Engineering, Johannesburg, South Africa.

Stacey, T.R and Page, C.H. (1986). *Practical Handbook for Underground Rock Mechanics (Series on Rock and Soil Mechanics).* Trans Tech Publications.

Stacey, T.R. (1981). A simple extension strain criterion for fracture of brittle rock. *International Journal of Rock Mechanics, Mining and Science,* vol. 18, pp. 469 – 474.

Terzaghi, K. (1943). *Theoretical Soil Mechanics*. John Wiley, New York.

Todal Mining Geology Data Base. (2008). A collection of geology data of the Bokai exploration site. (L. Saungweme, Ed.), Harare, Harare Metropolitan Province, Zimbabwe.

Todal Mining Geotechnical Data Base. (2009). A collection of geotechnical data of the Bokai exploration site. (M. Spengler, Ed.), Harare, Harare Metropolitan Province, Zimbabwe.

Van der Merwe, J. (1998). *Practical Coal Mining Strata Control* (Second Edition ed.). Johannesburg, Gauteng, South Africa: Itasca Africa Private Limited.

Van der Merwe, J. (2010). *MINN4010 Subsidence Lecture Notes.* University of the Witwatersrand, Department of Mining Engineering, Johannesburg, South Africa.

Van der Merwe, J.N. (2011). Project question document given to students: Probability and Risk in Rock Engineering Assignment. A Graduate Diploma in Engineering Course presented to rock engineering postgraduate students at the University of the Witwatersrand, School of Mining Engineering, Johannesburg, South Africa.

Von Kimmelmann, M.R., Hyde, B and Madgwick, R.J. (1984). The use of computer applications at BCL Limited in planning pillar extraction and design of mining layouts. In Brown-ET-Hudson-JA (Ed.), *Proceedings of the International Society for Rock Mechanics (ISRM) Symposium: Design and Performance of Underground Excavations,* pp. 53 – 63. London: British Geotechnical Society.

Wagner, H and Madden, B.J. (1984). Fifteen Years Experience with the Design of Coal Pillars in Shallow South African Collieries: An Evaluation of the Performance of the Design Procedures and Recent Improvements. Design and Performance of Underground Excavations. *International Society for Rock Mechanics/BGS*, pp. 391 – 399.

Wagner, H and Salamon, M.D.G. (1979). *Pillar design*. Series of Lectures given at Sappers Rust, Pretoria, South Africa, August.

Wagner, H. (1980). Pillar design in coal mines. *Journal of the South African Mining and Metallurgy*, vol. 80, pp. 37 – 45.

Wesseloo, J and T.R Stacey. (2006). Updated in situ stress database for Sothern Africa.

Wesseloo, J. (2000). Predicting the extent of fracturing around underground excavations in brittle rock. *Proceedings of the South African Young Geotechnical Engineers Conference. A joint venture between the South African Institute of Civil Engineering and the South African Institute for Engineering and Environmental Geologists*, 12pp. Western Cape, Republic of South Africa.

Wilson, A.H and Prendergast, M.D. (2002). Platinum-Group Element Mineralisation in the Great Dyke, Zimbabwe, and its Relationship to Magma Evolution and Magma Chamber Structure. *South African Journal of Geology,* vol. 104, no. 4, pp. 319 – 342.

Young, C.M. (1915). Percentage of Extraction of Bituminous Coal with Special Reference to Illinois Conditions. *Engineering Experiment Station Bulletin,* vol. 2, no. 100, 130pp.

APPENDIX 1: TABLE FOR BIENIAWSKI (1989) RMR SYSTEM

Table A.1: Rock Mass Rating System (Bieniawski, 1989)

A. CLASSIFICATION PARAMETERS AND THEIR RATINGS									
Parameter			Range of values						
1	Strength of intact rock material	Point-load strength index	>10 MPa	4 - 10 MPa	2 - 4 MPa	1 - 2 MPa	For this low range - uniaxial compressive test is preferred		
		Uniaxial comp. strength	>250 MPa	100 - 250 MPa	50 - 100 MPa	25 - 50 MPa	5 - 25 MPa	1 - 5 MPa	< 1 MPa
	Rating		15	12	7	4	2	1	0
2	Drill core Quality *RQD*		90% - 100%	75% - 90%	50% - 75%	25% - 50%	< 25%		
	Rating		20	17	13	8	3		
3	Spacing of discontinuities		> 2 m	0.6 - 2 . m	200 - 600 mm	60 - 200 mm	< 60 mm		
	Rating		20	15	10	8	5		
4	Condition of discontinuities (See E)		Very rough surfaces Not continuous No separation Unweathered wall rock	Slightly rough surfaces Separation < 1 mm Slightly weathered walls	Slightly rough surfaces Separation < 1 mm Highly weathered walls	Slickensided surfaces or Gouge < 5 mm thick or Separation 1-5 mm Continuous	Soft gouge >5 mm thick or Separation > 5 mm Continuous		
	Rating		30	25	20	10	0		
5	Ground water	Inflow per 10 m tunnel length (l/m)	None	< 10	10 - 25	25 - 125	> 125		
		(Joint water press)/ (Major principal σ)	0	< 0.1	0.1, - 0.2	0.2 - 0.5	> 0.5		
		General conditions	Completely dry	Damp	Wet	Dripping	Flowing		
	Rating		15	10	7	4	0		

B. RATING ADJUSTMENT FOR DISCONTINUITY ORIENTATIONS (See F)						
Strike and dip orientations		Very favourable	Favourable	Fair	Unfavourable	Very Unfavourable
Ratings	Tunnels & mines	0	-2	-5	-10	-12
	Foundations	0	-2	-7	-15	-25
	Slopes	0	-5	-25	-50	

C. ROCK MASS CLASSES DETERMINED FROM TOTAL RATINGS					
Rating	100 ← 81	80 ← 61	60 ← 41	40 ← 21	< 21
Class number	I	II	III	IV	V
Description	Very good rock	Good rock	Fair rock	Poor rock	Very poor rock

D. MEANING OF ROCK CLASSES					
Class number	I	II	III	IV	V
Average stand-up time	20 yrs for 15 m span	1 year for 10 m span	1 week for 5 m span	10 hrs for 2.5 m span	30 min for 1 m span
Cohesion of rock mass (kPa)	> 400	300 - 400	200 - 300	100 - 200	< 100
Friction angle of rock mass (deg)	> 45	35 - 45	25 - 35	15 - 25	< 15

E. GUIDELINES FOR CLASSIFICATION OF DISCONTINUITY conditions					
Discontinuity length (persistence) Rating	< 1 m 6	1 - 3 m 4	3 - 10 m 2	10 - 20 m 1	> 20 m 0
Separation (aperture) Rating	None 6	< 0.1 mm 5	0.1 - 1.0 mm 4	1 - 5 mm 1	> 5 mm 0
Roughness Rating	Very rough 6	Rough 5	Slightly rough 3	Smooth 1	Slickensided 0
Infilling (gouge) Rating	None 6	Hard filling < 5 mm 4	Hard filling > 5 mm 2	Soft filling < 5 mm 2	Soft filling > 5 mm 0
Weathering Ratings	Unweathered 6	Slightly weathered 5	Moderately weathered 3	Highly weathered 1	Decomposed 0

F. EFFECT OF DISCONTINUITY STRIKE AND DIP ORIENTATION IN TUNNELLING**			
Strike perpendicular to tunnel axis		Strike parallel to tunnel axis	
Drive with dip - Dip 45 - 90°	Drive with dip - Dip 20 - 45°	Dip 45 - 90°	Dip 20 - 45°
Very favourable	Favourable	Very unfavourable	Fair
Drive against dip - Dip 45-90°	Drive against dip - Dip 20-45°	Dip 0-20 - Irrespective of strike°	
Fair	Unfavourable	Fair	

* Some conditions are mutually exclusive. For example, if infilling is present, the roughness of the surface will be overshadowed by the influence of the gouge. In such cases use A.4 directly. ** Modified after Wickham et al (1972).

APPENDIX 2: BOREHOLES BO53A, BO54A AND BO54A CORE PHOTOGRAPHS

125-129 m

130-136 m

137-141 m

142-146 m

147 -151 m

152-157 m

158-163 m

164-169 m

169-170 m

BOREHOLE BO54A CORE

117-122 m

123-127 m

128-132 m

133-138 m

139-144 m

145-150 m

151-155 m

156-161 m

-161.5

BOREHOLE BO55A CORE

92-98 m

99-105 m

106-112 m

123-128 m

-129 m

APPENDIX 3: BOREHOLE BO54A GEOTECHNICAL LOGS

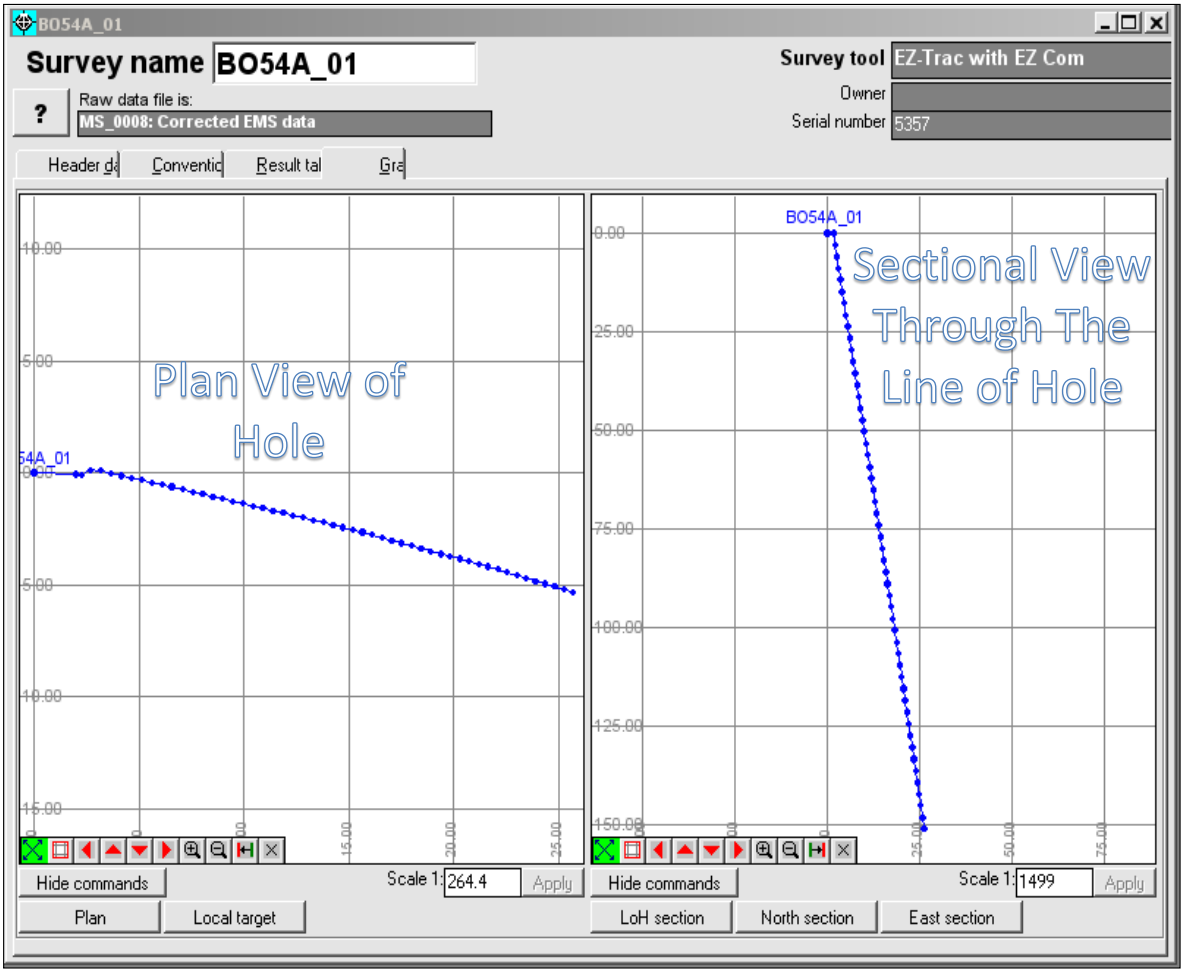

Figure A3.1: Downhole Survey Plan and Section of Borehole BO54A (Todal Mining Geotechnical Data Base, 2009).

Table A.2: Downhole survey results for borehole BO54A

African Mining & Exploration

Survey of Hole BO54A
For Todal Mining Private Limited
Surveyed 18/12/08 21:07
Hole size NQ
Surveyed By Darren Muirhead

Magnetic Reference Data
Magnetic Strength 29648 nT
Magnetic Dip 58.2 degrees
"MD"= Magnetic Dip Deviation > 0.5 degrees
"MT"= Magnetic Strenth Deviation > 1000 nT

Station	Quality	Dip	Azimuth	East	North	Elevation	Mag.Dip	Mag.Str.	Mag.Y	Mag.Z	Roll Angle	DLS	Comment
Metres	*	Degrees	Degrees	Metres	Metres	Metres	Degrees	nT	nT	nT	Degrees	deg./30m	
8	MD+MT	78.9	190.3	0.0	0.0	0.0	66.0	27565	0	25186	155.5	0.0	Casing interference
11	MD+MT	79.2	203.6	0.6	2.0	0.0	78.9	36496	0	35810	211.2	1581.9	Casing interference
14	MD+MT	79.2	104.1	0.5	2.4	3.0	59.7	30872	0	26658	59.6	164.9	Casing interference
17	OK+OK	78.8	102.8	0.1	2.5	5.9	58.3	29480	0	25094	0.7	4.4	
20	OK+OK	78.9	104.1	0.7	2.6	8.9	58.0	29417	0	24961	55.9	2.6	
23	OK+OK	79.0	105.0	1.2	2.8	11.8	57.9	29395	0	24890	116.5	2.3	
26	OK+OK	78.8	104.8	1.8	2.9	14.8	58.0	29377	0	24908	49.6	2.3	
29	OK+OK	78.9	103.4	2.3	3.1	17.7	58.2	29385	0	24972	349.4	2.9	
32	OK+OK	79.0	103.3	2.9	3.2	20.6	58.2	29381	0	24973	310.7	0.7	
35	OK+OK	79.0	103.4	3.5	3.3	23.6	58.2	29395	0	24985	298.0	0.9	
38	OK+OK	79.1	103.3	4.0	3.5	26.5	58.2	29385	0	24962	290.5	0.4	
41	OK+OK	79.1	103.8	4.6	3.6	29.5	58.2	29386	0	24964	268.7	1.0	
44	OK+OK	79.1	103.9	5.1	3.7	32.4	58.2	29381	0	24970	354.6	0.6	
47	OK+OK	79.3	104.7	5.7	3.9	35.4	58.0	29397	0	24943	150.4	2.6	
50	OK+OK	79.3	105.3	6.2	4.0	38.3	58.0	29387	0	24914	112.9	1.1	
53	OK+OK	79.3	105.2	6.7	4.2	41.3	58.0	29361	0	24888	123.3	0.6	
56	OK+OK	79.2	105.2	7.3	4.3	44.2	58.0	29385	0	24912	67.4	1.5	
59	OK+OK	79.2	105.8	7.8	4.5	47.2	58.0	29392	0	24919	71.4	1.4	
62	OK+OK	79.2	104.6	8.4	4.6	50.1	58.2	29393	0	24968	329.7	2.2	
65	OK+OK	79.4	104.5	8.9	4.8	53.1	58.1	29403	0	24972	248.5	1.5	
68	OK+OK	79.4	104.7	9.4	4.9	56.0	58.2	29434	0	25003	233.1	0.7	
71	OK+OK	79.3	105.0	10.0	5.0	59.0	58.1	29399	0	24971	356.7	1.6	
74	OK+OK	79.3	105.1	10.5	5.2	61.9	58.2	29425	0	24999	337.6	0.0	
77	OK+OK	79.4	104.6	11.0	5.3	64.8	58.2	29410	0	24999	283.1	1.7	
80	OK+OK	79.6	105.0	11.6	5.5	67.8	58.1	29420	0	24974	191.0	2.0	
83	OK+OK	79.6	104.6	12.1	5.6	70.7	58.2	29413	0	24989	232.7	0.7	
86	OK+OK	79.5	105.4	12.6	5.7	73.7	58.1	29404	0	24966	229.0	1.6	
89	OK+OK	79.4	106.0	13.2	5.9	76.6	58.1	29404	0	24963	356.6	2.0	
92	OK+OK	79.5	106.6	13.7	6.0	79.6	58.0	29391	0	24923	49.9	1.2	
95	OK+OK	79.5	106.0	14.2	6.2	82.5	58.2	29426	0	24999	358.1	0.9	
98	OK+OK	79.5	107.0	14.7	6.4	85.5	58.1	29430	0	24973	28.3	1.8	
101	OK+OK	79.7	107.8	15.3	6.5	88.4	57.9	29428	0	24935	91.4	2.2	
104	OK+OK	79.6	107.1	15.8	6.7	91.4	58.0	29403	0	24937	41.3	1.2	
107	OK+OK	79.6	107.1	16.3	6.8	94.3	58.1	29402	0	24971	359.2	0.0	
110	OK+OK	79.7	106.7	16.8	7.0	97.3	58.2	29393	0	24976	319.8	1.2	
113	OK+OK	79.9	107.2	17.3	7.2	100.3	58.1	29420	0	24981	207.4	2.4	
116	OK+OK	79.9	107.1	17.8	7.3	103.2	58.2	29401	0	24978	272.0	0.8	
119	OK+OK	80.0	108.7	18.3	7.5	106.2	58.0	29401	0	24926	129.4	3.0	
122	OK+OK	79.8	108.7	18.8	7.6	109.1	58.0	29422	0	24955	33.4	2.0	
125	OK+OK	80.0	108.0	19.3	7.8	112.1	58.0	29400	0	24946	177.2	2.8	
128	OK+OK	79.9	109.8	19.8	8.0	115.0	58.0	29420	0	24937	97.3	3.2	
131	OK+OK	80.0	108.3	20.3	8.1	118.0	58.1	29408	0	24968	233.8	2.8	
134	OK+OK	80.0	108.5	20.8	8.3	120.9	58.1	29388	0	24957	215.6	0.6	
137	OK+OK	80.1	109.6	21.3	8.5	123.9	58.0	29386	0	24924	166.7	1.9	
140	OK+OK	80.0	110.0	21.8	8.7	126.8	58.0	29362	0	24893	71.4	1.1	
143	OK+OK	80.1	110.7	22.2	8.8	129.8	57.9	29376	0	24892	108.4	1.9	
146	OK+OK	80.3	109.3	22.7	9.0	132.8	58.1	29386	0	24935	179.3	2.7	
149	OK+OK	80.2	109.3	23.2	9.2	135.7	57.9	29207	0	24752	216.2	0.3	
152	OK+OK	80.3	109.9	23.7	9.3	138.7	58.0	29371	0	24910	179.8	1.4	
155	OK+MT	80.4	112.3	24.2	9.5	141.6	57.7	28472	0	24075	187.0	4.1	
158	MD+MT	80.3	113.9	24.6	9.7	144.6	56.4	26765	0	22302	240.6	2.7	Unknown interference
161	OK+MT	80.2	108.3	25.1	9.9	147.5	58.3	28565	0	24303	339.7	9.6	
164	OK+OK	80.1	111.8	25.6	10.1	150.5	58.1	29137	0	24736	20.0	6.0	
167	OK+OK	80.2	111.9	26.0	10.3	153.4	57.7	29097	0	24599	77.9	0.7	
170	OK+OK	80.4	111.5	26.5	10.5	156.4	57.9	29078	0	24643	172.5	2.1	

Table A.3: Quick log per run for borehole BO54A

Log#1 - Quick Log Per Run

TODAL MINING - GEOTECHNICAL

Site: BOKAI
Logged by: TAWANDA
Hole Number: BO54A
Bearing: 102
Plunge: -80
BON @ 133.80
MH @ 142.17
Hole Position
X: 30 01 17.4
Y: 19 47 56.0
Z: 1 148
PC Input
By: TAWANDA
Checked: TAWANDA
Page no: 1 of 4

From (m)	To (m)	Rock Type	TCR (m)	SCR (m)	[RQD] Length >100mm	Photo Number	Comments
74.2	77.2	Anothositic norite	2.90	2.90	2.90	BO54A-1	Wholely intact rock
77.2	80.2	Anothositic norite	3.04	3.04	3.04	BO54A-1,2	Wholely intact rock
80.2	83.2	Anothositic norite	3.06	3.06	3.06	BO54A-2,3	Wholely intact rock
83.2	86.2	Anothositic norite	2.94	2.94	2.94	BO54A-3	Wholely intact rock
86.2	89.2	Anothositic norite	3.05	3.05	3.05	BO54A-3,4	Wholely intact rock
89.2	92.2	Anothositic norite	3.00	3.00	2.93	BO54A-4	OCJ @ 91.55, SZ btwn 91.93 & 92, RIR
92.2	95.2	Anothositic norite	2.91	2.91	2.91	BO54A-4,5	Wholely intact rock
95.2	98.2	Anothositic norite	3.04	3.04	3.04	BO54A-5	Wholely intact rock
98.2	101.2	Anothositic norite	3.00	3.00	3.00	BO54A-5,6	Wholely intact rock
101.2	104.2	Anothositic norite	3.05	3.05	3.05	BO54A-6	Wholely intact rock
104.2	107.2	Anothositic norite	3.03	3.03	3.03	BO54A-6,7	Wholely intact rock
107.2	110.2	Anothositic norite	2.94	2.94	2.94	BO54A-7	Wholely intact rock
110.2	113.2	Anothositic norite	2.97	2.97	2.97	BO54A-7,8	Wholely intact rock
113.2	116.2	Anothositic norite	3.02	3.02	3.02	BO54A-8	Oriantation starts @ 116.20, Wholely intact rock
116.2	119.5	Anothositic norite	3.19	3.19	2.68	BO54A-8,9	FZ btwn 118.1 & 118.48, FZ btwn 118.93 & 119.06, RIR
119.5	122.5	Anothositic norite	3.31	3.31	3.31	BO54A-9,10	OCJ @119.50, RIR
122.5	125.5	Anothositic norite	3.00	3.00	3.00	BO54A-10	FZ btwn 123.33 & 123.72, OCJ @ 124.32, RIR
125.5	128.5	Anothositic norite	3.00	2.92	2.92	BO54A-10,11	FZ btwn 128.50 & 128.58, RIR
128.5	131.5	Anothositic norite	2.98	2.98	2.98	BO54A-11	OCJ @ 131.16, RIR
131.5	134.5	Anothositic norite & Bronzitite @ 133.31	2.82	2.82	2.68	BO54A-11,12	OCJs @ 133.88, 134.14, 134.21, 134.28, RIR
134.5	137.5	Bronzitite	3.01	3.10	2.76	BO54A-12	F btwn 134.74 & 137.5, RIR
137.5	140.5	Bronzitite	3.14	3.14	2.27	BO54A-12,13	F btwn 137.50 & 138.37, RIR
140.5	143.5	Bronzitite	3.00	3.00	3.00	BO54A-13	OCJs @ 140.82, 143, 143.18, 143.43, RIR
143.5	146.5	Bronzitite	2.93	2.93	2.93	BO54A-13,14	Wholely intact rock
146.5	149.5	Bronzitite	3.14	3.14	3.03	BO54A-14,15	FZ btwn 147.42 & 147.53, OCJs @ 148.11, 148.34, 148.61, 148.86, 149.53, RIR
149.5	152.5	Bronzitite	2.96	2.96	2.96	BO54A-15	OCJs @ 149.75, 149.99, 150.50, 150.69, 151.05, 151.08, 151.41, RIR
152.5	155.5	Bronzitite	2.70	2.70	2.70	BO54A-15,16	Wholely intact rock
155.5	158.5	Bronzitite	3.09	3.09	3.09	BO54A-16	Wholely intact rock
158.5	161.5	Bronzitite	2.90	2.90	2.90	BO54A-17	OCJ @ 159.36, RIR

Table A.4: Major structures log for borehole BO54

Log#2 - Major Structures

TODAL MINING - GEOTECHNICAL

Site: BOKAI | Hole Number: BO54A | Hole Position | **PC Input**

Bearing: 102 | **X:** 30 01 17.4 | By: TAWANDA

Logged by: TAWANDA | Plunge: -80 | **Y:** 19 47 56.0 | Checked by: TAWANDA

Z: 1 148 | Page no 2 of 4

Distance or Interval		Visual Log	Structure Type		Typical Orientation			Brittle Structure Properties			Water Staining	Description
From	To		Code	Class	Alpha	Beta	Stick (T)op or (B)ottom	Micro-scale Geometry	Infill	Alteration		
74.20	77.20											Wholely intact rock
77.20	80.20											Wholely intact rock
80.20	83.20											Wholely intact rock
83.20	86.20											Wholely intact rock
86.20	89.20											Wholely intact rock
89.20	91.55		J	2	15			4	SP	1	√	1OCJ, faulted with displacement, RIR
91.55	91.93											Wholely intact rock
91.93	92.00		SZ	4				8	FD	2	√	Strongly sheared zone
92.00	95.20											Wholely intact rock
95.20	98.20											Wholely intact rock
98.20	101.20											Wholely intact rock
101.20	104.20											Wholely intact rock
104.20	107.20											Wholely intact rock
107.20	110.20											Wholely intact rock
110.20	113.20											Wholely intact rock
113.20	116.20											Orientation starts @ 116.20, Wholely intact rock
116.20	118.10											Wholely intact rock
118.10	118.48		FZ	3					SP	1	√	Rock mass weakened by strong fracturing
118.48	118.93											Wholely intact rock
118.93	119.06		FZ	3					SP	1	√	Rock mass weakened by strong fracturing
119.06	119.50		J	2	15	180	B	1	SP	1	√	1OCJ, faulted with displacement, RIR
119.50	123.33											Wholely intact rock
123.33	123.72		FZ	3					SP	3	√	Rock mass weakened by strong fracturing
123.72	124.32		J	2	15	108	T	7	SP	1	√	1OCJ, faulted with displacement, RIR
124.32	128.50											Wholely intact rock
128.50	128.58		FZ	3					SP	3	√	Rock mass weakened by strong fracturing
128.58	131.16		J	2	35	96	T	8	SP	1	√	1OCJ, faulted with displacement, RIR
131.16	133.88		J	2	45	127.2	B	8	SP	1	√	1OCJ, faulted with displacement, RIR
133.88	134.14		J	2	70	180	T	8	SP	1	√	1OCJ, faulted with displacement, RIR
134.14	134.21		J	2	70	180	T	8	SP	1	√	1OCJ, faulted with displacement, RIR

Structure Code Table

Structure		Code
Shear Zone		SZ
Fracture Zone		FZ
Fault		F
Fracture		Fr
Joint		J
Striation lineation		L
Fold Axis		FA
Vein		V
Dyke		D

Structure Class Table

Class	Description
1	Strongly sheared (cataclasite/mylonite), or brecciated
2	Clearly faulted with displacement or striations
3	The rock mass is weakened by alteration or strong fracturing, a nearby major structure is likely.
4	The core is completely broken because of poor core recovery. Possibly structure related
5	Core is strongly or completely altered/weathered to residual soil/mud.

Wall Alteration

1 - wall=rock hardness

2 - wall>rock hardness

3 - wall<rock hardness

Fill Type

Q - Quartz	G - Gouge
C - Calcite	M - Magnesium
FE - Iron oxide	H - Haematite
CL - Clay	S - Sulphide
B - Breccia	O - Other

Micro/Small Scale Joint Expression

Rough/Stepped/Irregular - 1

Smooth Stepped - 2

Slickensided Stepped - 3

Rough Undulating - 4

Smooth Undulating - 5

Slickensided Undulating - 6

Rough Planar - 7

Smooth Planar - 8

Polished - 9

Table A.5: Major structures log for borehole BO54 (Continuation)

Log#2 - Major Structures

TODAL MINING - GEOTECHNICAL

Site: BOKAI
Logged by: TAWANDA
Hole Number: BO54A
Bearing: 102
Plunge: -80
Hole Position
X: 30 01 17.4
Y: 19 47 56.0
Z: 1 148
PC Input
By: TAWANDA
Checked by: TAWANDA
Page no 3 of 4

Distance or Interval		Visual Log	Structure Type		Typical Orientation			Brittle Structure Properties			Water Staining	Description
From	To		Code	Class	Alpha	Beta	Stick (T)op or (B)ottom	Micro-scale Geometry	Infill	Alteration		
134.21	134.28		J	2	70	180	T	8	SP	1	√	1OCJ, faulted with displacement, RIR
134.28	134.74		_	_	_	_	_	_	_	_	_	Wholely intact rock
134.74	137.5		F	2	60	180	T	7	SP	3	√	28OCJs, 29CJs, faulted with displacement, RIR
137.5	138.37		F	2	60	180	T	7	SP	3	√	9OCJs, 11CJs, faulted with displacement, RIR
138.37	140.82		J	2	65	120	T	5	SP	3	√	1OCJ, faulted with displacement, RIR
140.82	143		J	2	55	100.8	T	8	SP	1	√	1OCJ, faulted with displacement, RIR
143	143.18		J	2	55	100.8	T	8	SP	1	√	1OCJ, faulted with displacement, RIR
143.18	143.43		J	2	55	100.8	T	8	SP	1	√	1OCJ, faulted with displacement, RIR
143.43	146.5		_	_	_	_	_	_	_	_	_	Wholely intact rock
146.5	147.42		_	_	_	_	_	_	_	_	_	Wholely intact rock
147.42	147.53		FZ	3	_	_	_	_	SP	1	√	Rock mass weakened by strong fracturing
147.53	148.11		J	2	65	72	B	5	SP	1	√	1OCJ, faulted with displacement, RIR
148.11	148.34		J	2	60	108	B	8	SP	1	√	1OCJ, faulted with displacement, RIR
148.34	148.61		J	2	60	108	B	8	SP	1	√	1OCJ, faulted with displacement, RIR
148.61	148.86		J	2	60	108	B	8	SP	1	√	1OCJ, faulted with displacement, RIR
148.86	149.53		J	2	60	108	B	8	SP	1	√	1OCJ, faulted with displacement, RIR
149.53	149.75		J	2	60	108	B	8	SP	1	√	1OCJ, faulted with displacement, RIR
149.75	149.99		J	2	88	180	B	8	SP	1	√	1OCJ, faulted with displacement, RIR
149.99	150.5		J	2	60	90	B	2	SP	1	√	1OCJ, faulted with displacement, RIR
150.5	150.69		J	2	70	90	B	8	SP	1	√	1OCJ, faulted with displacement, RIR
150.69	151.05		J	2	85	180	B	8	SP	1	√	1OCJ, faulted with displacement, RIR
151.05	151.08		J	2	15	108	B	8	SP	1	√	1OCJ, faulted with displacement, RIR
151.08	151.41		J	2	80	175	B	8	SP	1	√	1OCJ, faulted with displacement, RIR
151.41	155.5		_	_	_	_	_	_	_	_	_	Wholely intact rock
155.5	158.5		_	_	_	_	_	_	_	_	_	Wholely intact rock
158.5	159.36		J	2	75	180	B	8	SP	1	√	1OCJ, faulted with displacement, RIR
159.36	161.5		_	_	_	_	_	_	_	_	_	Wholely intact rock

Structure Code Table

Structure		Code
Shear Zone		SZ
Fracture Zone		FZ
Fault		F
Fracture		Fr
Joint		J
Striation lineation		L
Fold Axis		FA
Vein		V
Dyke		D

Structure Class Table

Class	Description
1	Strongly sheared (cataclasite/mylonite), or brecciated
2	Clearly faulted with displacement or striations
3	The rock mass is weakened by alteration or strong fracturing, a nearby major structure is likely.
4	The core is completely broken because of poor core recovery. Possibly structure related
5	Core is strongly or completely altered/weathered to residual soil/mud.

Wall Alteration

1 - wall=rock hardness
2 - wall>rock hardness
3 - wall<rock hardness

Fill Type

Q - Quartz	G - Gouge
C - Calcite	M - Magnesium
FE - Iron oxide	H - Haematite
CL - Clay	S - Sulphide
B - Breccia	O - Other

Micro/Small Scale Joint Expression

Rough/Stepped/Irregular - 1
Smooth Stepped - 2
Slickensided Stepped - 3
Rough Undulating - 4
Smooth Undulating - 5
Slickensided Undulating - 6
Rough Planar - 7
Smooth Planar - 8
Polished - 9

Table A.6: Detailed geotechnical log for borehole BO54A

Log#3 - Detail Geotech Log

TODAL MINING- GEOTECHNICAL

Site: BOKAI

Logged by: TAWANDA

Hole Number: BO54A
Bearing: 102
Plunge: -80

Hole Position
x: 30 01 17.4
y: 19 47 56.0
z: 1 148

PC Input
By: TAWANDA
Checked by: TAWANDA
Page no: 4 of 4

From	To	Rock Type	Intact Rock Strength			Fracture Frequency						Joint Condition (Micro/Filling/Alteration)						Cemented Joints		Micro Fractures	
												Set 1		Set 2		Set 3					
			Strong Mpa	Weak Mpa	% Weak	Total	Natural	Foliation	Set 1	Set 2	Set 3	α/β	MFA	α/β	MFA	α/β	MFA	Count	Fill Type	Intensity Count/m	Fill Type (if any)
74.2	77.2	Anothositic norite	R5																		
77.2	80.2	Anothositic norite	R5																		
80.2	83.2	Anothositic norite	R5																		
83.2	86.2	Anothositic norite	R5																		
86.2	89.2	Anothositic norite	R5																		
89.2	92.2	Anothositic norite	R5	R4	0.233	5	6		1	4								5	SP		
92.2	95.2	Anothositic norite	R5																		
95.2	98.2	Anothositic norite	R5																		
98.2	101.2	Anothositic norite	R5																		
101.2	104.2	Anothositic norite	R5																		
104.2	107.2	Anothositic norite	R5																		
107.2	110.2	Anothositic norite	R5																		
110.2	113.2	Anothositic norite	R5																		
113.2	116.2	Anothositic norite	R5																		
116.2	119.5	Anothositic norite	R5	R4	15.99	1	1		1												
119.5	122.5	Anothositic norite	R5			1	1		1			0.0833	1SP1					1	SP		
122.5	125.5	Anothositic norite	R5			1	1		1												
125.5	128.5	Anothositic norite	R5	R0	2.67	MTPL	√		√												
128.5	131.5	Anothositic norite	R5			1	1		1			0.36	8SP1					1	SP		
131.5	134.5	Anothositic norite & Bronzitite @ 133.31	R5			4	4		1	3		0.389	8SP1	0.354	8SP1			4	SP		
134.5	137.5	Bronzitite	R4	R3	8.31	57	57		28	29		0.333	7SP3	0.333	_SP3			57	SP		
137.5	140.5	Bronzitite	R4	R3	27.71	20	20		9	11		0.333	7SP3	0.333	_SP3			20	SP		
140.5	143.5	Bronzitite	R4			4	4		4			0.555	8SP1					4	SP		
143.5	146.5	Bronzitite	R5																		
146.5	149.5	Bronzitite	R5	R4	3.5	5	5		4	1			_SP1	0.903	5SP1			5	SP		
149.5	152.5	Bronzitite	R5			7	7		3	2	2	0.444	8SP1	0.666	8SP1	0.139	8SP1	7	SP		
152.5	155.5	Bronzitite	R5																		
155.5	158.5	Bronzitite	R5																		
158.5	161.5	Bronzitite	R5			1	1		1			0.417	8SP1					1	SP		

Micro/Small Scale Joint Expression

Rough/Stepped/Irregular - 1
Smooth Stepped - 2
Slickensided Stepped - 3
Rough Undulating - 4
Smooth Undulating - 5
Slickensided Undulating - 6
Rough Planar - 7
Smooth Planar - 8
Polished - 9

Fill Type	
Q - Quartz	G - Gouge
C - Calcite	M - Magnesium
FE - Iron oxide	H - Haematite
CL - Clay	S - Sulphide
B - Breccia	O - Other

Wall Alteration
1 - wall=rock hardness
2 - wall>rock hardness
3 - wall<rock hardness

APPENDIX 4: GEOTECHNICAL LOGS FOR BOREHOLE BO55A

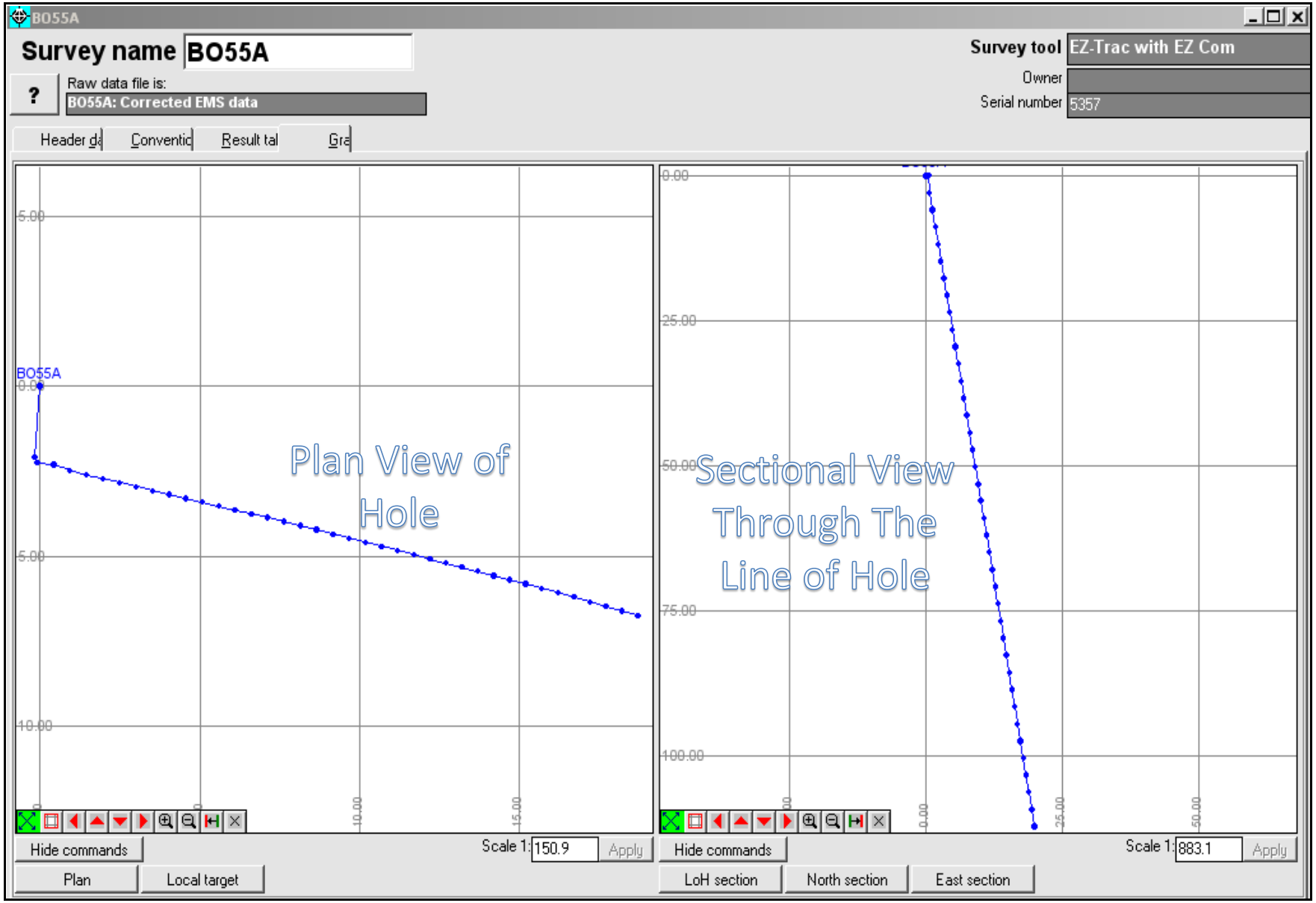

Figure A4.1: Downhole Survey Plan and Section of Borehole BO55A (Todal Mining Geotechnical Data Base, 2009).

Table A.7: Downhole survey results for borehole BO55A

African Mining & Exploration

Survey of Hole BO55A
For Todal Mining Private Limited
Surveyed 14/01/09 14:44
Hole size NQ
Surveyed By Darren Muirhead

Magnetic Reference Data
Magnetic Strength 29708 nT
Magnetic Dip 58.4 degrees
"MD"= Magnetic Dip Deviation > 0.5 degrees
"MT"= Magnetic Strenth Deviation > 1000 nT

Station Metres	Quality *	Dip Degrees	Azimuth Degrees	East Metres	North Metres	Elevation Metres	Mag.Dip Degrees	Mag.Str. nT	Mag.Y nT	Mag.Z nT	Roll Angle Degrees	DLS deg./30m	Comment
11	MD+MT	79.0	148.5	0.0	0.0	0.0	74.7	46481	0	44823	262.4	0.0	Casing interference
14	MD+MT	79.0	221.4	0.2	2.1	0.0	78.1	44250	0	43306	340.6	1623.6	Casing interference
17	MD+MT	79.4	78.8	0.1	2.3	3.0	69.5	10700	0	10023	43.1	203.9	Casing interference
20	MD+MT	79.7	112.3	0.4	2.3	5.9	25.5	13935	0	6009	120.1	59.9	Casing interference
23	MD+MT	79.8	106.9	0.9	2.5	8.9	64.6	37106	0	33521	63.4	9.7	Casing interference
26	MD+OK	79.9	101.7	1.4	2.6	11.8	59.1	30358	0	26038	128.1	9.2	Casing interference
29	MD+OK	79.7	102.3	2.0	2.7	14.8	59.0	30071	0	25769	271.5	2.0	Casing interference
32	OK+OK	79.6	103.0	2.5	2.8	17.7	58.8	29992	0	25661	279.2	1.4	
35	OK+OK	79.8	102.6	3.0	3.0	20.7	58.7	29960	0	25609	35.8	1.5	
38	OK+OK	79.9	102.8	3.5	3.1	23.7	58.6	29965	0	25580	78.1	1.2	
41	OK+OK	80.0	102.2	4.0	3.2	26.6	58.6	29957	0	25569	137.8	1.2	
44	OK+OK	79.8	102.4	4.6	3.3	29.6	58.7	29954	0	25606	230.4	1.7	
47	OK+OK	79.9	101.7	5.1	3.4	32.5	58.7	29963	0	25593	170.4	2.0	
50	OK+OK	79.9	102.8	5.6	3.5	35.5	58.6	29954	0	25567	79.8	2.0	
53	OK+OK	79.8	103.0	6.1	3.6	38.4	58.7	29948	0	25592	6.7	0.7	
56	OK+OK	80.0	102.2	6.6	3.8	41.4	58.6	29966	0	25588	132.5	2.2	
59	OK+OK	80.0	102.4	7.1	3.9	44.3	58.6	29961	0	25577	117.4	0.4	
62	OK+OK	79.9	103.8	7.6	4.0	47.3	58.7	29935	0	25577	11.1	2.7	
65	OK+OK	80.0	102.3	8.1	4.1	50.2	58.6	29965	0	25580	150.0	3.1	
68	OK+OK	79.9	103.5	8.7	4.2	53.2	58.6	29965	0	25581	42.9	2.5	
71	OK+OK	79.9	104.1	9.2	4.3	56.1	58.6	29958	0	25572	25.8	1.0	
74	OK+OK	80.1	103.1	9.7	4.5	59.1	58.6	29970	0	25573	130.3	2.8	
77	OK+OK	79.9	103.6	10.2	4.6	62.0	58.8	29956	0	25623	265.4	2.5	
80	OK+OK	80.0	103.0	10.7	4.7	65.0	58.8	29976	0	25631	222.4	1.4	
83	OK+OK	80.0	103.7	11.2	4.8	68.0	58.8	29967	0	25630	270.2	1.2	
86	OK+OK	80.0	104.6	11.7	5.0	70.9	58.6	29974	0	25597	7.2	1.6	
89	OK+OK	80.2	103.6	12.2	5.1	73.9	58.5	29986	0	25578	121.3	2.3	
92	OK+OK	80.1	104.0	12.7	5.2	76.8	58.5	29974	0	25555	97.1	0.8	
95	OK+OK	80.2	103.3	13.2	5.3	79.8	58.6	29985	0	25590	124.9	1.3	
98	OK+OK	80.1	104.3	13.7	5.4	82.7	58.5	29980	0	25569	79.9	1.9	
101	OK+OK	80.2	103.6	14.2	5.6	85.7	58.6	29975	0	25573	119.7	1.5	
104	OK+OK	80.1	104.4	14.7	5.7	88.6	58.5	29965	0	25545	84.1	1.6	
107	OK+OK	80.0	103.8	15.2	5.8	91.6	58.7	29963	0	25607	229.6	1.8	
110	OK+OK	80.0	103.3	15.7	5.9	94.6	58.7	29912	0	25550	221.3	0.8	
113	OK+OK	79.9	105.3	16.2	6.1	97.5	58.5	29866	0	25478	333.1	3.7	
116	OK+OK	80.0	104.4	16.7	6.2	100.5	58.4	29724	0	25329	220.0	1.9	
119	OK+OK	80.2	105.6	17.2	6.3	103.4	58.5	29601	0	25232	98.4	2.8	
122	MD+OK	80.1	106.5	17.7	6.5	106.4	59.7	29744	0	25672	186.4	1.7	
125	OK+OK	80.1	103.0	18.2	6.6	109.3	58.1	29549	0	25082	198.5	5.9	
128	OK+OK	80.0	105.7	18.7	6.7	112.3	58.7	30138	0	25744	352.8	4.6	

Table A.8: Quick log per run for borehole BO55A

Log#1 - Quick Log Per Run

TODAL MINING - GEOTECHNICAL

Site: BOKAI
Logged by: TAWANDA
Hole Number: BO55A
Bearing: 102
Plunge: -80
BON @ 113.74 MH @ 122.95

Hole Position
X: 30 01 27.5
Y: 19 48 00.3
Z: 1 145

PC Input
By: TAWANDA
Checked: TAWANDA
Page no: 1 of 4

From (m)	To (m)	Rock Type	TCR (m)	SCR (m)	[RQD] Length >100mm	Photo Number	Comments
92.08	95.08	Anothositic norite	3.00	3.00	3.00	BO55A-1	OCJs @ 93.2, 93.53, 94.08, RIR
95.08	98.08	Anothositic norite	3.00	3.00	2.96	BO55A-1	OCJs @ 96.94, 96.98, 97.10, RIR
98.08	101.08	Anothositic norite	3.00	3.00	3.00	BO55A-1,2	OCJ @ 99.54, RIR
101.08	104.40	Anothositic norite	3.00	3.00	2.92	BO55A-2	OCJs @ 101.76, 101.82, 101.99, 102.07, Oriantation starts @ 101.08, OCJs @ 102.44, 103.03, 103.4, 104.4, RIR
104.40	107.40	Anothositic norite	3.00	3.00	1.32	BO55A-2	OCJ @ 105.09, CJ @ 105.51, F btwn 105.68 & 107.4 (20OCJs & 4CJs), RIR
107.40	110.40	Anothositic norite	3.02	3.02	3.02	BO55A-2,3	OCJs @ 107.56, 107.67, 107.91, RIR
110.40	113.04	Anothositic norite	3.01	3.01	3.01	BO55A-3	Wholely intact rock
113.04	116.40	Anothositic norite & Bronzitite @ 113.74	2.98	2.29	1.47	BO55A-3	OCJs @ 113.51, 113.7, OCJs 113.82, 114.06, F btwn 114.89 & 116.4 (32OCJs), RIR
116.40	119.04	Bronzitite	3.00	2.80	2.14	BO55A-3,4	FZ btwn 116.4 & 116.74, FZ btwn 117.66 & 118.08, OCJs @118.42, 118.47, 118.59, 118.81, 118.86, RIR
119.04	122.40	Bronzitite	2.98	2.98	2.89	BO55A-4	OCJs @ 119.2, 119.91, CJs @ 119.96, 120.0, OCJs @ 120.15, 120.36, 120.43, 120.52, 120.71, 121.38, RIR
122.40	125.40	Bronzitite	3.03	3.03	3.03	BO55A-4	Wholely intact rock
125.40	128.40	Bronzitite	3.00	3.00	3.00	BO55A-4,5	OCJ @ 128.34, RIR

Table A.9: Major structures log for borehole BO55A

Log#2 - Major Structures

TODAL MINING - GEOTECHNICAL

Site: BOKAI
Logged by: TAWANDA
Hole Number: BO55A
Bearing: 102
Plunge: -80
BON @ 113.74 MH @ 122.95
Hole Position
X: 30 01 27.5
Y: 19 48 00.3
Z: 1 145
PC Input
By: TAWANDA
Checked: TAWANDA
Page no: 2 of 4

Distance or Interval		Visual Log	Structure Type		Typical Orientation			Brittle Structure Properties			Water Staining	Description
From	To		Code	Class	Alpha	Beta	Stick (T)op or (B)ottom	Micro-scale Geometry	Infill	Alteration		
92.08	93.20		J	2	88	_	_	8	SP	1	√	1OCJ, faulted with displacement, RIR
93.20	93.53		J	2	88	_	_	8	SP	1	√	1OCJ, faulted with displacement, RIR
93.53	94.08		J	2	45	_	_	8	SP	1	√	1OCJ, faulted with displacement, RIR
94.08	96.94		J	2	75	_	_	7	SP	1	√	1OCJ, faulted with displacement, RIR
96.94	96.98		J	2	75	_	_	7	SP	1	√	1OCJ, faulted with displacement, RIR
96.98	97.10		J	2	75	_	_	7	SP	1	√	1OCJ, faulted with displacement, RIR
97.10	99.54		J	2	85	_	_	8	SP	1	√	1OCJ, faulted with displacement, RIR
99.54	101.76		J	2	50	268.8	B	8	SP	1	√	1OCJ, faulted with displacement, RIR
101.76	101.82		J	2	50	268.8	B	8	SP	1	√	1OCJ, faulted with displacement, RIR
101.82	101.99		J	2	50	268.8	B	8	SP	1	√	1OCJ, faulted with displacement, RIR
101.99	102.07		J	2	50	268.8	B	8	SP	1	√	1OCJ, faulted with displacement, RIR
102.07	102.44		J	2	50	268.8	B	8	SP	1	√	1OCJ, faulted with displacement, RIR
102.44	103.03		J	2	75	129.6	B	8	SP	1	√	1OCJ, faulted with displacement, RIR
103.03	103.40		J	2	75	129.6	B	8	SP	1	√	1OCJ, faulted with displacement, RIR
103.40	104.40		J	2	45	180	T	8	SP	1	√	1OCJ, faulted with displacement, RIR
104.40	105.09		J	2	85	0	T	8	SP	1	√	1OCJ, faulted with displacement, RIR
105.09	105.51		J	2	85	_	_	_	SP	1	√	1OCJ, faulted with displacement, RIR
105.51	105.68		_	_	_	_	_	_	_	_	_	Wholely intact rock
105.68	107.40		F	2	60	180	B	8	SP	1	√	1OCJ, faulted with displacement, RIR
107.40	107.56		J	2	50	199.2	B	8	SP	1	√	1OCJ, faulted with displacement, RIR
107.56	107.67		J	2	50	199.2	B	8	SP	1	√	1OCJ, faulted with displacement, RIR
107.67	107.91		J	2	45	204	B	8	SP	1	√	1OCJ, faulted with displacement, RIR
107.91	110.40		_	_	_	_	_	_	_	_	_	Wholely intact rock
110.40	113.04		_	_	_	_	_	_	_	_	_	Wholely intact rock
113.04	113.51		J	2	45	_	_	_	SP	1	√	1OCJ, faulted with displacement, RIR
113.51	113.70		J	2	45	_	_	_	SP	1	√	1OCJ, faulted with displacement, RIR
113.70	113.82		J	2	60	336	B	8	SP	1	√	1OCJ, faulted with displacement, RIR
113.82	114.06		J	2	60	336	B	8	SP	1	√	1OCJ, faulted with displacement, RIR
114.06	114.89		_	_	_	_	_	_	_	_	_	

Structure Code Table

Structure		Code
Shear Zone		SZ
Fracture Zone		FZ
Fault		F
Fracture		Fr
Joint		J
Striation lineation		L
Fold Axis		FA
Vein		V
Dyke		D

Structure Class Table

Class	Description
1	Strongly sheared (cataclasite/mylonite), or brecciated
2	Clearly faulted with displacement or striations
3	The rock mass is weakened by alteration or strong fracturing, a nearby major structure is likely.
4	The core is completely broken because of poor core recovery. Possibly structure related
5	Core is strongly or completely altered/weathered to residual soil/mud.

Wall Alteration

1 - wall=rock hardness
2 - wall>rock hardness
3 - wall<rock hardness

Fill Type

Q - Quartz	G - Gouge
C - Calcite	M - Magnesium
FE - Iron oxide	H - Haematite
CL - Clay	S - Sulphide
B - Breccia	O - Other

Micro/Small Scale Joint Expression

Rough/Stepped/Irregular - 1
Smooth Stepped - 2
Slickensided Stepped - 3
Rough Undulating - 4
Smooth Undulating - 5
Slickensided Undulating - 6
Rough Planar - 7
Smooth Planar - 8
Polished - 9

Table A.10: Major structures log for borehole BO55A (Continuation)

Log#2 - Major Structures

TODAL MINING - GEOTECHNICAL

Site: BOKAI
Logged by: TAWANDA
Hole Number: BO55A
Bearing: 102
Plunge: -80
BON @ 113.74 MH @ 122.95

Hole Position
X: 30 01 27.5
Y: 19 48 00.3
Z: 1 145

PC Input
By: TAWANDA
Checked: TAWANDA
Page no: 3 of 4

Distance or Interval		Visual Log	Structure Type		Typical Orientation			Brittle Structure Properties			Water Staining	Description
From	To		Code	Class	Alpha	Beta	Stick (T)op or (B)ottom	Micro-scale Geometry	Infill	Alteration		
114.89	116.40		F	2	55	340.8	B	8	SP	3	√	1OCJ, faulted with displacement, RIR
116.40	116.74		FZ	3	_	_	_	_	SP	3	√	Rock mass weakened by strong fracturing
116.74	117.66		_	_	_	_	_	_	_	_	_	Wholely intact rock
117.66	118.08		FZ	3	_	_	_	_	SP	3	√	Rock mass weakened by strong fracturing
118.08	118.42		J	2	65	156	T	8	SP	1	√	1OCJ, faulted with displacement, RIR
118.42	118.47		J	2	65	156	T	8	SP	1	√	1OCJ, faulted with displacement, RIR
118.47	118.59		J	2	65	156	T	8	SP	1	√	1OCJ, faulted with displacement, RIR
118.59	118.81		J	2	65	156	T	8	SP	1	√	1OCJ, faulted with displacement, RIR
118.81	118.86		J	2	65	156	T	8	SP	1	√	1OCJ, faulted with displacement, RIR
118.86	119.20		J	2	15	28.8	B	8	SP	1	√	1OCJ, faulted with displacement, RIR
119.20	119.91		J	2	50	28.8	B	8	SP	1	√	1OCJ, faulted with displacement, RIR
119.91	119.96		J	2	50	28.8	B	8	SP	1	√	1OCJ, faulted with displacement, RIR
119.96	120.00		J	2	50	28.8	B	8	SP	1	√	1OCJ, faulted with displacement, RIR
120.00	120.15		J	2	50	28.8	B	8	SP	1	√	1OCJ, faulted with displacement, RIR
120.15	120.36		J	2	50	28.8	B	8	SP	1	√	1OCJ, faulted with displacement, RIR
120.36	120.43		J	2	50	28.8	B	8	SP	1	√	1OCJ, faulted with displacement, RIR
120.43	120.52		J	2	50	28.8	B	8	SP	1	√	1OCJ, faulted with displacement, RIR
120.52	120.71		J	2	50	28.8	B	8	SP	1	√	1OCJ, faulted with displacement, RIR
120.71	121.38		J	2	50	28.8	B	8	SP	1	√	1OCJ, faulted with displacement, RIR
121.38	122.40		_	_	_	_	_	_	_	_	_	Wholely intact rock
122.40	125.40		_	_	_	_	_	_	_	_	_	Wholely intact rock
125.40	128.34		J	2	50	300	T	7	SP	1	√	1OCJ, faulted with displacement, RIR
128.34	128.40		_	_	_	_	_	_	_	_	_	Wholely intact rock

Structure Code Table

Structure		Code
Shear Zone		SZ
Fracture Zone		FZ
Fault		F
Fracture		Fr
Joint		J
Striation lineation		L
Fold Axis		FA
Vein		V
Dyke		D

Structure Class Table

Class	Description
1	Strongly sheared (cataclasite/mylonite), or brecciated
2	Clearly faulted with displacement or striations
3	The rock mass is weakened by alteration or strong fracturing, a nearby major structure is likely.
4	The core is completely broken because of poor core recovery. Possibly structure related
5	Core is strongly or completely altered/weathered to residual soil/mud.

Fill Type

Q - Quartz	G - Gouge
C - Calcite	M - Magnesium
FE - Iron oxide	H - Haematite
CL - Clay	S - Sulphide
B - Breccia	O - Other

Wall Alteration

1 - wall=rock hardness
2 - wall>rock hardness
3 - wall<rock hardness

Micro/Small Scale Joint Expression

Rough/Stepped/Irregular - 1
Smooth Stepped - 2
Slickensided Stepped - 3
Rough Undulating - 4
Smooth Undulating - 5
Slickensided Undulating - 6
Rough Planar - 7
Smooth Planar - 8
Polished - 9

Table A.11: Detailed geotechnical log for borehole BO55A

Log#3 - Detail Geotech Log

TODAL MINING- GEOTECHNICAL

Site: BOKAI

Logged by: TAWANDA

Hole Number: BO55A
Bearing: 102
Plunge: -80
BON @ 113.74 MH @ 122.95

Hole Position
x: 30 01 27.5
y: 19 48 00.3
z: 1 145

PC Input
By: TAWANDA
Checked: TAWANDA
Page no: 4 of 4

From	To	Rock Type	Intact Rock Strength			Fracture Frequency						Joint Condition (Micro/Filling/Alteration)						Cemented Joints		Micro Fractures	
												Set 1		Set 2		Set 3					
			Strong Mpa	Weak Mpa	% Weak	Total	Natural	Foliation	Set 1	Set 2	Set 3	α/β	MFA	α/β	MFA	α/β	MFA	Count	Fill Type	Intensity Count/m	Fill Type (if any)
92.08	95.08	Anothositic norite	R5	_	_	3	3	_	2	1	_	_	8SP1	_	8SP1	_	_	3	SP	_	_
95.08	98.08	Anothositic norite	R5	_	_	3	3	_	3	_	_	_	8SP1	_	_	_	_	3	SP	_	_
98.08	101.08	Anothositic norite	R5	_	_	1	1	_	1	_	_	_	8SP1	_	_	_	_	1	SP	_	_
101.08	104.40	Anothositic norite	R5	_	_	8	8	_	5	2	1	0.186	8SP1	0.579	8SP1	0.25	8SP1	8	SP	_	_
104.40	107.40	Anothositic norite	R5	_	_	26	26	_	2	24	_	∞	8SP1	0.333	8SP1	_	_	26	SP	_	_
107.40	110.40	Anothositic norite	R5	_	_	3	3	_	2	1	_	0.251	8SP1	0.221	8SP1	_	_	3	SP	_	_
110.40	113.04	Anothositic norite	R5	_	_	_	_	_	_	_	_	_	_	_	_	_	_	_	_	_	_
113.04	116.40	Anothositic norite & Bronzitite @ 113.74	R4	R2	50.67	36	36	_	2	2	32	_	_SP1	0.179	8SP1	0.161	8SP3	36	SP	_	_
116.40	119.04	Bronzitite	R4	R2	28.67	16	16	_	3	2	5	_	_SP1	_	_SP1	0.4167	8SP1	5	SP	_	_
119.04	122.40	Bronzitite	R5	_	_	10	10	_	1	9	_	0.521	8SP1	1.736	8SP1	_	_	10	SP	_	_
122.40	125.40	Bronzitite	R5	_	_	_	_	_	_	_	_	_	_	_	_	_	_	_	_	_	_
125.40	128.40	Bronzitite	R5	_	_	1	1	_	1	_	_	0.1	7SP1	_	_	_	_	1	SP	_	_

Micro/Small Scale Joint Expression

Rough/Stepped/Irregular - 1
Smooth Stepped - 2
Slickensided Stepped - 3
Rough Undulating - 4
Smooth Undulating - 5
Slickensided Undulating - 6
Rough Planar - 7
Smooth Planar - 8
Polished - 9

Fill Type	
Q - Quartz	G - Gouge
C - Calcite	M - Magnesium
FE - Iron oxide	H - Haematite
CL - Clay	S - Sulphide
B - Breccia	O - Other

Wall Alteration
1 - wall=rock hardness
2 - wall>rock hardness
3 - wall<rock hardness